Final Report

DEVELOPMENT OF A TEST METHOD THAT WILL ALLOW EVALUATION AND QUANTIFICATION OF THE EFFECTS OF HEALING ON ASPHALT MIXTURE

UF Project No.: 00084223

Contract No.: BDK75 977-26

Submitted to:

Florida Department of Transportation
605 Suwannee Street
Tallahassee, FL, 32399

Dr. Reynaldo Roque, P.E.
Reebie Simms
Yu Chen
Chulseung Koh
George Lopp

Department of Civil and Coastal Engineering
College of Engineering
365 Weil Hall, P.O. Box 116580
Gainesville, FL, 32611-6580
Tel: (352) 392-9537 extension 1458
Fax: (352) 392-3394

April 2012

DISCLAIMER

The opinions, findings and conclusions expressed in this publication are those of the authors and not necessarily those of the Florida Department of Transportation.

Prepared in cooperation with the State of Florida Department of Transportation.

SI* (MODERN METRIC) CONVERSION FACTORS

APPROXIMATE CONVERSIONS TO SI UNITS

Symbol	When You Know	Multiply By	To Find	Symbol
	LENGTH			
in	inches	25.4	millimeters	mm
ft	feet	0.305	meters	m
yd	yards	0.914	meters	m
mi	miles	1.61	kilometers	km
	AREA			
in^2	square inches	645.2	square millimeters	mm^2
ft^2	square feet	0.093	square meters	m^2
yd^2	square yards	0.836	square meters	m^2
ac	acres	0.405	hectares	ha
mi^2	square miles	2.59	square kilometers	km^2
	VOLUME			
fl oz	fluid ounces	29.57	milliliters	ml
gal	gallons	3.785	liters	l
ft^3	cubic feet	0.028	cubic meters	m^3
yd^3	cubic yards	0.765	cubic meters	m^3

NOTE: Volumes greater than 1000 l shall be shown in m^3.

	MASS			
oz	ounces	28.35	grams	g
lb	pounds	0.454	kilograms	kg
T	short tons (2000 lb)	0.907	megagrams	Mg
	TEMPERATURE (exact)			
°F	Fahrenheit temperature	5(F-32)/9 or (F-32)/1.8	Celcius temperature	°C
	ILLUMINATION			
fc	foot-candles	10.76	lux	l
fl	foot-Lamberts	3.426	candela/m^2	cd/m^2
	FORCE and PRESSURE or STRESS			
lbf	poundforce	4.45	newtons	N
psi	poundforce per square inch	6.89	kilopascals	kPa

APPROXIMATE CONVERSIONS FROM SI UNITS

Symbol	When You Know	Multiply By	To Find	Symbol
	LENGTH			
mm	millimeters	0.039	inches	in
m	meters	3.28	feet	ft
m	meters	1.09	yards	yd
km	kilometers	0.621	miles	mi
	AREA			
mm^2	square millimeters	0.0016	square inches	in^2
m^2	square meters	10.764	square feet	ft^2
m^2	square meters	1.195	square yards	yd^2
ha	hectares	2.47	acres	ac
km^2	square kilometers	0.386	square miles	mi^2
	VOLUME			
ml	milliliters	0.034	fluid ounces	fl oz
l	liters	0.264	gallons	gal
m^3	cubic meters	35.71	cubic feet	ft^3
m^3	cubic meters	1.307	cubic yards	yd^3
	MASS			
g	grams	0.035	ounces	oz
kg	kilograms	2.202	pounds	lb
Mg	megagrams	1.103	short tons (2000 lb)	T
	TEMPERATURE (exact)			
°C	Celcius temperature	1.8C + 32	Fahrenheit temperature	°F
	ILLUMINATION			
lx	lux	0.0929	foot-candles	fc
cd/m^2	candela/m^2	0.2919	foot-Lamberts	fl
	FORCE and PRESSURE or STRESS			
N	newtons	0.225	poundforce	lbf
kPa	kilopascals	0.145	poundforce per square inch	psi

* SI is the symbol for the International System of Units. Appropriate rounding should be made to comply with Section 4 of ASTM E380.

(Revised August 1992)

Technical Report Documentation Page

1. Report No.	2. Government Accession No.	3. Recipient's Catalog No.

4. Title and Subtitle	5. Report Date
Development Of A Test Method That Will Allow Evaluation And Quantification Of The Effects Of Healing On Asphalt Mixture	April 2012
	6. Performing Organization Code 00084223
7. Author(s) Reynaldo Roque, Reebie Simms, Yu Chen, Chulseung Koh, George Lopp	8. Performing Organization Report No.
9. Performing Organization Name and Address University of Florida Department of Civil and Coastal Engineering 365 Weil Hall P.O. Box 116580 Gainesville, FL 32611-6580	10. Work Unit No. (TRAIS)
	11. Contract or Grant No. BDK75 977-26
12. Sponsoring Agency Name and Address Florida Department of Transportation Research Management Center 605 Suwannee Street, MS 30 Tallahassee, FL 32399	13. Type of Report and Period Covered Final Report 10/13/09-04/15/12
	14. Sponsoring Agency Code

15. Supplementary Notes

16. Abstract

Repeated traffic loading will result in accumulation of damage, but this damage will heal during periods of no traffic loading. Consequently, this healing will extend the fatigue life of the asphalt pavement. Traditional fatigue analysis does not consider this and, as a result, will often underpredict field fatigue life. In this study, a test was developed to evaluate the healing behavior of asphalt mixture, both dense-graded and open-graded, using the Superpave Indirect Tensile Test (IDT) testing system. The healing test comprises of two phases: a damage phase and a healing phase. The testing procedure consists of repeated loading damage tests (resilient modulus tests) during the damage phase followed by a healing phase during which resilient modulus tests are performed only periodically to measure modulus recovery (healing). A decrease in resilient modulus with an increasing number of load cycles is indicative of accumulation of microdamage during the damage phase. Recovery of resilient modulus during the healing phase is indicative of damage recovery or healing. Rate of healing was found to not be constant but rather changed with time at a decreasing rate for any given mixture. Since healing rate varies with time, a healing rate parameter was defined to allow for comparison between mixtures. Results showed that, in general, mixtures at higher temperatures healed at a faster rate than those at lower temperatures. Lastly, recommendations are made for continued development and validation of testing using the proposed healing test.

17. Key Word	18. Distribution Statement
Healing, Damage, Asphalt Mixture, Modified Brittleness Index, Resilient Modulus	No restrictions. This document is available to the public through the National Technical Information Service, Springfield, VA, 22161.

19. Security Classif. (of this report)	20. Security Classif. (of this page)	21. No. of Pages	22. Price
Unclassified	Unclassified	115	

Form DOT F 1700.7 (8-72) Reproduction of completed page authorized

ACKNOWLEDGMENTS

The authors would like to acknowledge and thank the Florida Department of Transportation (FDOT) for providing technical and financial support and materials for this project. Special thanks go to project manager Gregory Sholar and engineers and technicians of the Bituminous Section of the State Materials Office for their contributions in terms of their expert knowledge, experience, and constructive advice throughout the course of this work.

EXECUTIVE SUMMARY

Fatigue cracking in flexible pavement is one of the most common and crucial modes of pavement distress experienced in Florida. It affects both the service quality and life of flexible pavement. These cracks start as micro-cracks (microdamage) which propagate and join together to form macro-cracks. It is now well recognized that microdamage healing may strongly influence fatigue life during micro-crack initiation and macro-crack propagation. Many researchers have developed different ways to evaluate these effects, but current evaluation methods for healing remain inadequate. Even though there are researchers who have been successful in characterizing healing effects, for the most part, these researchers have failed to quantify it. This is due to the lack of an appropriate testing and interpretation system to measure damage recovery rates, or healing rates, of asphalt mixture. Therefore, there is a strong need to develop an appropriate and systematic evaluation method for healing characteristics of asphalt mixtures as well as to quantify healing potential of asphalt mixtures.

In this study, a healing test was developed and validated to both evaluate healing characteristics and measure healing potential of asphalt mixture. The developed healing test consists of two phases: a damage phase and a healing phase. During the damage phase, repeated loading is applied. During the healing phase, no load is applied, except for occasional application of low load levels to monitor modulus recovery (healing). For purposes of practicality, protocols were developed to limit each phase to 30 min, but there are no restrictions on testing time as long as enough time has been given to induce proper damage during the damage phase and recover the damage during the healing phase.

It was determined that the standard Superpave Indirect Tensile Test (IDT) testing system should be utilized throughout this research because of its practicality and ability to yield

reasonable and accurate damage/fracture properties of asphalt mixture. One advantage of the Superpave IDT over other tension testing systems is that both laboratory-compacted specimens and field cores can be tested.

It was also concluded that the use of the resilient modulus (MR) test is appropriate both for the damage phase and the healing phase since it is a convenient way to measure effective stiffness of asphalt mixture, which is capable of indicating damage and damage recovery. The resilient modulus test also allows for the incorporation of varying lengths of rest period between load applications which will indicate the significance of rest period duration when inducing microdamage into the asphalt mixture.

Standard Superpave IDT tests (Resilient Modulus, Creep, and Strength tests) were performed on all asphalt mixtures before performing any healing tests. These tests provided essential mixture properties needed to determine appropriate load levels and rest period duration for the damage phase of the healing test. In an effort to identify appropriate load levels and rest periods for use during the damage phase of the healing test, repeated load damage tests were performed on asphalt mixtures encompassing a range of brittleness, load amplitude, and rest period duration. From these initial tests, appropriate load levels and rest period durations for use during the damage phase were determined and validated.

Rest periods can have a huge effect on healing. As a result, rest periods lasting 0.1, 0.4, and 0.9-second were examined to observe their effect on healing potential of asphalt mixture. The 0.4-second rest period was determined to be the most appropriate as it sufficiently minimized healing to allow for accumulation of targeted damage levels within a reasonable period of time (30 min). In addition, the 0.4-second rest period resulted in longer steady-state

damage range than shorter rest periods, which led to more controllable damage rates. Lastly, the 0.4-second rest period allows overall testing time to be relatively short.

It was discovered that appropriate load levels for use during the damage phase actually depended on brittleness of the asphalt mixture. A relationship between brittleness and loading level was established and validated for all asphalt mixtures tested. One concern regarding load level was that excessively high damage rates would make testing difficult to control and results hard to analyze. Loading levels given by the established relationship resulted in damage rates that were manageable. While loading levels given by the relationship did not necessarily induce the same amount of damage in each asphalt mixture tested, they did induce sufficient microdamage – 10% - 25% reduction in resilient modulus. During the healing phase, loading level was simply reduced by 5% as to not induce additional microdamage in the mixture while obtaining resilient modulus measurements. Results indicated that brittle mixtures were more sensitive to changes in loading level than those that were more ductile in nature. As a result, it was recommended that brittle mixture be tested at or below 40% of the failure strength of the mixture, while ductile mixture be tested at or above 20% of the failure strength.

After appropriate load levels and rest period duration were determined, testing protocol, data reduction and interpretation methods for standardization of the healing test were established. The healing test was then performed on all asphalt mixtures to evaluate the effects of mixture type, binder type, temperature, and degree of oxidative aging on healing potential of asphalt mixture. Results indicated that the modified brittleness index (strength divided by failure strain from Superpave IDT test) introduced in this study worked well in not only separating brittleness of asphalt mixture both by oxidative aging and temperature, but also in determining appropriate load levels to induce microdamage in the asphalt mixture.

Rate of healing measurements were made for all mixtures and, in general, were in good agreement with expected trends. Rate of healing was found to not be constant but rather changed with time at a decreasing rate for any given mixture. Although it would be ideal to wait for complete healing to occur in order to determine healing rate, this would be impractical for routine laboratory evaluation. Consequently, the healing test was limited to a run time of one hour, so complete healing of the asphalt mixture may or may not occur. To overcome this dilemma, a method to determine the undamaged normalized resilient modulus value at which complete healing occurs was devised. Once this value was known, percentage of healing with time (rate of healing) was determined for each mixture. Since healing rate was found to vary with time, a healing rate parameter was defined using a logarithmic relation to allow for comparison between mixtures. Results showed that, in general, faster healing rates were observed for mixtures at higher temperatures, less oxidative aging, and Styrene-Butadiene-Styrene (SBS) modification.

TABLE OF CONTENTS

LIST OF TABLES

LIST OF FIGURES

CHAPTER 1
INTRODUCTION

1.1 Background

Fatigue cracking in flexible pavement is one of the most common and crucial distresses that clearly affects the service quality and life of flexible pavement. Therefore, fatigue cracking is an important structural and functional deficiency that should be addressed in pavement design and maintenance planning. These cracks start as micro-cracks (microdamage) which propagate and join together to form macro-cracks. It is now well recognized that microdamage healing strongly influences the fatigue life during micro-crack initiation and macro-crack growth. Many empirical and mechanistic approaches have been investigated in order to evaluate and develop appropriate models for predicting asphalt pavement performance with respect to fatigue cracking. Pavement cracking and performance models used for development of pavement and mixture design in addition to specifications have traditionally been limited to considering only the effects of structure (layer thickness and stiffness) on bending stresses at the bottom of the pavement and their effects on fatigue cracking.

The most commonly used fatigue failure criterion was developed by Monismith et al. (1985) in the form:

$$N_f = K \cdot \left(\frac{1}{\varepsilon_t}\right)^a \cdot \left(\frac{1}{E}\right)^b$$

where,
N_f = the number of cycles to failure;
K, a, and b = regression coefficients;
ε_t = tensile strain; and

E = stiffness of the mixture.

However, observations in the asphalt pavement community indicate that this classic fatigue failure relationship under predicts field fatigue life. Monismith and Finn (1977) indicated that laboratory-based fatigue life required a shift factor of 13 to match actual fatigue cracking in the AASHO Road Test. Furthermore, laboratory to field shift factors from other research efforts ranged from 3 to 100. This implies that important factors are not properly accounted for in classic fatigue criteria. The difference between laboratory and field results may be attributed to loading conditions, including rest periods. Rest periods between loading applications in the laboratory are generally constant, while there are rest periods in the field which are of random length. Francken (1979) found that rest periods significantly increased the fatigue life of asphalt mixtures. This appears to indicate that asphalt concrete has the potential to heal during rest periods.

Many researchers have observed and verified healing effects in asphalt mixture and as a result, have developed different ways to evaluate these effects. Kim and Kim (1997) evaluated fatigue damage and healing of asphalt concrete pavements at the FHWA Turner Fairbank Highway Research Center in McLean, Virginia using the stress wave method. Asphalt pavements were loaded using the accelerated loading facility to induce fatigue damage and wave transients measured at different loading cycles and after rest periods were evaluated. The results indicated that the analysis technique used in this study provided a sensitive means of evaluating the changes in asphalt surface layer properties during fatigue loading and rest periods. Also, it was found that the effective modulus of the asphalt layer increased as the rest period between loading cycles increased. Daniel and Kim (2001) evaluated healing of asphalt concrete mixtures in the laboratory using the impact resonance test method. This study indicated that this method

can be used successfully to evaluate micro-crack healing of asphalt concrete. Si et al. (2002a) indicated that the pseudo stiffness was found to decrease consistently with an increasing number of stress loading cycles. The recovery of pseudo stiffness after rest periods indicates that healing took place. The degree of healing was found to be a function of binder properties. Stiff mixtures were found to have better healing potential, and induction of longer rest periods were found to result in more healing. Song et al. (2005) addressed the development of a comprehensive methodology for the characterization of damage and healing in asphalt mastics. Healing in asphalt mastics was captured using X-ray Computed Tomography (CT) imaging of specimens subjected to cyclic loading with and without rest periods. They concluded that the influence of healing was substantially greater at earlier stages of loading where damage is small (micro-cracks are small) while the healing potential was minimal at points beyond the failure point. Kim and Roque (2006) developed an approach to determine the healing rate of asphalt mixture in terms of recovered dissipated creep strain energy (DCSE) per unit time. For the binders and mixtures evaluated, they found that microdamage healing was more affected by the aggregate structure characteristics than by polymer binder modification. These research efforts have not only shown evidence of healing in asphalt mixture but have also implied that microdamage is permanent only if the mixture is no longer capable of healing. Thus, in addition to measuring fatigue damage properties of asphalt mixture, it is also important to measure healing properties to more accurately predict fatigue life of asphalt pavement.

The latest version of the new Mechanistic-Empirical Pavement Design Guide (MEPDG) design guide for pavement structures attempts to consider the effects of asphalt mixture aging by including an age-hardening model that predicts asphalt mixture stiffness changes with time and the resulting effects on bending stresses and strains, which affect fatigue cracking predictions.

However, there are currently no existing models that consider changes due to the effects of damage recovery (healing), which is known to occur in asphalt mixtures during rest periods, particularly at relatively warm in-service temperatures. Recent work completed using the Heavy Vehicle Simulator (HVS) at the FDOT's Accelerated Pavement Testing (APT) facility has clearly indicated that an asphalt mixture's potential for damage recovery or healing may have a major impact on top-down cracking performance of flexible pavement, which is the predominant mode of distress in Florida pavements.

Still yet, evaluation methods for healing are inadequate at this time. Even though some researchers have been successful in showing healing effects, for the most part, they have failed to quantify it. This is because of the lack of an appropriate testing and interpretation system to measure damage recovery rates of asphalt mixture. Therefore, there is a strong need to develop an appropriate and systematic evaluation method for healing characteristics of asphalt mixtures as well as to quantify healing potential of asphalt mixtures.

1.2 Objectives

The main objective of this study is to develop a testing and data interpretation system to measure damage recovery rates of asphalt mixture. The system will be suitable for testing of laboratory-compacted specimens and field cores and will be based on the Superpave IDT. In addition, the system will follow the Hot-Mix Asphalt (HMA) Fracture Mechanics concepts developed in previous FDOT research efforts, which are currently being integrated as part of the top-down cracking model that will be incorporated into the new MEPDG design guide.

Detailed objectives of this research are as follows:

- Review and define microdamage and healing in asphalt mixture

- Develop an appropriate and systematic methodology to induce microdamage in asphalt mixture without inducing macro-cracking
- Develop an appropriate and systematic methodology to evaluate and quantify the healing potential of asphalt mixture
- Use the system developed to measure and characterize healing for a range of asphalt mixtures
- Evaluate the testing and data interpretation method developed by comparing measured effects to expected trends

1.3 Scope

This study primarily focuses on development of a testing and data interpretation system for determination of damage recovery rates of asphalt mixture. While the system is capable of handling both laboratory-compacted specimens and field cores, this study will focus on the former in an effort to reduce complication and variability. For determination of damage recovery rates, healing tests consisting of two phases, a damage phase and a healing phase, were performed on asphalt mixtures.

Damage is characterized by resilient modulus and healing by a recovery in resilient modulus. Damage refers to micro-crack initiation or growth. If and when a micro-crack becomes a macro-crack, it is considered to be no longer healable and as a result, is outside the scope of this project. Therefore, damage induced in all asphalt mixtures will always remain below the failure point.

Standard Superpave IDT tests (resilient modulus, creep, and strength tests) were performed before all healing tests to obtain necessary mixture properties. Healing tests were performed in two back-to-back test phases consisting of a damage phase and a healing phase.

Two mixture types, one dense-graded and one open-graded, were used to evaluate healing potential. Binder types PG 67-22 and 76-22 were used for the dense-graded mixture, while binder types PG 76-22 and ARB-12 were used for the open-graded mixture. The PG 76-22 binder is a blend of PG 67-22 and Styrene-Butadiene-Styrene (SBS) polymer and the ARB-12 is a blend of PG 67-22 with 12% ground tire rubber by weight. Each mixture was tested at three test temperatures: 0°C, 10°C, and 20°C. Aging conditions included both Short-Term Oven Aging (STOA) and Long-Term Oven Aging (LTOA).

1.4 Research Approach

Because current evaluation methods for healing are few and far between, a systematic methodology for the evaluation and quantification of the effects of healing on asphalt mixture was developed. The research approach taken to develop such a system involved the following steps:

- Review knowledge regarding the assessment of healing in asphalt binders and mixtures. This review of literature should include definitions of microdamage and healing along with current understandings of healing mechanisms. Existing approaches used to characterize and/or quantify damage and healing should be presented as well. Efforts with the most promising findings should be used in the development of a test to measure healing potential.
- Develop a healing test method and associated data interpretation method for evaluation of healing characteristics of asphalt mixture. Said test should be capable of inducing microdamage into the asphalt mixture without inducing macrodamage

and in addition should be able to evaluate and quantify healing potential.

Development of such a tests includes identification of the following:

1) Appropriate mode of loading (static or repeated)
2) Appropriate loading procedure (magnitude and duration)
3) Reasonable testing and data interpretation time
4) Adequate frequency of data acquisition

- Perform laboratory tests using the Superpave IDT and the developed healing test on laboratory-compacted specimens subjected to various conditions to evaluate healing potential. Lastly, compare test results to expected trends.

CHAPTER 2
LITERATURE REVIEW

2.1 Definitions of Damage and Healing

Loosely speaking, damage can be defined as a loss of structural integrity, either local (at the material level) or global (at the structural level). This in turn, can be thought of as a reduction in stiffness. A recovery in stiffness is then thought to be healing. Damage and healing are best described by Bhasin et al. (2011):

> "The growth of a microcrack is associated with the creation of new fracture surfaces. A precursor to the growth of a microcrack is damage in the vicinity of the crack tip. This damage is associated with the deformation and rearrangement of molecules in the failure zone. The mechanism of self-healing can therefore be regarded as a reversal of these processes. More specifically, self-healing entails reversal of crack opening followed by reversal of the microdamage that occurred in the failure zone."

Many researchers characterize healing in asphalt mixture by simply an increase in stiffness because the healing mechanism is not clearly understood. Because the healing mechanism is not understood, it is difficult to truly define microdamage and healing. Therefore, in this paper, damage will be characterized using resilient modulus, and healing will be characterized by a recovery in resilient modulus. Additionally, in this paper, the terms "damage" and "micro-crack" are synonymous and are used interchangeably. The terms "failure" and "fracture" refer to macro-crack initiation or growth. It should be noted however that terminology used in the following sections of this literature review is that of each individual work, which may or may not adhere to the definitions of damage and healing given above.

2.2 Evidence of Healing

In recent years, the concept of healing in asphalt binder, binder-rich sand mixture, and asphalt mixture has gained worldwide interest. However, the concept of healing is nothing new. As early as the 1960s, Oliensis (1964) examined crack-healing tendencies of binders through prolonged weather tests. While there are still researchers who question the existence of healing today, there has been evidence both in the field and in the lab that suggests otherwise.

2.2.1 Evidence of Healing in the Field

Using the stress wave propagation method, Kim and Kim (1997) evaluated changes in surface waves velocities of asphalt concrete surface layers due to fatigue and rest periods. Results showed that in general, as the number of loading cycles increased, the phase velocity decreased and therefore the effective elastic modulus decreased. When rest periods were introduced however, the phase velocity was seen to increase resulting in an increase in effective modulus. This increase in phase velocity was attributed to three factors including relaxation of the asphalt material, steric hardening of the asphalt binder, and actual healing of the induced micro-cracks. Since it is difficult to determine how much of each factor contributes to healing, the cumulative effect of these factors was termed “microdamage healing”.

2.2.2 Evidence of Healing in the Lab

Daniel and Kim (2001) monitored changes in the dynamic modulus of elasticity and flexural stiffness of asphalt concrete specimens using the impact resonance test and the third-point bending beam fatigue machine. When specimens were subjected to rest periods, an increase in dynamic modulus of elasticity was observed. Daniel and Kim attributed this increase

in modulus to "microcrack healing" since the impact resonance method measures only the elastic response of the material. In other words, no viscoelastic relaxation is present. An increase in flexural stiffness was observed as well. In addition, Daniel and Kim noted that higher temperatures appeared to increase the amount of healing that occurred during the rest periods.

2.3 Healing Mechanism

Many researchers characterize healing in asphalt mixture by simply using an increase in stiffness without specifically defining microdamage and healing. This is likely due to the fact that healing mechanisms are still not clearly understood. In general, most researches use the concept of wetting and intrinsic healing as a means of explaining healing in asphalt mixture.

2.3.1 Crack Wetting and Intrinsic Healing

Some researchers describe healing using two steps: (1) crack wetting (closing of micro-cracks) and (2) intrinsic healing (strength gain). Intrinsic healing is then divided into two additional components: instantaneous strength gain due to interfacial cohesion between the surfaces of the wetted crack interface and time-dependent strength gain due to randomization of molecules across the wetted crack interface (Bhasin et al., 2011). According to Little and Bhasin (2007), healing should not be confused with viscoelastic recovery due to rearrangement of molecules within the bulk of the material even when damage has not been induced with the material.

Using the process described above, Wool and O'Connor (1981) described the net macroscopic recovery, or rate of healing, within a material as the combination of two functions: rate of crack wetting [$\varphi(t)$] and rate of intrinsic healing [$R_h(t)$]. The net macroscopic recovery, R(t), is defined below:

$$R(t) = \int_{\tau=-\infty}^{\tau=t} R_h(t-\tau)\frac{d\varphi(\tau)}{d\tau}d\tau$$

where,
$R_h(t)$ = the intrinsic healing function;
$\varphi(t)$ = the wetting function; and
τ = the time variable.

$R_h(t)$ is controlled by inherent material properties such as surface free energy of the binder and molecular morphology and external factors such as temperature (Wool and O'Connor, 1981 and Bhasin et al., 2011). $\varphi(t)$ is controlled by factors such as surface free energy of the binder, crack geometry, and mechanical properties of the binder or mixture (Wool and O'Connor, 1981 and Bhasin et al., 2011).

2.4 Quantification of Healing in the Lab

In this section, four approaches for quantification of healing are presented. It should be noted that some approaches characterize healing more so than quantify it by introducing parameters that provide a relative comparison of healing between mixtures while other approaches provide a more absolute measure of healing through proposed parameters. In the end however, each approach provides a physical quantity as a means of describing healing.

2.4.1 Continuum Damage Mechanics Approach

In the continuum damage mechanics approach, strains in viscoelastic materials are not regarded as actual physical quantities, but are rather thought of as pseudo variables (Schapery, 1984). For an undamaged nonlinear viscoelastic material, the plot of the measured stress versus pseudo-strain is a hysteresis loop. The area within the hysteresis loop for an undamaged material is the dissipated pseudo-strain energy. Since asphalt concrete is a viscoelastic material, it is

highly time and history dependent. By using the dissipated pseudo-strain energy as opposed to the dissipated strain energy, the time-dependent characteristics can be eliminated as long as the initial stress or strain is relatively small (Kim, 1988). Nonlinearity of the material can then be eliminated by using the reference modulus of an undamaged nonlinear viscoelastic material as a correction factor (Si et al., 2002a). For an undamaged nonlinear viscoelastic material, the resulting plot of measured stress versus corrected pseudo-strain is a straight line. Any departure from this straight line indicates damage. This dissipated pseudo-strain energy is thought to be the real damage since both the time dependent and nonlinear behavior effects have been eliminated (Si et al., 2002a).

Using pseudo-stiffness, slope of the linear regression of the pseudo hysteresis loop, Si et al. (2002a) evaluated the effects of rest periods on microdamage and healing. During fatigue, pseudo stiffness will decrease with increasing number of cycles indicating damage of the asphalt concrete material. Recovery of pseudo stiffness after the introduction of rest periods therefore indicates healing of the asphalt concrete material. Healing is then described by the Healing Index (HI), the percent in pseudo stiffness increase which is defined below:

$$HI = \frac{\varphi_{after} - \varphi_{before}}{\varphi_{before}}$$

where,
φ_{before} = the pseudo stiffness before a rest period, and
φ_{after} = the pseudo stiffness after a rest period.

Results showed that stiffer mixtures exhibited greater healing capacity. It should be noted however that the HI only allows a relative comparison between mixtures. For example, mixture

A has a higher HI as compared to mixture B; therefore it has greater healing potential. The HI does not however actually quantify healing. It only provides a means of evaluating healing.

Si et al. (2002b) also proposed a healing rate. According to the researchers, two components of thermodynamic surface energy, Lifshitz-Van der Waals and Lewis Acid-Base, can be used to explain cohesive and adhesive fracture and healing. In cohesive fracture and healing, micro-cracks extend or heal within the binder or asphalt mastic. In adhesive fracture and healing, micro-cracks extend or heal at the asphalt-aggregate interface. The authors proposed that the actual rate of healing of an asphalt mixture is governed by two healing mechanisms, one controlled by the Lifshitz-Van der Waals component and one controlled by the Lewis Acid-Base component. The first mechanism is dominant in the short-term healing process and the second is dominant in the long-term healing process, but both occur simultaneously. The actual healing rate, $\dot{h}$, is defined as follows and is illustrated in Figure 2-1:

$$\dot{h} = \dot{h_2} + \frac{\dot{h_1} - \dot{h_2}}{1 + \frac{\dot{h_1} - \dot{h_2}}{h_\beta}(\Delta t)_h}$$

where,
$\dot{h_1}, \dot{h_2}$ = healing rates generated by the Lifshitz-Van der Waals and Lewis Acid-Base surface energies, respectively;
$(\Delta t)_h$ = the rest period between load applications; and
h_β = a factor that represents the maximum percent of healing that can be achieved by the asphalt binder.

Results showed that the healing rate did not only depend on surface energy of the binder, but also on surface energy of the aggregate and that the degree of healing was mixture dependent. Si et al. (2002b) noted however, that most healing occurred within the cohesive regions as stated by other researchers (Bhasin et al., 2011 and Shen et al., 2010).

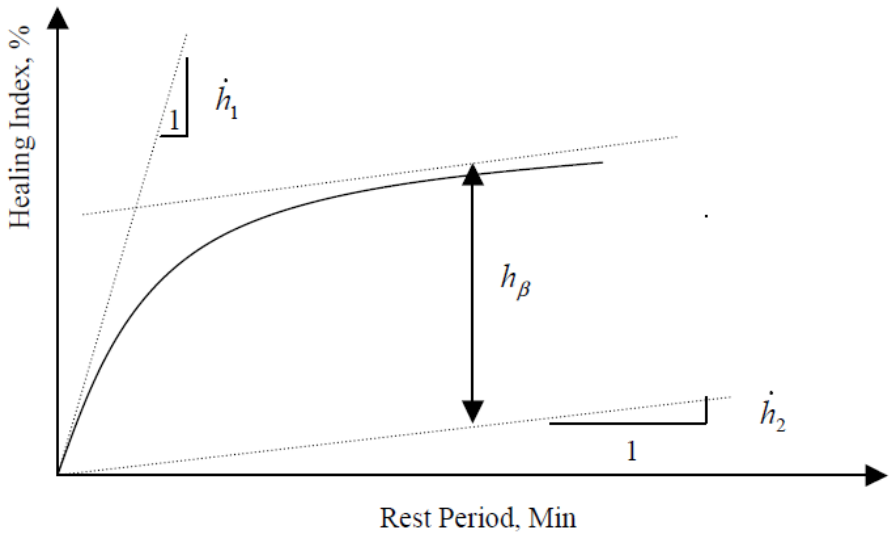

Figure 2-1. Graphical illustration of healing rate on typical healing curve (Si et al., 2002b)

2.4.2 HMA Fracture Mechanics Approach

Kim and Roque (2006) developed a method to both identify and quantify healing characteristics of asphalt mixture using the HMA Fracture Mechanics Model developed at the University of Florida. In the model, DCSE per cycle for a haversine load of 0.1-second and 0.9-second rest period is defined as follows:

$$DCSE/cycle = \int_0^{0.1} \sigma_{AVE} \sin(10\pi t)\dot{\varepsilon}_{p\,max} \sin(10\pi t)dt$$

where,
σ_{AVE} = the average stress applied; and
$\dot{\varepsilon}_{p\,max}$ = the creep strain rate.

In the HMA fracture mechanics approach, damage is characterized by the DCSE and healing is characterized by the recovered DCSE per unit time. The DCSE concept is illustrated in Figure 2-2.

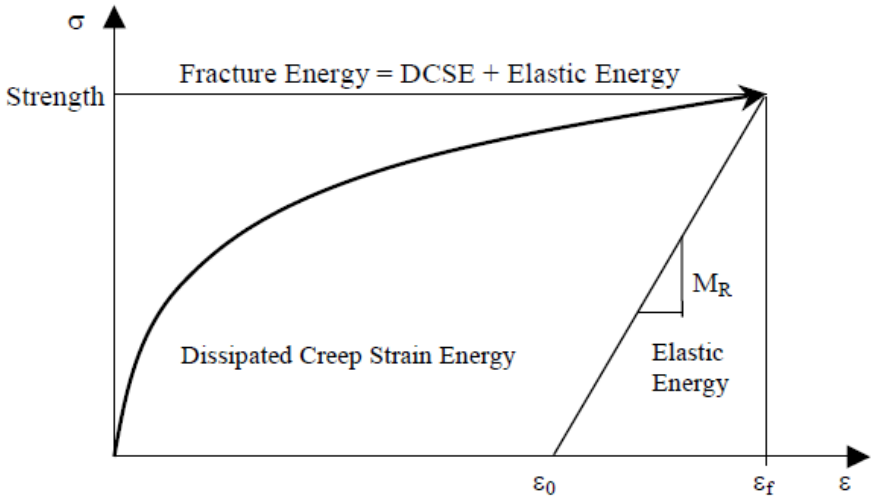

Figure 2-2. Dissipated creep strain energy concept (Kim and Roque, 2006)

Kim and Roque developed two healing tests. In the first, a normalized damage parameter ($DCSE/DCSE_{applied}$) which is defined as the DCSE divided by the accumulated DCSE was developed to characterize healing of the asphalt mixture. This parameter was found to be independent of the damage incurred in the mixture, but could not differentiate damage related healing from overall healing. Recall, that this was the problem with the stress wave method used by Kim and Kim (1997). So, a second healing test was developed. In the second test, pure damage recovery was separated from overall healing by eliminating the effects of steric hardening and cooling. During the loading and healing phases, the total increase in resilient deformation can be thought of as two parts: one related to damage ($\Delta\delta_D$) and one related to steric softening and heating ($\Delta\delta_{SS}$). Similarly, the total decrease in resilient deformation during healing can thought of as two parts: one that is damage recovery ($\Delta\delta_{DR}$) and one that is steric hardening and cooling ($\Delta\delta_{SH}$). This concept is illustrated in Figure 2-3. In the figure, t_D is the time when loading stops, t_{DR} is the time when damage recovery finishes, and t_H is the time when the mixture is fully healed, and dH_N is the rate of damage recovery.

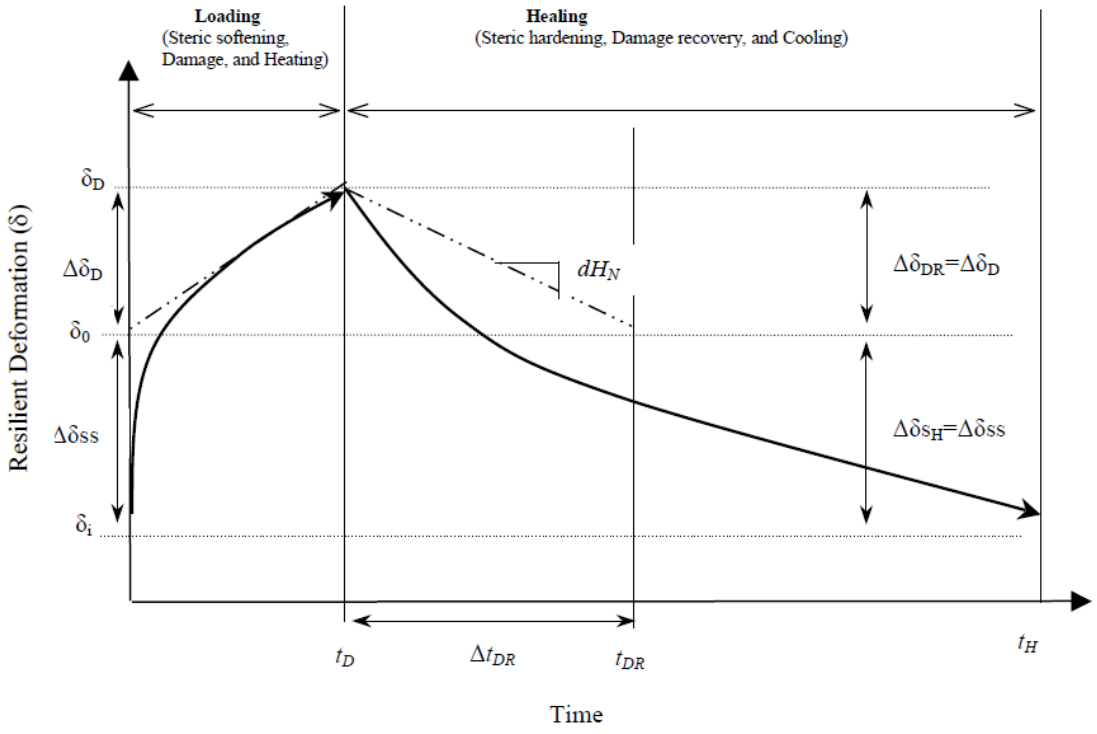

Figure 2-3. Resilient deformation during loading and healing (Kim and Roque, 2006)

For the second healing test, healing was evaluated using a new parameter – the rate of normalized damage recovery. As discussed above, this new parameter excludes the effects of steric softening and heating. Kim and Roque noted that in general, mixtures with lower asphalt contents exhibited higher damage recovery rates than those with higher asphalt contents. Interestingly, there was no difference in damage recovery rates between unmodified and modified mixtures. Polymer modification did however reduce the rate of damage accumulation. Figure 2-4 shows damage recovery rates for mixtures with asphalt contents of 6.1 and 7.2 %, denoted by 6.1 and 7.2 in the figure, and their corresponding polymer modified counterparts. Kim and Roque later went on to note that the total healing rate and the rate of damage recovery were found to be directly proportional and as a result, the DCSE/$DCSE_{applied}$ damage parameter

could be used for relative comparisons between mixtures since the total healing rate is far easier to measure.

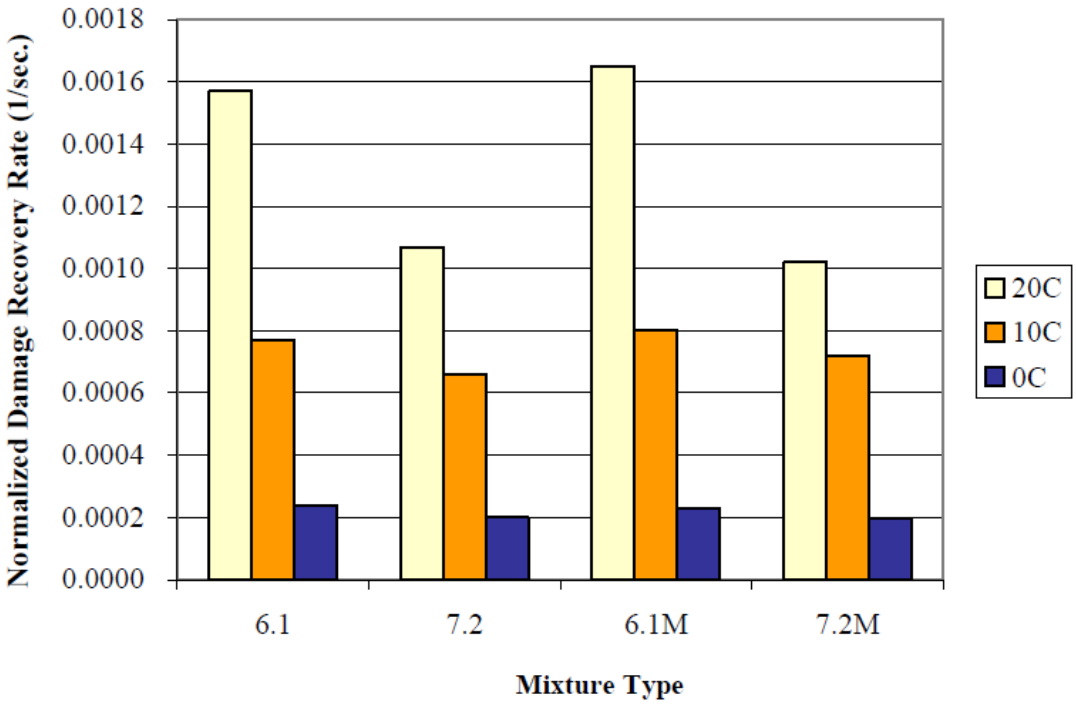

Figure 2-4. Normalized damage recovery rates (Kim and Roque, 2006)

2.4.3 Dissipated Energy Approach

Unlike the continuum damage mechanics approach, in the dissipated energy approach, stresses and strains in viscoelastic materials are regarded as actual physical quantities. For an undamaged nonlinear viscoelastic material, the plot of the measured stress versus strain is a hysteresis loop. The area within the hysteresis loop for an undamaged material is the dissipated energy. Since asphalt concrete is a viscoelastic material, it is highly time and history dependent, meaning that the dissipated energy in one loading cycle will depend on the dissipated energy in previous loading cycles.

According to Carpenter and Shen (2006), not all dissipated energy is responsible for damage. Only the relative amount of dissipated energy created by each additional load cycle will produce further damage, excluding dissipated energy due to plastic deformation and heat dissipation. By definition, Ratio of Dissipated Energy Change (RDEC) is the ratio of dissipated energy change between two loading cycles divided by the number of cycles between them and is written as follows:

$$RDEC_n = \frac{(DE_n - DE_m)}{DE_m \cdot (n - m)}$$

where,
$RDEC_n$ = the average ratio of dissipated energy change at cycle n;
DE_m and DE_n = dissipated energies at cycle m and n, respectively; and
m and n = loading cycles m and n, respectively.

It is thought that the RDEC provides a true indication of the damage being done to the mixture from one cycle to another by comparing the previous cycle's energy level and determining how much of it caused damage (Carpenter and Shen, 2006). A typical RDEC versus load curve is shown in Figure 2-5. Of particular interest is zone II, where the RDEC is more or less constant. This zone is referred to as the plateau stage. The RDEC value corresponding to the number of loading cycles at 50% reduction in stiffness is defined as the Plateau Value (PV). Using the RDEC approach, Carpenter and Shen obtained plateau values (PVs) from healing tests with varying rest periods. Results showed that healing capacity could be indicated using the PV recovery per second of rest period.

Following the RDEC concept, Shen et al. (2010) used Dynamic Shear Rheometer (DSR) testing with intermittent loading to evaluate healing behavior of asphalt binders. Healing was quantified using a healing rate, slope of the PV versus rest period curve. As shown in Figure 2-6,

the higher the slope of the PV – (RP+1) curve, the higher the healing rate, and thus, the greater healing capacity of the binder.

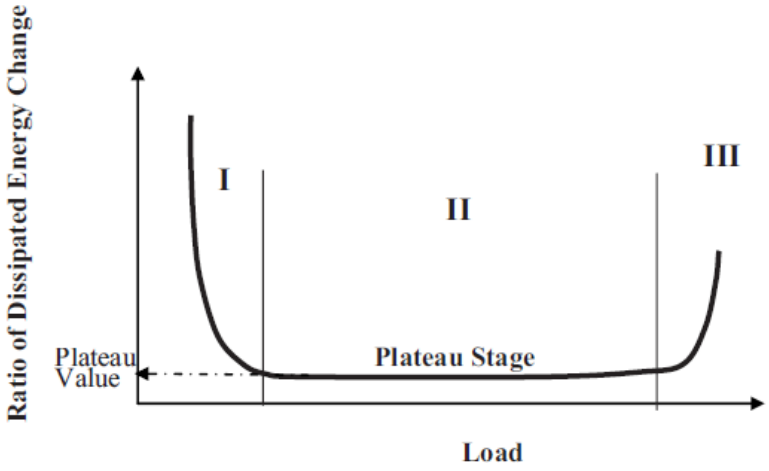

Figure 2-5. Typical RDEC plot (Shen et al., 2010)

The RDEC concept is promising because the plateau value has been found to be a fundamental property, meaning it is independent of mode of loading and testing condition (Shen and Carpenter, 2005). However, the RDEC still utilizes 50% reduction in initial modulus as is used in traditional fatigue analysis as a failure criterion. This 50% reduction in initial modulus has been shown to be inconsistent when predicting failure (Ghuzlan and Carpenter, 2000). Interestingly, the plateau value is defined as the RDEC corresponding to the number of load cycles at a 50% reduction in initial modulus while failure is defined as the point where the RDEC increases rapidly (zone III). This seems to be a contradiction within itself. Furthermore, failure is determined by visual inspection which may not prove easy due to significant scatter of data.

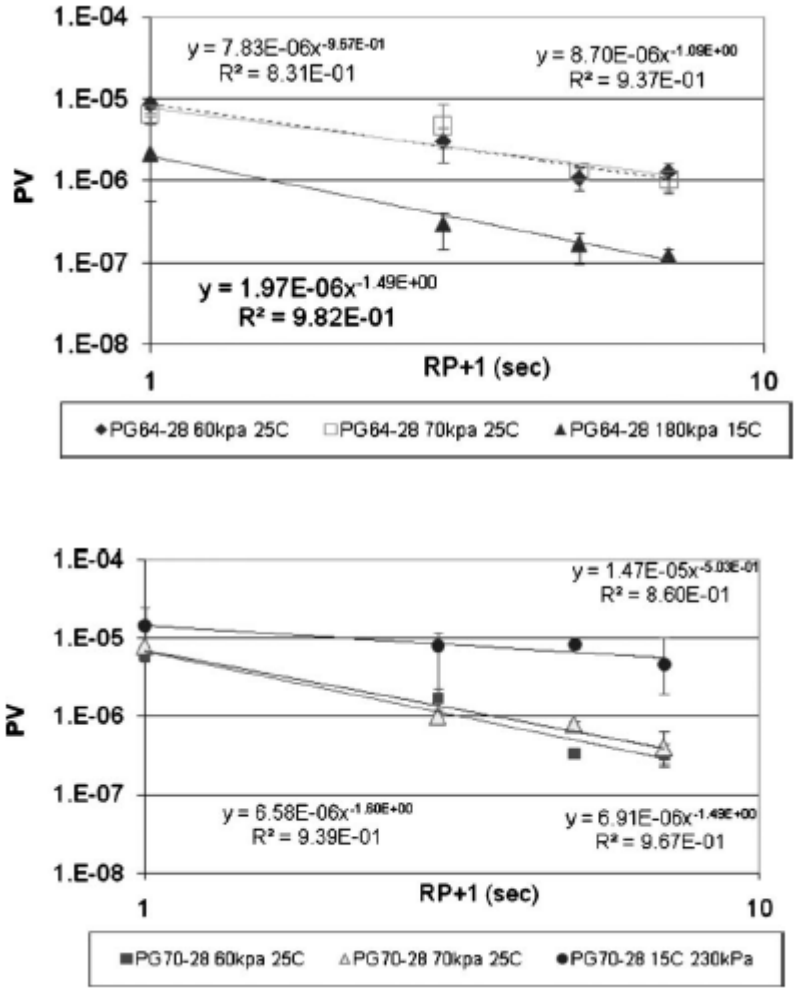

Figure 2-6. RDEC versus rest period for two binders (Shen et al., 2010)

2.4.4 X-ray Computed Tomography

Using X-ray CT, Song et al. (2005) captured healing in asphalt mastics (asphalt and mineral filler) specimens subjected to cyclic loading with and without rest periods. X-ray CT is an attractive technique as it allows for the capturing of the internal structure of the asphalt material while remaining nondestructive throughout the imaging process. Before specimens were imaged, they were damaged with a Dynamic Mechanical Analyzer (DMA). It should be noted that specimen dimensions were 500 mm in length with a diameter of 12 mm which may bring the

concept of Representative Volume Element (RVE) into question. Since only asphalt mastic was tested, this may not be an issue.

Images of specimens were captured at four different levels of damage as shown in Figure 2-7. Step 1 represents an initial condition where no damage has occurred. Steps 2 and 3 are at the first and second inflection points, respectively. Step 4 represents a point after failure has occurred.

From the X-ray CT results, Song and associates used a damage parameter that quantifies the percentage of voids (cracks and air voids) in a specimen as a means of characterizing healing. This damage parameter, ξ, was developed by Tashman et al. (2004) and is defined as follows:

$$\xi = \frac{1}{A}\sum_{i=1}^{N} A_{vi}$$

where,
A_{vi} = the void area (cracks and air voids);
A = cross-sectional area of a slice; and
N = the number of voids of in a slice.

Results showed that specimens with and without rest periods started with the same ξ value as expected or percentage of voids. However, when rest periods were introduced, specimens exhibited a smaller ξ value. Song et al. stated that the difference between specimens with and without rest periods became smaller at the last step (some point beyond failure) where voids were large and healing was not as effective as in steps 2 and 3. That is, the healing effect is greater at earlier stages of loading where damage is small. Figure 2-8 shows the difference in damage parameter ξ at steps 1, 2, 3, and 4. It is unclear as to whether images of specimens were captured immediately after being damaged or if specimens had to be transferred from the DMA

to the X-ray CT apparatus. If so, it is possible that healing took place during transfer of the specimens.

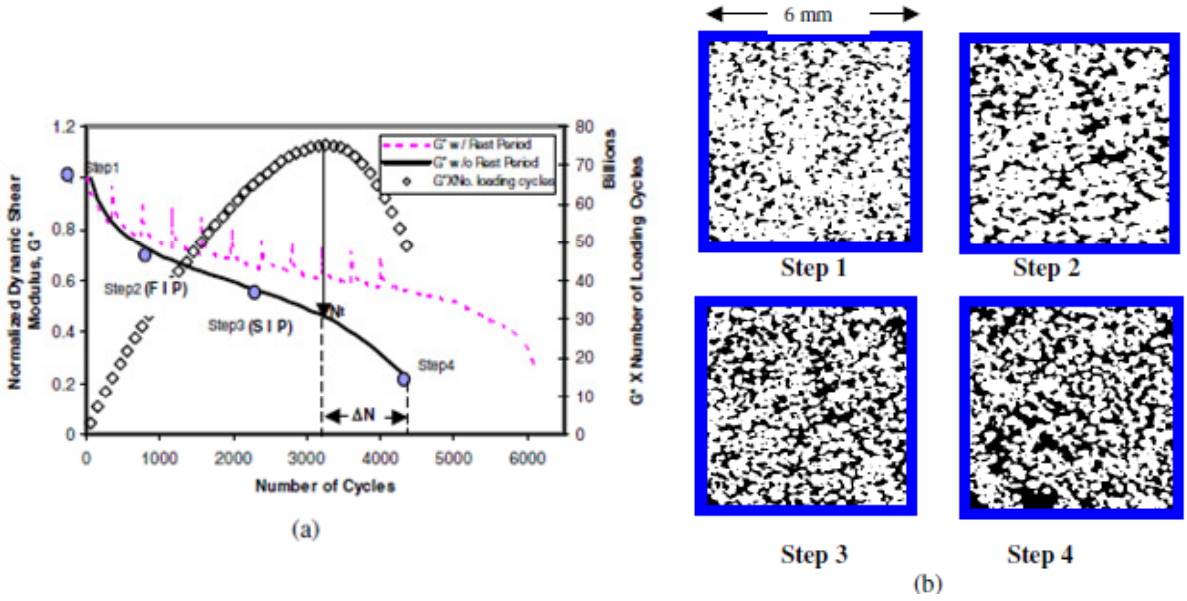

Figure 2-7. (a) Location of points selected for imaging, and (b) images of specimens captured at different levels of damage (voids space in black) (Song et al., 2005)

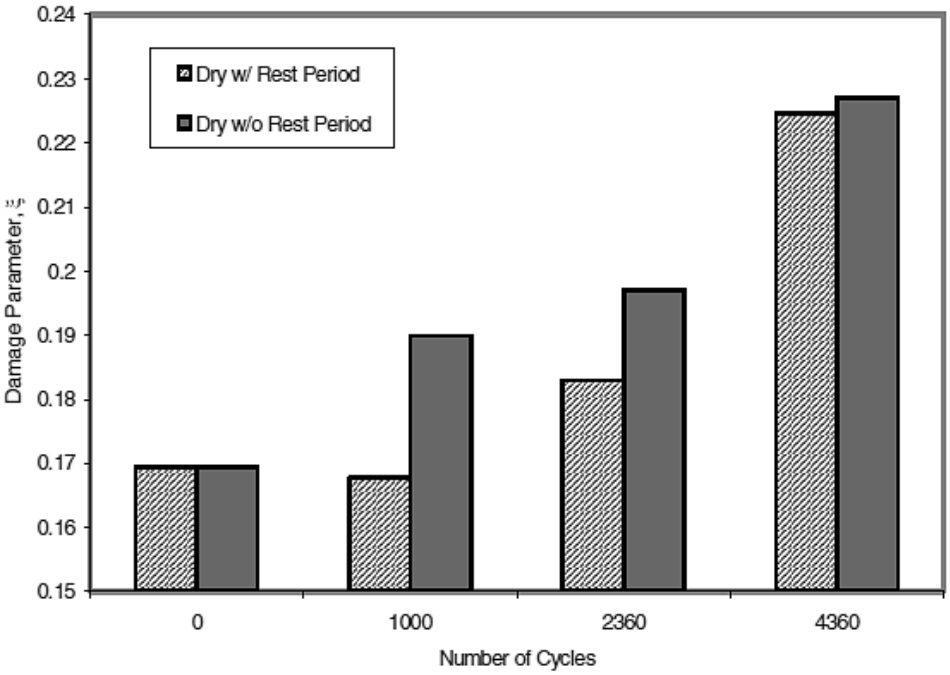

Figure 2-8. Damage parameter ξ in specimens with and without rest periods (Song et al., 2005)

The main advantage of X-ray CT is that it is a nondestructive and imaging technique that provides both two-dimensional and three-dimensional images of the internal structure of a solid material or object. In addition, X-ray CT has the ability to distinguish different phases and/or components of a material. This is particularly useful because micro-cracks which are invisible to the naked eye can be visualized via X-ray CT. However, this ability comes at a cost. The X-ray CT technique itself requires expertise in both electronics and physics and the image processing analysis program that analyzes measurements taken may require advanced knowledge in mathematics and statistics. Further, analysis of results may prove to be time-consuming. In the work described above, Song and associates had to analyze 700 slices per specimen.

2.5 Summary

From the literature review, it can be seen that there exists no universal method for either evaluating or quantifying healing. Four approaches for quantification of healing were presented. Of these four approaches, some characterized healing more so than quantified healing by introducing parameters that provide some relative measure of healing while other approaches provided a more absolute measure of healing. In addition, some researchers chose to evaluate healing by examining only the asphalt binder, while others tried evaluating healing by examining the asphalt mixture, or binder-rich sand mixture. It has been discovered that there are differences between results when considering binder versus mixture. Shen et al. (2010) found that when considering only asphalt binder, healing rates for polymer modified binders were greater than those of neat binders. In contrast, Kim and Roque (2006) found that when considering asphalt mixture, healing rates were more affected by the aggregate structure characteristics, than by polymer modification. Likewise, Si et al. (2002b) found that healing rates depended on surface

energies of both the asphalt binder and aggregate. In any case, evaluation methods for healing remain inadequate.

CHAPTER 3
TEST MATERIALS AND METHOD

3.1 Asphalt Mixture Design

Materials selected were chosen to be those representative of materials used in the state of Florida. Limestone and granite, two commonly used aggregate types in Florida, were used. Using Superpave (AASHTO M323-07) and FDOT Specifications Sections 334 and 337 (FDOT 2007), two gradations of asphalt mixture, one dense-graded and one open-graded (FC-5 mixture), were used. Dense-graded asphalt mixtures are typically used for structural purposes while open-graded asphalt mixtures usually serve as wearing courses which provide frictional characteristics such as skid resistance.

3.1.1 Dense-Graded Asphalt Mixture

All dense-graded asphalt mixtures were prepared using Georgia granite. Aggregate sources for the dense-graded mixtures are shown in Table 3-1. Aggregates were selected based upon availability and experience from previous research. In any case, the chosen aggregate met the consensus and source property criteria as stipulated by the Superpave mix design process to ensure quality aggregates in the production of asphalt mixture.

Following Superpave specification, the dense-graded mixtures were designed to have a 12.5 mm nominal maximum aggregate size. The gradation, or particle size distribution, with control points for the dense-graded mixture can be seen in Figure 3-1. Detailed information regarding the gradation can also be found in Appendix A.

Table 3-1. Aggregate sources for dense-graded mixtures

Type of Material	FDOT Code	Producer	Pit No.
# 78 Stone	43	Junction City Mining	GA-553
# 89 Stone	51	Junction City Mining	GA-553
W-10 Screenings	20	Junction City Mining	GA-553
Local Sand	-	V. E. Whitehurst & Sons	Starvation Hill

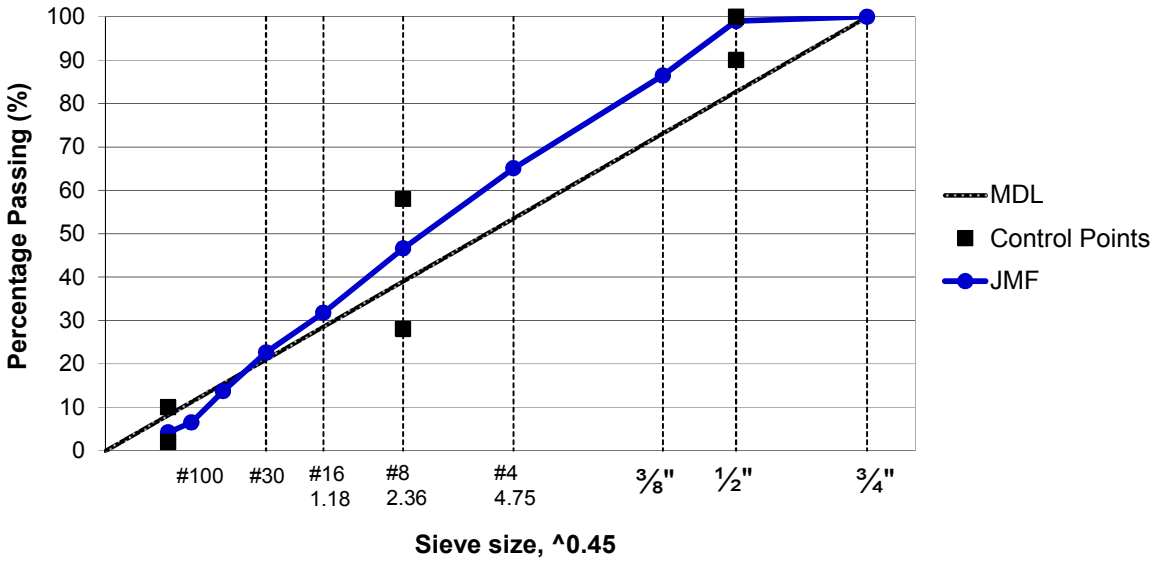

Figure 3-1. Gradation for dense-graded mixtures

Asphalt binders used in this study were obtained from the CITGO Asphalt Refining Company. Two binders including a control binder, PG 67-22 and a polymer modified binder, PG 76-22 with SBS, were used for evaluation of dense-graded asphalt mixtures.

3.1.1.1 Batching and Mixing

Aggregates and binders were oven-heated at the desired mixing temperature for approximately 3 hours before mixing. For the unmodified mixture and modified mixture, this temperature was determined to be 315°F and 325°F, respectively. After heating, the aggregates

were removed from the oven and mixed with binder using a mechanical mixer (see Figure 3-2) until the aggregates were well coated. The resulting mixtures were then placed in pans and put into the oven set at 275°F and short-term oven aged for 2 hours. To ensure a uniformly aged sample, each sample was stirred after an hour of STOA. For a detailed version of the mixing process see the "Specimen Preparation and Compaction" section of Asphalt Institute (2001). Batching sheets for the 4500 g samples can be found in Appendix A.

Figure 3-2. Mechanical asphalt mixer

3.1.1.2 Compaction

After STOA, samples were removed from the oven and compacted using the Servopac Superpave Gyratory Compactor (SGC) at the desired compaction temperature (see Figure 3-3). Using a ram pressure of 600 kPa and a gyratory external angle of 1.25° as specified by Superpave specification, samples were compacted to the number of gyrations corresponding to traffic level C. Traffic levels and the corresponding gyratory compaction efforts as stipulated by

the FDOT can be seen in Table 3-2. It should be noted that even though the dense-graded asphalt mixtures were designed to have 4% air void content, they were compacted in the SGC to achieve 7.0 ± 0.5% air voids. For a detailed version of the compaction process see the "Specimen Preparation and Compaction" section of Asphalt Institute (2001).

Figure 3-3. Servopac gyratory compactor

Table 3-2. Traffic levels and gyratory compaction efforts

Traffic Level	Million ESALs	$N_{initial}$	N_{design}	$N_{maximum}$
A	< 0.3	6	50	75
B	0.3 to < 3	7	75	115
C	3 to < 10	7	75	115
D	10 to < 30	8	100	160
E	≥ 30	8	100	160

Note: ESAL=Equivalent single axle load.

3.1.1.3 Optimum Asphalt Content

In the Superpave mix design process, the Optimum Asphalt Content (OAC) is selected as the asphalt content that achieves 4% air voids at N_{des}, granted volumetric mix design criteria are met. Using densification data from the compaction process, the OAC was determined to be 4.80% and 4.82% for the unmodified mixture and modified mixture, respectively. Volumetric properties resulting from the OAC are shown in Table 3-3. For more details on determining the optimum asphalt content, see the "Data Analysis and Presentation" section of Asphalt Institute (2001).

Table 3-3. Volumetrics for dense-graded asphalt mixture

AC (%)	G_{sb}	G_{mm}	VMA (%)	VFA (%)
4.8	2.770	2.579	14.9	73.1

Note: AC=Asphalt content; G_{sb}=Bulk specific gravity; G_{mm}=Rice specific gravity; VMA=Volume of voids in mineral aggregate; VFA=Volume of voids filled with asphalt

3.1.1.4 Long-Term Oven Aging

To evaluate the effects of aging on healing potential, in addition to being short-term oven aged, specimens were also subjected to a second level of aging. Following the procedure in AASHTO (2001a), specimens were subjected to LTOA for 5 days at 185 ± 0.5°F. Because of the high temperature specified for LTOA, there is always a possibility that specimens can fall apart during the conditioning process. To ensure an intact specimen during LTOA, a procedure developed by Varadhan (2004) was used. While the procedure was actually intended for open-graded compacted specimens, it was used for dense-graded specimens as well. As described in the procedure, compacted specimens were wrapped with a wire mesh with openings of 1/8 inch. The 1/8 inch openings allow for good air circulation while preventing smaller aggregates from

falling through the mesh. Two metal bands were then clamped to the mesh and specimen as shown in Figure 3-4. Special care was taken not to apply too much pressure when attaching the bands. Lastly, the specimens were placed on porous metal plates and then placed into the oven.

Figure 3-4. Wire mesh setup

3.1.2 Open-Graded Asphalt Mixture

All open-graded asphalt mixtures were prepared using Florida oolitic limestone. Aggregate sources for the open-graded mixtures are shown in Table 3-4. Again, aggregates were selected based upon availability and experience from previous research. Florida limestone is often used for open-graded friction courses throughout the state of Florida and is FDOT approved for road construction and rehabilitation projects.

Open-graded mixtures were designed according to FDOT specification Section 337 for FC-5 mixture type (FDOT 2007). The gradation for the open-graded mixture can be seen in Figure 3-5. It should be noted that the gradation falls within the acceptable ranges as specified by the FDOT. Detailed information regarding the gradation can also be found in Appendix A.

Table 3-4. Aggregate sources for open-graded mixtures

Type of Material	FDOT Code	Producer	Pit No.
S1A Stone	41	White Rock Quarries	87-339
S1B Stone	53	White Rock Quarries	87-339
Screenings	22	White Rock Quarries	87-339
Filler	-	-	-

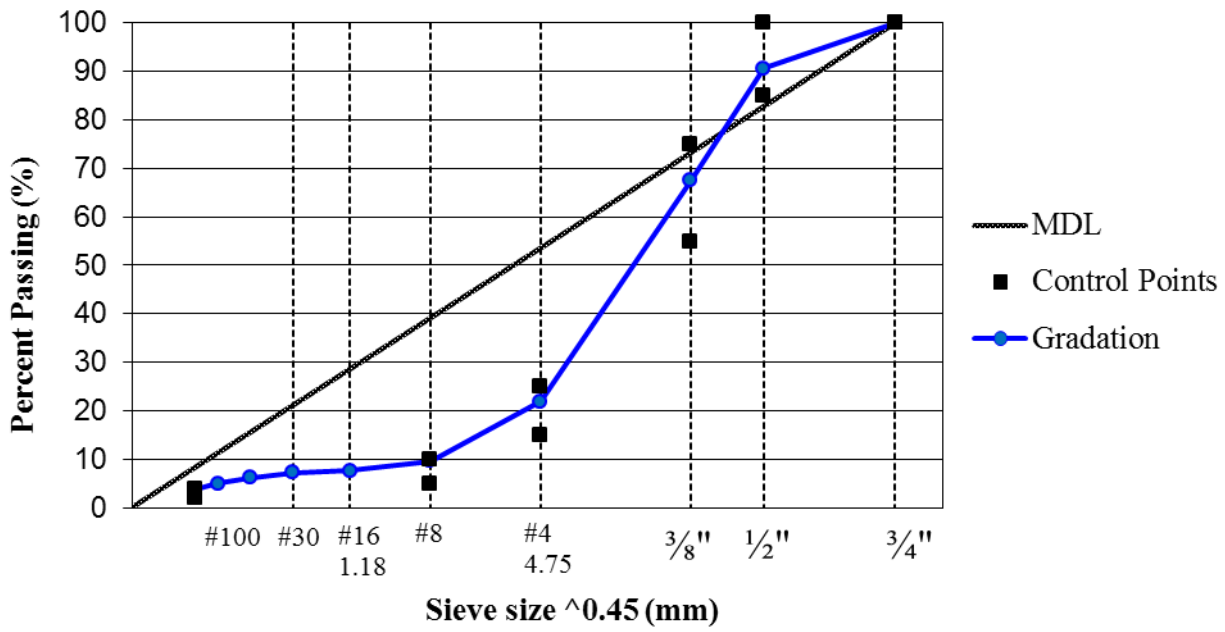

Figure 3-5. Gradation for open-graded mixtures

Asphalt binders used in this study were obtained from the CITGO Asphalt Refining Company. Two binders including a polymer modified binder, PG 76-22 with SBS, and a rubber

modified binder, ARB-12, were used for evaluation of open-graded asphalt mixtures. To achieve the desired Asphalt Rubber Binder (ARB), 12% ground tire rubber was blended with PG 67-22 to produce ARB-12.

3.1.2.1 Batching and Mixing

Aggregates and binders were oven-heated at the desired mixing temperature for approximately 3 hours before mixing. For the polymer modified and asphalt rubber modified mixture, this temperature was determined to be 315°F and 325°F, respectively. After heating, the aggregates were removed from the oven and mixed with binder using a mechanical mixer (see Figure 3-2) until the aggregates were well coated. The resulting mixtures were then placed in pans and put into the oven set at 275°F and short-term oven aged for 2 hours. To ensure a uniformly aged sample, each sample was stirred after an hour of STOA. For a detailed version of the mixing process see the "Specimen Preparation and Compaction" section of Asphalt Institute (2001). Batching sheets for the 4500 g samples can be found in Appendix A.

3.1.2.2 Compaction

After STOA, samples were removed from the oven and compacted using the SGC at the desired compaction temperature (see Figure 3-3). Using a ram pressure of 600 kPa and a gyratory angle of 1.25 ° as specified by Superpave specification, samples were compacted to 75 gyrations as suggested by previous research (Mallick et al., 2000; Varadhan, 2004). After compaction, specimens were allowed to cool for approximately 2 hours before being ejected from the mold to prevent collapse of the specimen due to the inherent high air void content of the

mixture. The compacted specimens were then allowed to cool for at least 24 hours at room temperature before any additional usage.

3.1.2.3 Optimum Asphalt Content

For the open-graded mixtures, the OAC was selected as the asphalt content resulting in the lowest VMA granted sufficient effective asphalt film thickness. Sufficient film thickness is needed to ensure adequate durability of the mixture. For both the polymer modified and rubber modified mixtures, the OAC was determined to be 6.40%.

3.1.2.4 Long-Term Oven Aging

To evaluate the effects of aging on healing potential, in addition to being short-term oven aged, specimens were also subjected to a second level of aging. Following the procedure in AASHTO (2001a), specimens were subjected to LTOA for 5 days at 185 ± 0.5°F. Because of the high temperature specified for LTOA, there is always a possibility that specimens can fall apart during the conditioning process. To ensure an intact specimen during LTOA, a procedure developed by Varadhan (2004) was used. As described in the procedure, compacted specimens were wrapped with a wire mesh with openings of 1/8 inch. The 1/8 inch openings allow for good air circulation while preventing smaller aggregates from falling through the mesh. Two metal bands were then clamped to the mesh and specimen as shown in Figure 3-4. Special care was taken not to apply too much pressure when attaching the bands. Lastly, the specimens were placed on porous metal plates and then placed into the oven.

3.1.2.5 Determination of Bulk Specific Gravity

When determining bulk specific gravity (G_{mb}) of compacted asphalt mixture, it is standard practice to use water-displacement methods such as those outlined in AASHTO T166 (AASHTO, 2001b) and ASTM D2726 (ASTM, 2002a). For the most part, when considering fine-graded mixtures, these methods result in accurate G_{mb}. However, when testing coarser gradations such as open-graded mixture and Stone Matrix Asphalt (SMA), it has been found that these methods result in erroneous measurement of G_{mb} (Buchanan and White, 2005; Cooley et al., 2002). Therefore, for good measure, G_{mb} was determined using the Corelok device as suggested by Buchanan and White (2005) and Cooley et al. (2002). The Corelok device is shown in Figures 3-6 and 3-7. The procedure for determination of G_{mb} using the Corelok device can be found in ASTM D6752 (ASTM, 2002b). Bulk specific gravity results for open-graded mixture are presented in Appendix B.

Figure 3-6. Corelok device

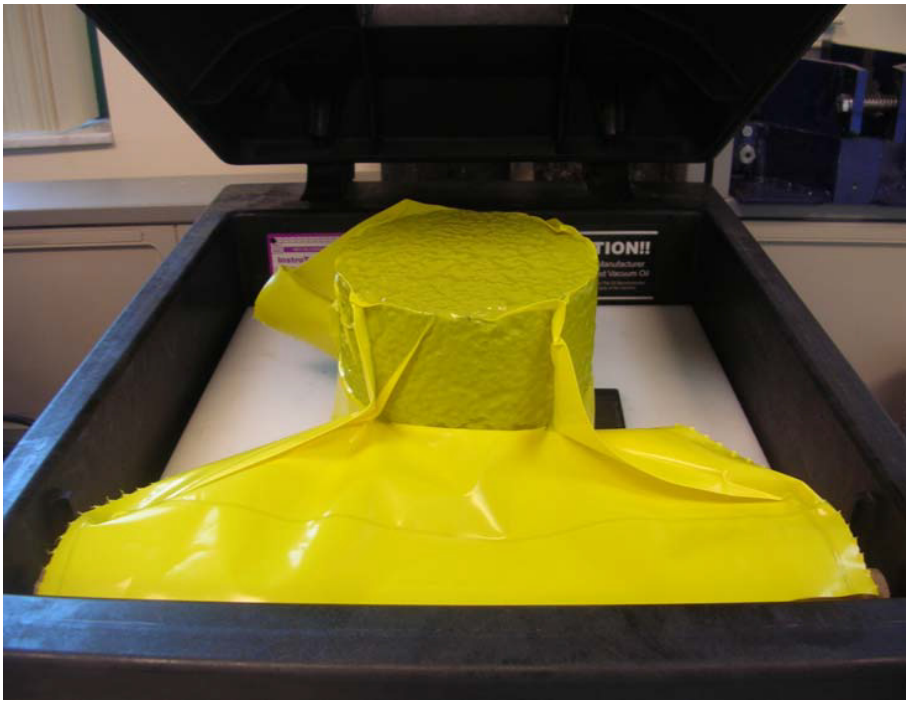

Figure 3-7. Vacuum-sealing in Corelok device

CHAPTER 4
DEVELOPMENT OF THE HEALING TEST

4.1 Introduction

Through comprehensive literature review, it was determined that the Superpave IDT testing system (MTS (Material testing System), environmental chamber, measurement and data acquisition system) should be utilized throughout this research because of its practicality and ability to provide reasonable and accurate damage/fracture properties of asphalt mixture including open graded asphalt mixture (Koh and Roque, 2010a; Koh and Roque 2010b). Another advantage of the Superpave IDT over other testing systems is that field core samples can be used as well. The standard Superpave IDT tests (Resilient Modulus, Creep, and Strength tests) can also be used to identify appropriate damage levels along with other mixture information.

After exhaustive analysis and discussion, it was concluded that the use of the Resilient Modulus (MR) test is appropriate for both the damage phase and the healing phase since it is a convenient way to measure effective stiffness of asphalt mixture, which could indicate damage and damage recovery. The resilient modulus test also allows for the incorporation of rest periods which will indicate the significance of rest period duration during damaging.

4.2 Selection of Loading Mode

One concern regarding damaging of the asphalt mixture is selection of the mode of loading. Two types of loading modes often used to evaluate damage and fracture of asphalt mixture are static and repeated (cyclic) loading. Static loading is performed with either a

constant rate of loading or constant rate of displacement, and repeated loading is performed with or without introduction of rest periods.

In many cases, the use of static loading is advantageous in that it results in significantly reduced testing time. However, delayed elasticity becomes an issue and may cause error during healing phases if static loading is employed. Roque et al. (1997a) showed that delayed elasticity is present for static loading conditions even when load durations are very short. The purpose of the healing test is to measure the rate of damage recovery after loading has ceased. If static loading were used during the damage phase, it would be nearly impossible to separate the delayed elastic response from actual damage recovery. Since true healing does not include delayed elasticity, it would be inappropriate to use the static loading mode. Therefore, the repeated loading mode was selected since it is possible to incorporate rest periods between load applications, thereby minimizing delayed elasticity while at the same time mimicking traffic loading conditions. This also allows for the use of the resilient modulus test, which has been determined to be an appropriate and convenient way to measure effective stiffness of asphalt mixture, during both the damage and healing phases.

4.3 Experimental and Theoretical Analysis of Load Characteristics

When using the repeated or cyclic mode of loading, three factors need to be considered, including load shape, load amplitude, and duration of rest period between load applications. Each of these factors will have an effect on the amount of microdamage accumulation and thus, healing. Each of the three factors is discussed in the following sections.

4.3.1 Load Shape

A haversine load shape of 0.1-second was chosen. Technically, the MTS is capable of applying both haversine and square load shapes. However, in the case of square shape loading, issues arise. The first is that the square shape cannot be fully achieved. This is because the load cannot be instantaneously removed when commanded to do so by the control program which will lead to additional undesired damage in the asphalt concrete specimen. Further, it is possible that testing times would have to be longer to ensure delayed elasticity has been recovered. Neither of these issues is a concern with haversine loading and since the Superpave IDT resilient modulus test utilizes the haversine load shape and has been identified as being suitable for inducing damage in the asphalt material, no modifications to load shape have to be made. This is of great convenience as procedures for calculation of resilient modulus are already established (Roque and Buttlar, 1992; Buttlar and Roque, 1994; Roque et al., 1997a). Therefore, the haversine load shape was selected as being an appropriate load shape.

4.3.2 Load Amplitude

An appropriate load amplitude, or load level, should result in development of significant damage within the steady-state range as shown in Figure 4-1. If load amplitude is selected such that it is in the linear range, then material response will be stress-state independent. Figure 4-2 shows data from a typical Superapve IDT strength test. Below 40 % of the load at failure, the stress-strain relationship could be considered linear. As a result, it is necessary to know in what load amplitude range the asphalt mixture will behave like an elastic material before the healing test is performed. Consequently, there is most likely no one load that would be appropriate for a range of asphalt mixture.

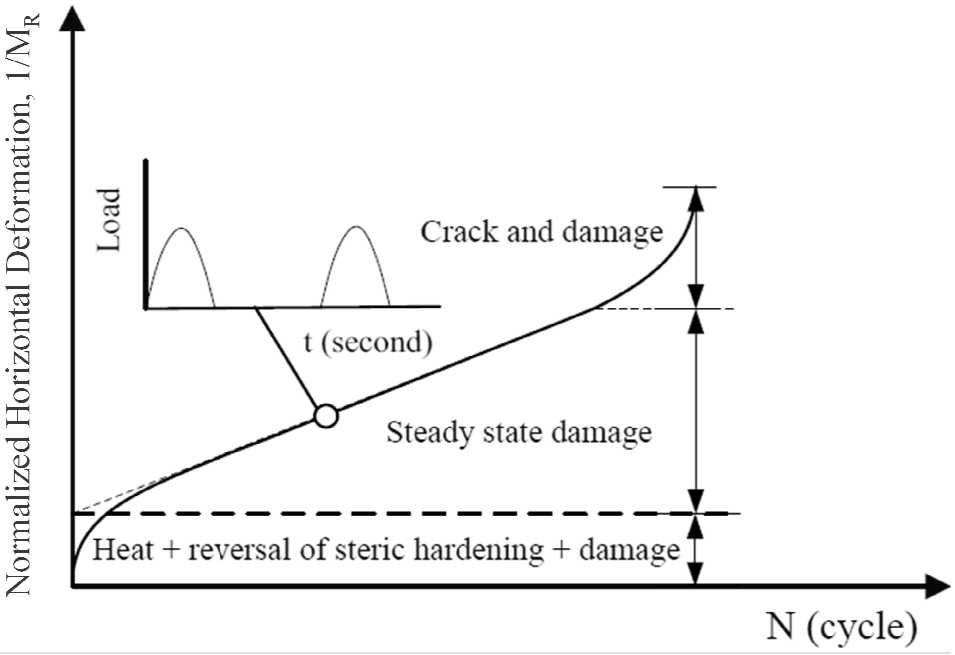

Figure 4-1. Asphalt mixture fatigue curve due to cyclic loading

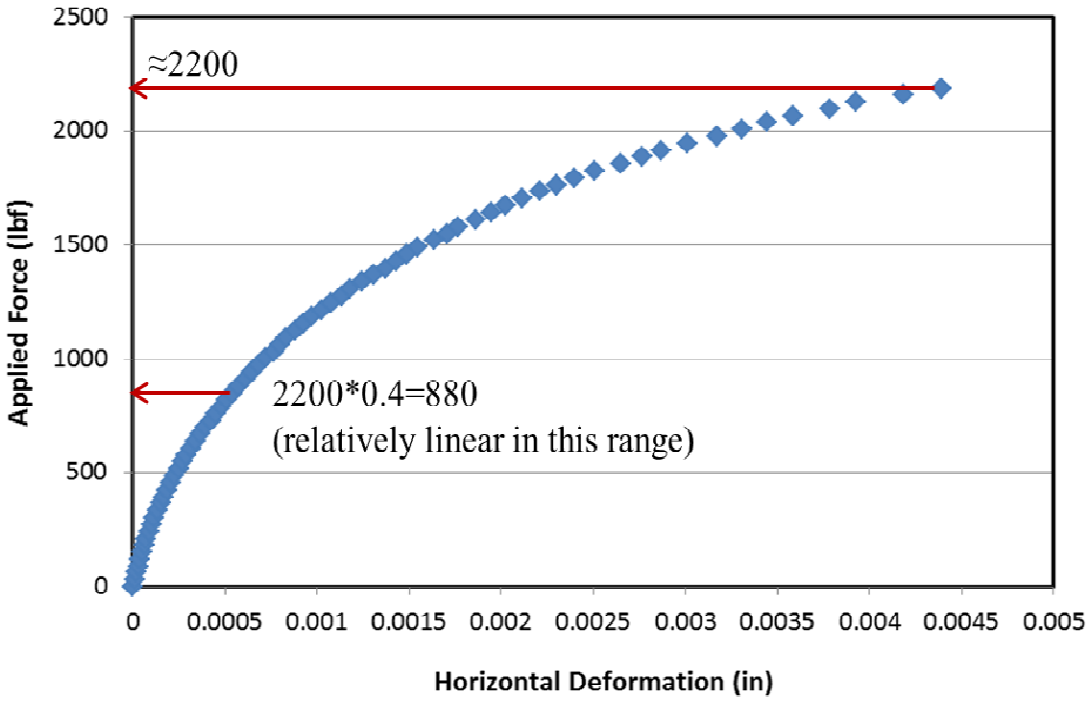

Figure 4-2. Linearity check for relationship between load and deformation

While the load level should be in the linear range, this does not necessarily ensure an appropriate load level has been chosen. From a practical point of view, loads too high may result in excessively high rates of damage which would make testing difficult to control and results hard to analyze. In addition, high loads might also lead to stress concentration at the loading strip which may result in failure in the loading strip region (Varadhan, 2004). On the other hand, loads too low in amplitude might result in excessively long testing times to induce the same amount damage.

One need also consider the stiffness or brittleness of the asphalt mixture. Brittle materials or materials tested at low temperatures will exhibit lower strain at failure than more ductile materials or those tested at high temperatures, which mean these materials may not be able to sustain loads of great magnitude.

4.3.3 Rest Period Duration

The standard Superpave IDT resilient modulus test uses a haversine wave with a 0.1-second load pulse followed by a 0.9-second rest period. It is important however that rest period duration be studied because rest period can have a huge effect on healing. Shorter rest periods may result in high damage rates, while longer rest periods will yield relatively long testing times. From a practical point of view, the most effective rest period duration should be long enough to allow recovery of most of the delayed elasticity, yet be short enough to minimize healing during the damage phase. Rest periods lasting 0.1, 0.4, and 0.9-second were examined to see their effect on healing as shown in Figure 4-3.

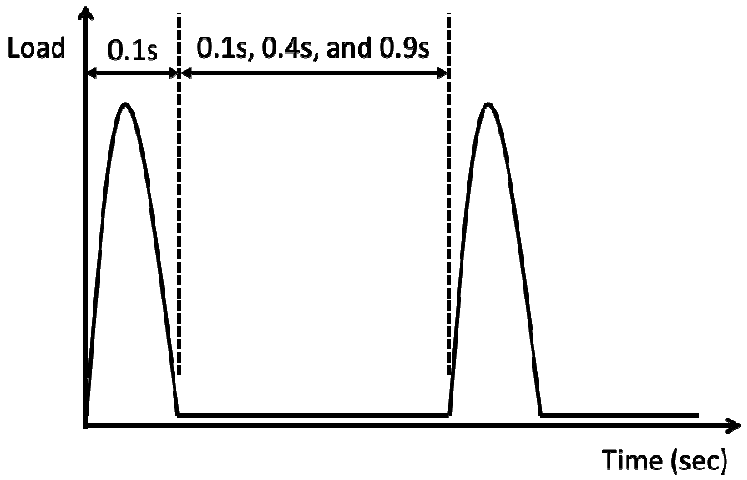

Figure 4-3. Load level and rest period duration

4.4 Modified Brittleness Index

It is postulated that determination of an appropriate load level to induce damage in an asphalt mixture might depend on the brittleness of the mixture. Traditionally, in the field of rock mechanics, a reversible energy based approach is used to determine brittleness. The brittleness index (I_B) used in rock mechanics, is a ratio of the specific elastic energy (S) accumulated in the material up to the point of fracture and the total specific energy (W) dissipated due to deformation up to the point of failure. This concept is illustrated in Figure 4-4 (a) and in the following equation:

$$I_B = \frac{reversible\ energy}{total\ energy} = \frac{S}{W} = \frac{Area\ DCE}{Area\ OABCE}$$

This concept can be applied to asphalt mixture by using parameters from the HMA fracture mechanics model developed at the University of Florida (see Figure 4-4 (b)). Using

these parameters, the above equation can be rewritten while still retaining the meaning of its original form. Rewritten, the new brittleness index is defined as follows:

$$I_{B,HMA} = \frac{EE}{FE} = \frac{FE - DCSE}{FE}$$

where,
$I_{B,HMA}$ = the brittleness index based the HMA fracture mechanics model;
EE = the elastic energy;
FE = the fracture energy; and
DCSE = the dissipated creep strain energy.

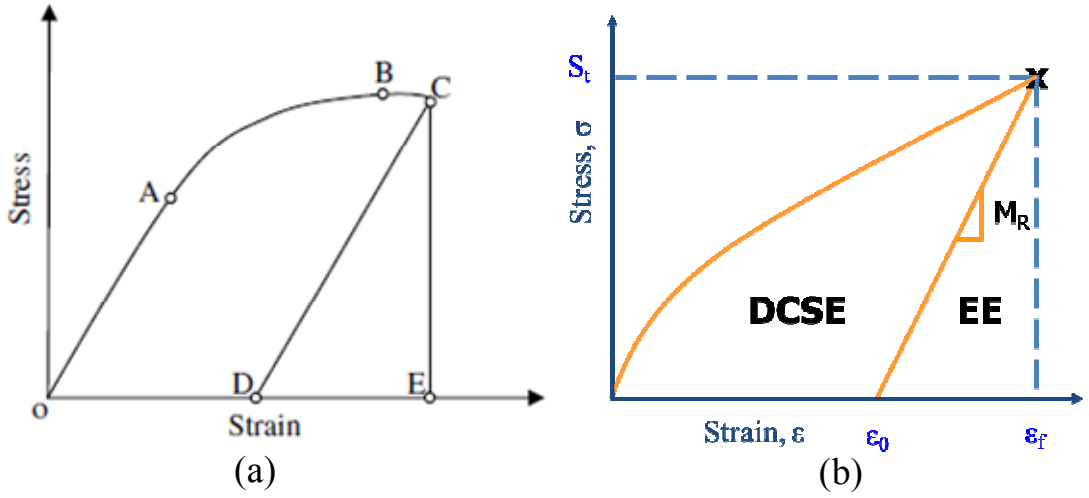

Figure 4-4. Illustration of (a) brittleness index and (b) brittleness index based on HMA fracture mechanics

Figure 4-5 shows the brittleness index based on the HMA fracture mechanics model ($I_{B,HMA}$) for 24 mixture combinations used in this study. The data was ranked from highest $I_{B,HMA}$ to lowest $I_{B,HMA}$. However, no trend seems to emerge from the data. For example, one would expect that brittle materials or low temperature materials would exhibit higher values of brittleness index while more ductile materials or high temperature materials would exhibit lower

values brittleness index. When looking at the figure though, the data seems to be scattered. This inconsistency seems to indicate that the energy-based approach is not appropriate to properly rank asphalt mixture brittleness versus temperature. Consequently, a second approach had to be developed.

Figure 4-6 illustrates typical strength versus failure strain curves for asphalt mixtures. From this plot, it can be said that Mixture 1 is more brittle than Mixture 2. This is based on the observation that strength is higher and failure strain is lower as test temperature is reduced; therefore, a new brittleness index called the modified brittleness index (I_{MB}) was proposed. The I_{MB} is the secant slope of the stress-strain curve as illustrated in Figure 4-7 and is defined below:

$$I_{MB} = \frac{Strength\ (kPa)}{Failure\ Strain\ (\mu\varepsilon)}$$

Figure 4-8 shows ranking of the mixtures used in this study using the modified brittleness index (I_{MB}). As can be seen in the figure, this approach is capable of separating the brittleness of asphalt mixture with temperature with the exception of two data points (OML20 and DMS10). Based on these results, it is thought that this approach is more appropriate for assessing the brittleness of asphalt mixtures. For initial trial testing for appropriate loading level, the asphalt mixture was categorized into three distinct groups based on I_{MB}. These groups were labeled: brittle, medium, or ductile (shown in Figure 4-8). The initial loading level was adjusted according to modified brittleness index and knowledge from tests ran. When labeling mixtures, the following nomenclature was used: O (open-graded), D (dense-graded), M (modified binder), U (unmodified binder), R (asphalt rubber binder), L (LOTA), S (STOA), 00 (0°C), 10 (10°C), and 20 (20°C).

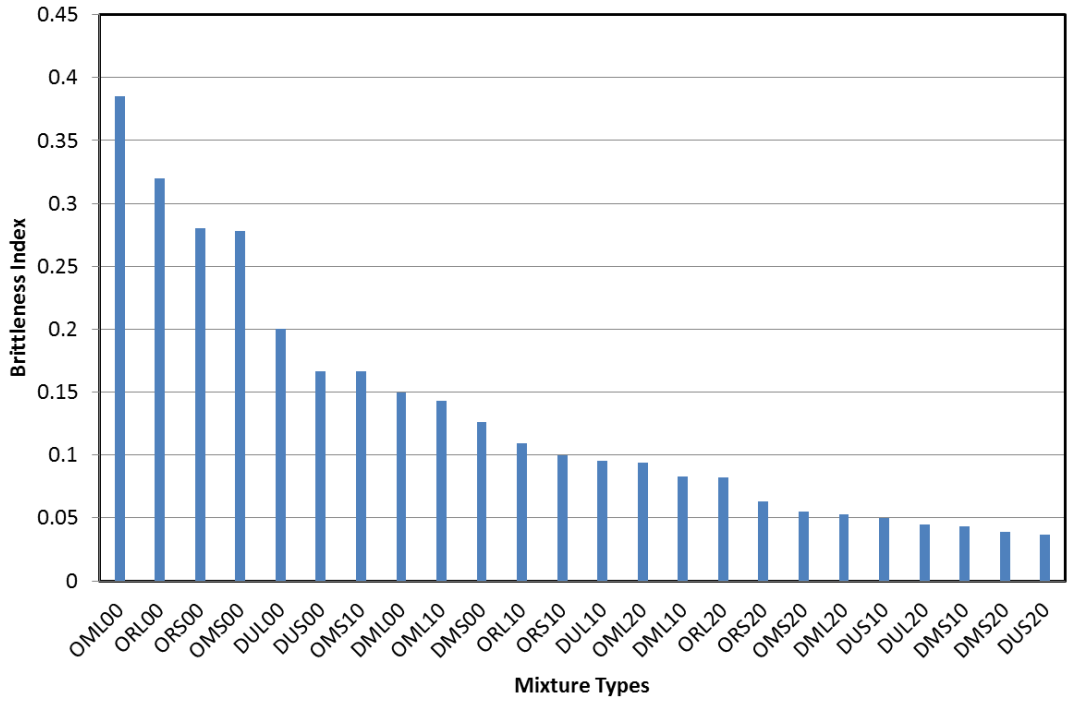

Note: O- open-graded, D- dense-graded, M- modified binder (PG 76-22), U- unmodified binder (PG 67-22), R- asphalt rubber binder (ARB-12), L- long term oven aging, S- short term oven aging, 00- test temperature 0°C, 10- test temperature 10°C, and 20- test temperature 20°C

Figure 4-5. HMA fracture mechanics-based brittleness index

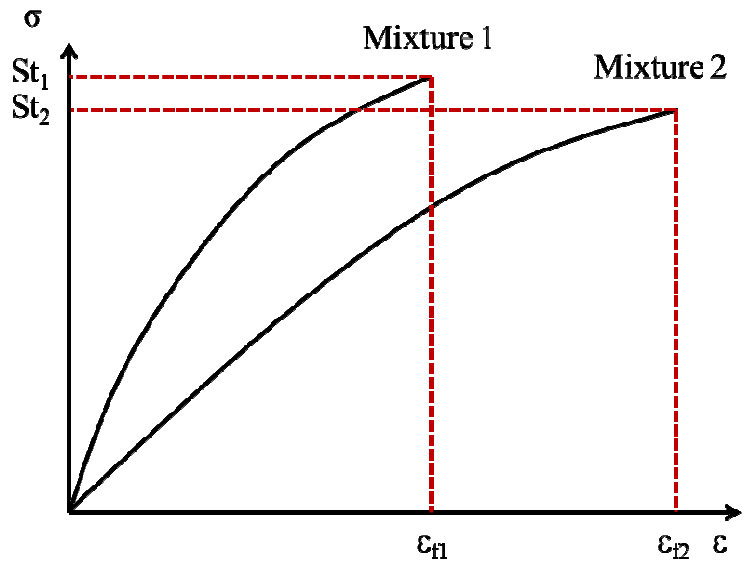

Figure 4-6. Comparison of brittleness for two asphalt mixtures

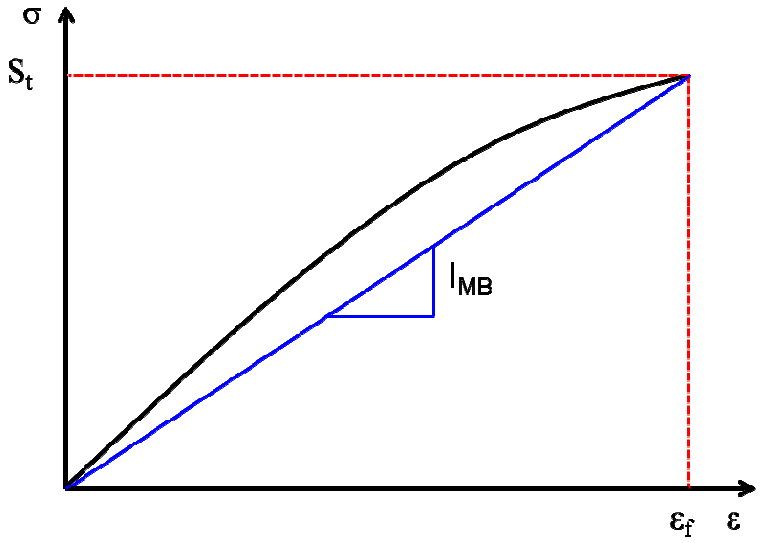

Figure 4-7. Illustration of modified brittleness index

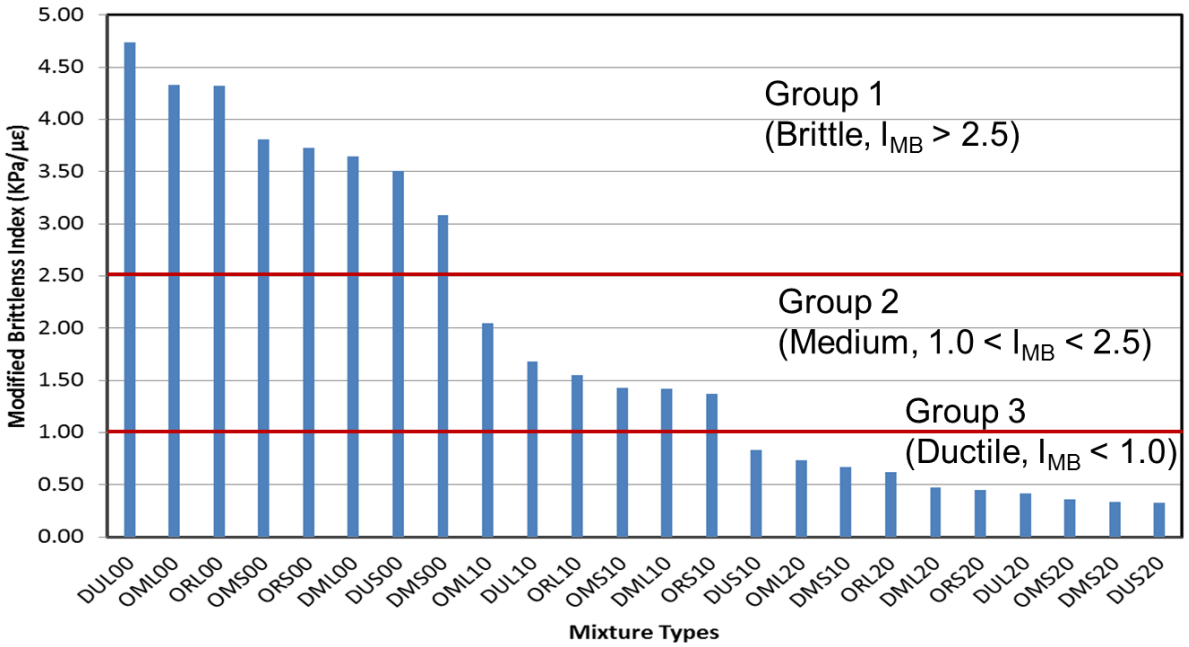

Note: O- open-graded, D- dense-graded, M- modified binder (PG 76-22), U- unmodified binder (PG 67-22), R- asphalt rubber binder (ARB-12), L- long term oven aging, S- short term oven aging, 00- test temperature 0°C, 10- test temperature 10°C, and 20- test temperature 20°C

Figure 4-8. Ranking asphalt mixtures with modified brittleness index

Standard Superpave IDT tests preceded the healing tests. The Superpave IDT tests were performed on all asphalt mixtures as they provided essential properties which were used for the purpose of determining loading functions for damage and healing. Results for the IDT tests can be found in Appendix C. Next, appropriate loading levels and rest period were determined and validated. Lastly, healing tests were performed on all asphalt mixtures. A detailed schematic of this process is presented in Figure 4-9.

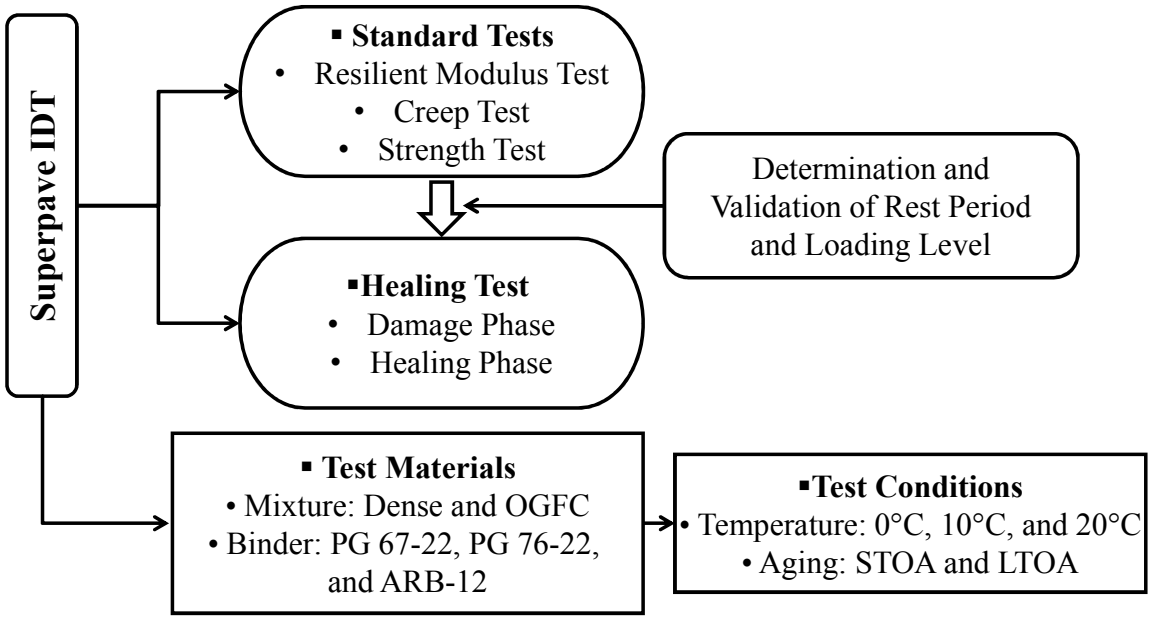

Figure 4-9. Schematic of testing plan

4.5 Determination and Validation of Rest Period and Load Level

During development of a candidate testing procedure for the healing test, it was felt that determination of appropriate load levels and rest periods for use during the damage phase of the healing test would be a challenge. Determination of appropriate load levels and rest periods should result in development of significant damage within the steady-state damage range. However, load levels and rest periods selected should not result in excessively high accumulation of damage, as this makes testing difficult to control. On the other hand, load levels should not be too low and rest periods too long as to create excessively long testing times. Additionally, damage is likely mixture dependent, so it is possible that damage criteria should be dependent on specific mixture characteristics. As is discussed in the following sections, many of these factors will in fact interact with one another, making it difficult to examine their effects separately.

4.5.1 Determination of Rest Period Duration

As stated previously, determination of an appropriate load level and rest period should result in development of significant damage within the steady-state damage range (see Figure 4-1). Figure 4-10 shows normalized resilient deformation for a typical STOA mixture with a 0.9-second rest period, which is traditionally used in the resilient modulus test. As seen in the figure, regardless of load level, resilient deformation remains more or less constant during damaging. This implies that not only does the 0.9-second rest period allow enough time for recovery of delayed elasticity, but allows enough time for complete healing of the asphalt mixture. To illustrate further, even when loading amplitude was increased from 30% to 50% of the strength, horizontal deformation remained constant with time through 60 min of loading, indicating no damage had accumulated during the "damage" phase. These results indicate that the 0.9-second rest period is inappropriate, as it allows for complete healing of the induced microdamage during the "damage" phase. This is undesirable, as the entire point of the damage phase is to damage the asphalt material.

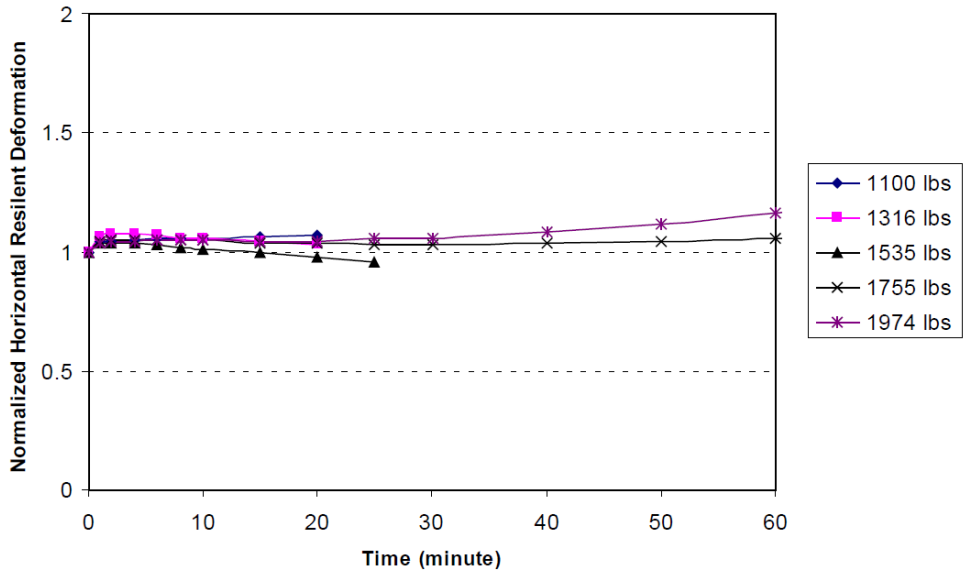

Figure 4-10. Normalized resilient deformation for a 0.9-second rest period with different load levels

Figure 4-11, which shows results of tests for the same mixture, indicated that significant damage was accumulated when shorter rest periods were used. Based on these results, it appears that the shortest rest periods (0.1 and 0.2-second) result in excessively rapid damage development, which would make it difficult to maintain microdamage within the steady-state damage range. Also, the shorter the rest period, the greater the accumulation of delayed elasticity during the damage phase. In this study, damage is characterized by reduction in effective stiffness, which can be measured by changes in resilient modulus. Resilient modulus is in turn affected by recovery of delayed elasticity. The more accumulated delayed elasticity in the specimen, the greater the error in resilient modulus, and thus the greater the error in characterizing damage.

As compared to the 0.1 and 0.2-second rest periods, the 0.4-second rest period resulted in more controllable damage development and a longer steady-state damage range. For instance, it took about 20 min with a loading level of 45% of the strength to reduce effective stiffness by 30%. Ideally, the most effective rest period duration should be long enough to allow recovery of most of the delayed elasticity, yet be short enough to minimize healing during the damage phase.

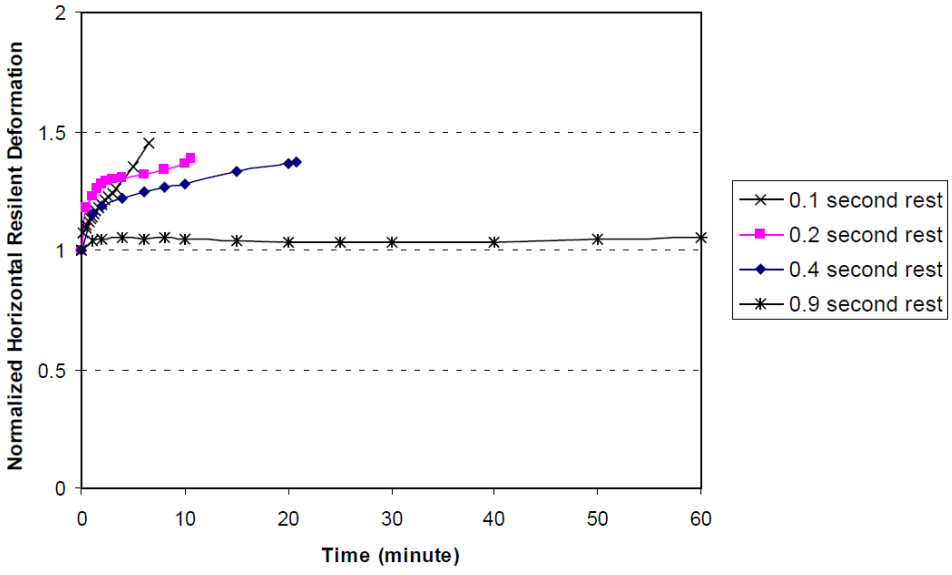

Figure 4-11. Normalized resilient deformation for different rest periods (45% of Strength, 1755 lb)

4.5.2 Determination of Load Level

Several potential approaches to determine appropriate load levels for damage and healing tests were considered including failure strain (ε_f), FE, DCSE and strength (S_t). The percent of strength approach was selected as the most practical approach because of the consistency and simplicity of interpretation of strength test results.

A percent of the ultimate load from the standard Superpave IDT strength test is a practical starting point to proceed in determining appropriate loading levels. The strength value and Poisson's ratio from these tests are used for determination of an appropriate applied force. Since dimensions will vary from specimen to specimen, strength values are corrected using the following equations:

$$P_{applied} = \frac{S_t \cdot \pi \cdot d \cdot t}{2 \cdot CSX} \cdot A$$

$$CSX = 0.9480 - 0.01114\left(\frac{t}{d}\right) - 0.2693(\nu) + 1.4360\left(\frac{t}{d}\right)(\nu)$$

where,
$P_{applied}$ = load to be applied in lb;
S_t = the strength from strength test in psi;
d = the diameter of the specimen in inches;
t = thickness of the specimen in inches;
A = percentage of strength;
ν = Poisson's ratio from the strength test; and
CSX = a stress correction factor.

It should be noted that Poisson's ratio of the asphalt mixture is unknown before performing damage phase testing. According to previous research done by Li (2009), the Poisson's ratio from the strength test is similar to that obtained from the repeated loading mode; therefore, this value will be used for the damage phase.

Recall, that for load level to be considered appropriate, it should result in development of significant damage within the steady-state range (see Figure 4-1). If load amplitude is selected such that it is in the linear range, the material response will be stress-state independent. For convenience, to check linearity, resilient moduli were determined at different loading levels. If the resilient moduli are more or less constant, then load level is within the linear damage range. An example is shown in Figure 4-12.

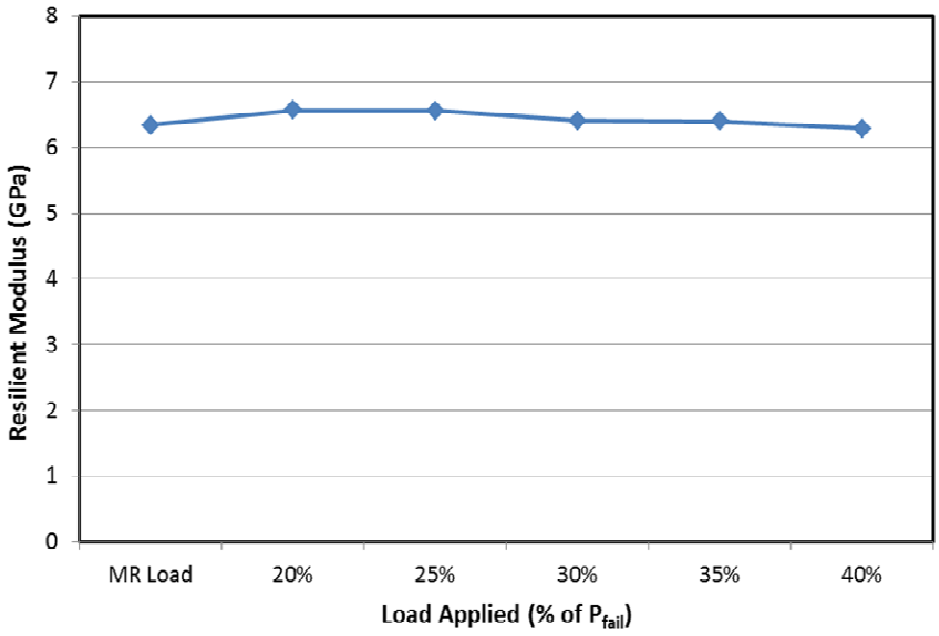

Figure 4-12. Linearity check for ductile group

4.5.3 Validation of Rest Period and Load Level

For initial trial testing, repeated load damage tests were performed on asphalt mixtures encompassing a range of brittleness, load level, and rest period to identify appropriate load levels and rest periods for use during the damage phase of the healing test. Asphalt mixtures were categorized into three distinct groups based on modified brittleness index (I_{MB}). These groups

were labeled brittle, medium, and ductile as shown in Table 4-1. Two mixtures from each of these three groups (see Figure 4-13) were selected to determine appropriate load levels and rest periods for the damage phase of the healing test. Loading levels and rest periods for initial trial testing for these six mixtures are shown in Table 4-2.

Table 4-1. Grouping of asphalt mixture using modified brittleness index

Group	Mixture Condition	Modified Brittleness Index (I_{MB})	Initial Loading Level
Group 1	Ductile	$I_{MB}<1.0$	20% to 40% of P_{fail}
Group 2	Medium	$1.0<I_{MB}<2.5$	25% to 50% of P_{fail}
Group 3	Brittle	$I_{MB}>2.5$	30% to 50% of P_{fail}

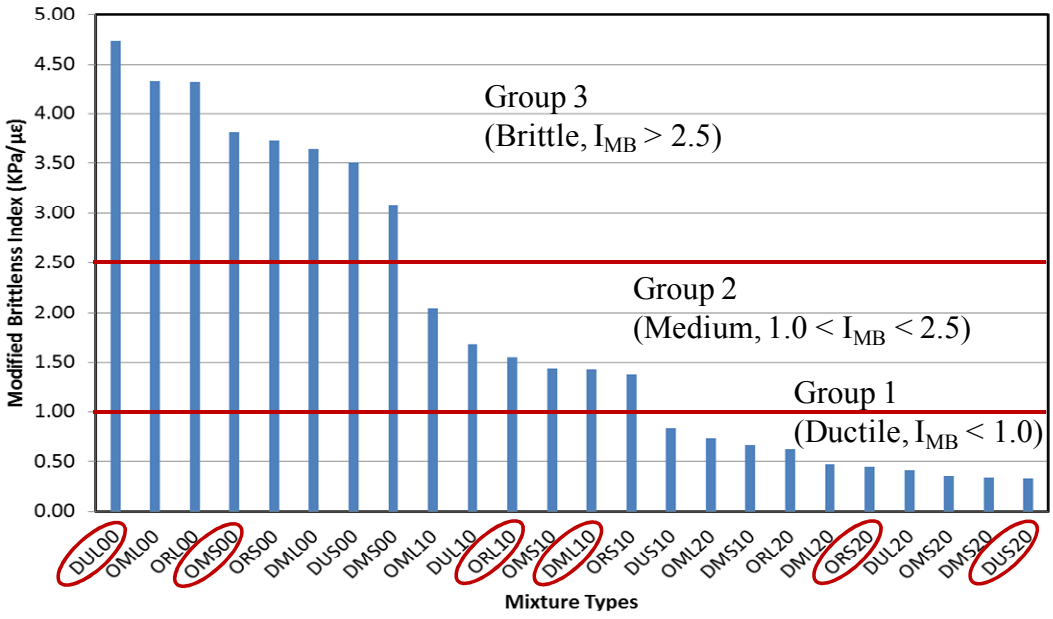

Figure 4-13. Selection of mixtures based on modified brittleness index

Table 4-2. Loading level and rest periods for initial testing

Rest Period	Mix Condition	Mixture Types		Loading Level (% of Strength)				
0.9 sec	Ductile	DUS20	ORS20	0.2	0.25	0.3	0.35	0.4
	Medium	DML10	ORL10	0.4	0.45	0.5	0.55	0.6
	Brittle	DUL00	OMS00	0.6	0.65	0.7	0.75	0.8
0.4 sec	Ductile	DUS20	ORS20	0.2	0.25	0.3	0.35	0.4
	Medium	DML10	ORL10	0.4	0.45	0.5	0.55	0.6
	Brittle	DUL00	OMS00	0.6	0.65	0.7	0.75	0.8
0.1 sec	Ductile	DUS20	ORS20	0.2	0.25	0.3	0.35	0.4
	Medium	DML10	ORL10	0.4	0.45	0.5	0.55	0.6
	Brittle	DUL00	OMS00	0.6	0.65	0.7	0.75	0.8

Figures 4-14 through 4-21 show changes in normalized effective modulus for repeated damage tests performed on the dense-graded (D), unmodified (U), short-term oven aged (S) mixture tested at 20°C (20). Here, normalized effective modulus refers to normalized resilient modulus. In general, results were in good agreement with expected trends. Figures 4-16 and 4-21 clearly indicate that higher load levels and/or shorter rest periods result in greater reduction of effective modulus. It was also observed that higher load levels and/or shorter rest periods caused more heating and reversal of steric hardening. It would be difficult to separate these effects from the actual microdamage induced. Also, from a practical point of view, as shown in Figures 4-16, 4-20, and 4-21, higher load levels and/or shorter rest periods may result in excessively high damage rates which would make testing difficult to control and results hard to analyze. Of particular concern with shorter rest periods is that of delayed elasticity. With shorter rest periods, the delayed elastic response is not given ample time to recover. This results in an underestimation of resilient modulus. Ideally, the rest period should be long enough to allow most of the delayed elasticity to recover, yet short enough to minimize healing while inducing damage.

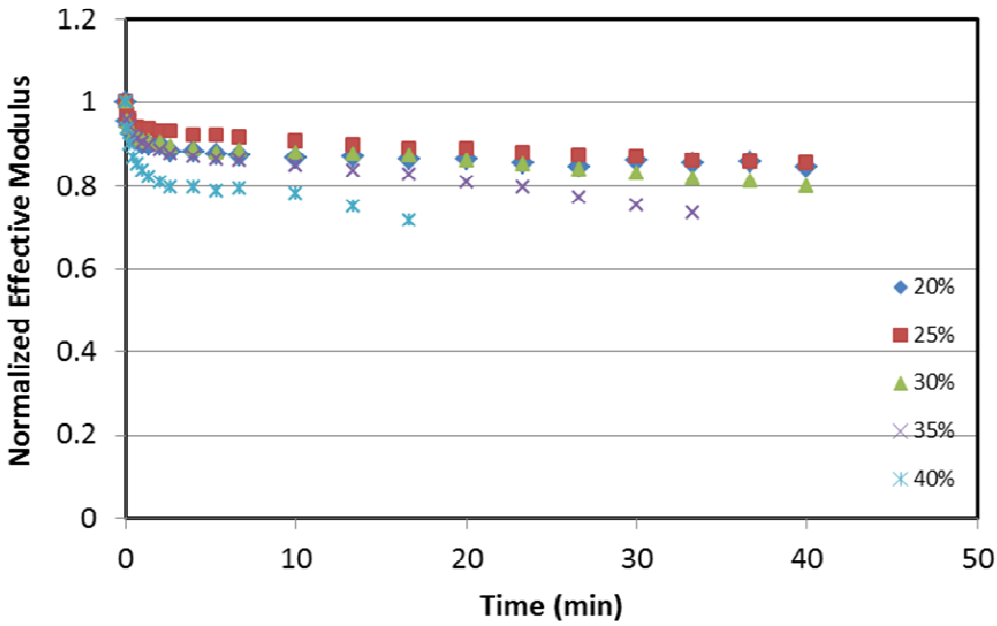

Figure 4-14. Effect of loading amplitude with 0.9-second rest period (DUS20)

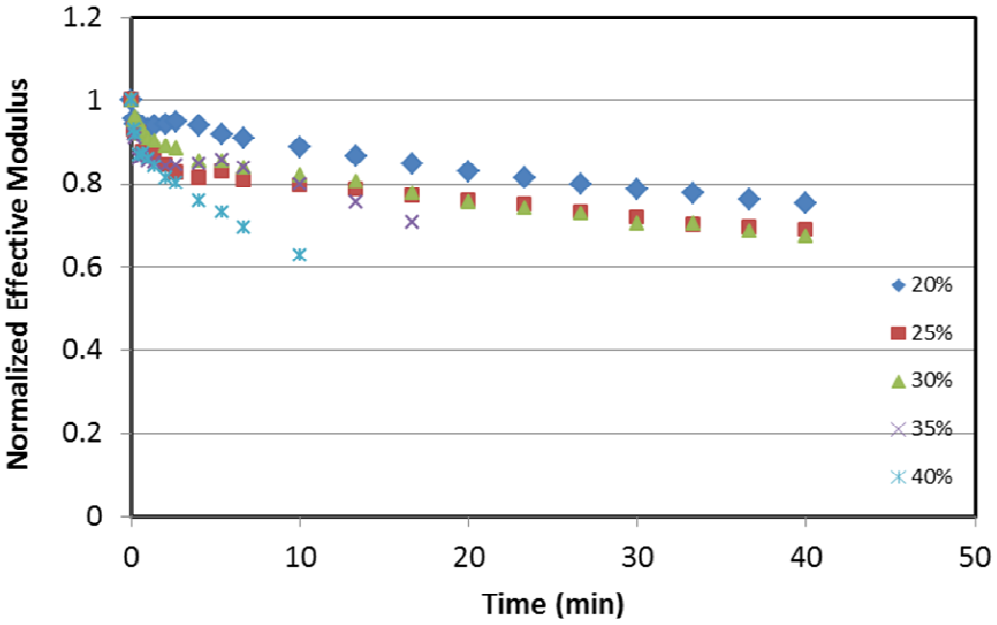

Figure 4-15. Effect of loading amplitude with 0.4-second rest period (DUS20)

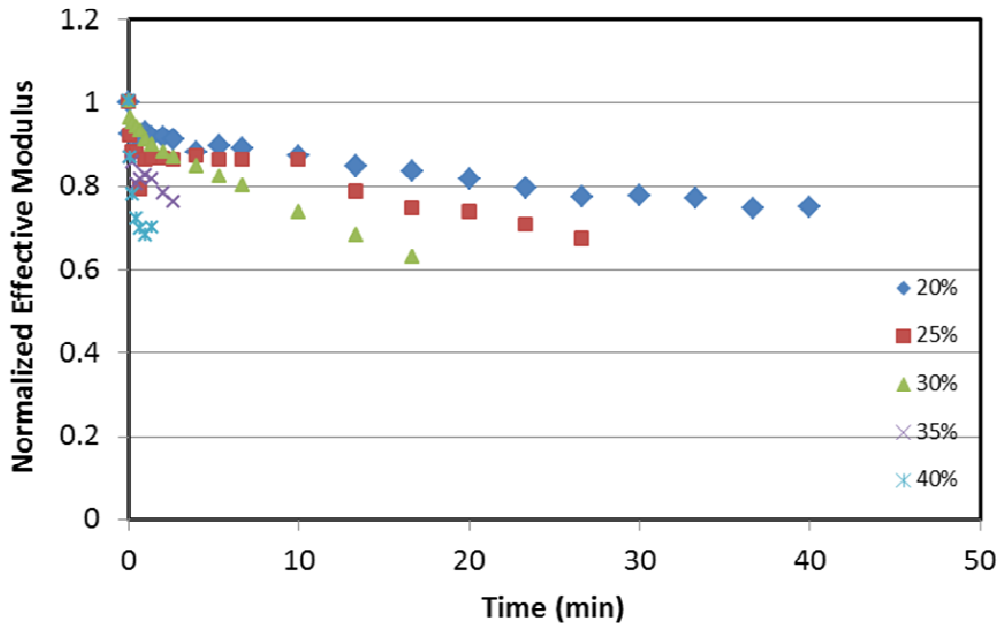

Figure 4-16. Effect of loading amplitude with 0.1-second rest period (DUS20)

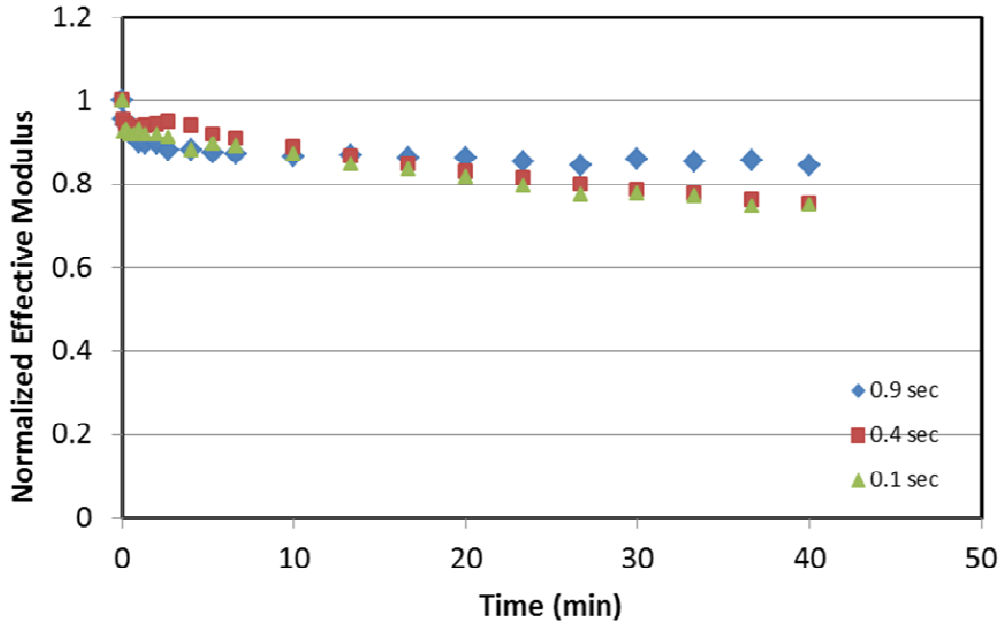

Figure 4-17. Effect of rest period with 20% loading of P_{fail} (DUS20)

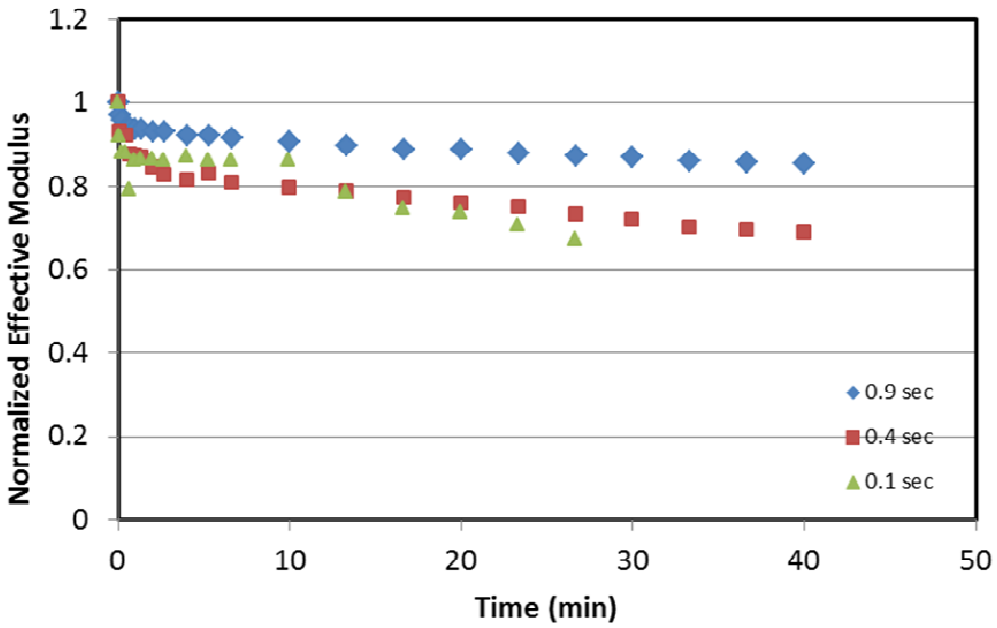

Figure 4-18. Effect of rest period with 25% loading of P_{fail} (DUS20)

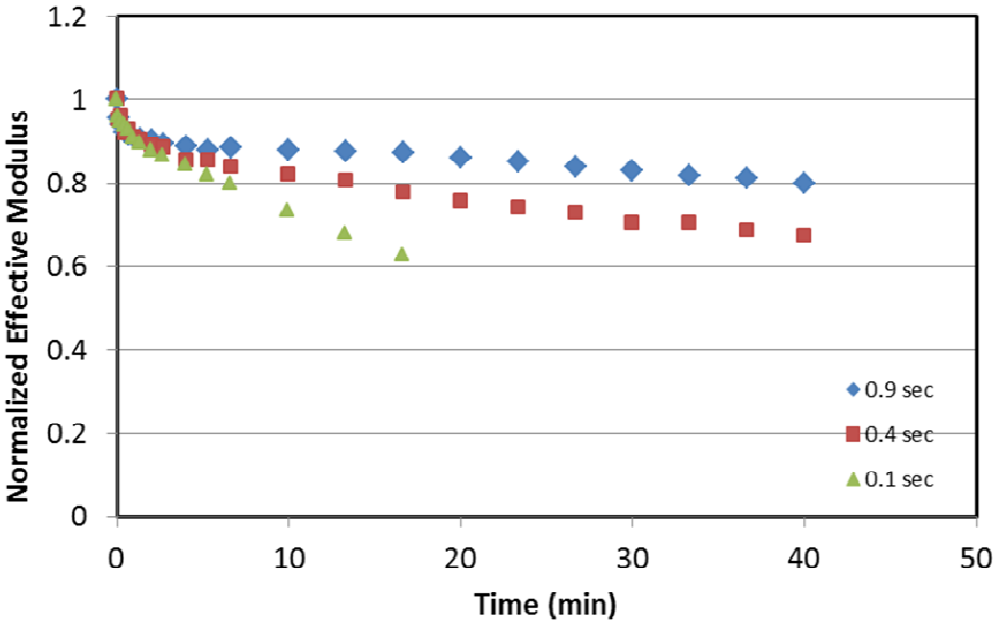

Figure 4-19. Effect of rest period with 30% loading of P_{fail} (DUS20)

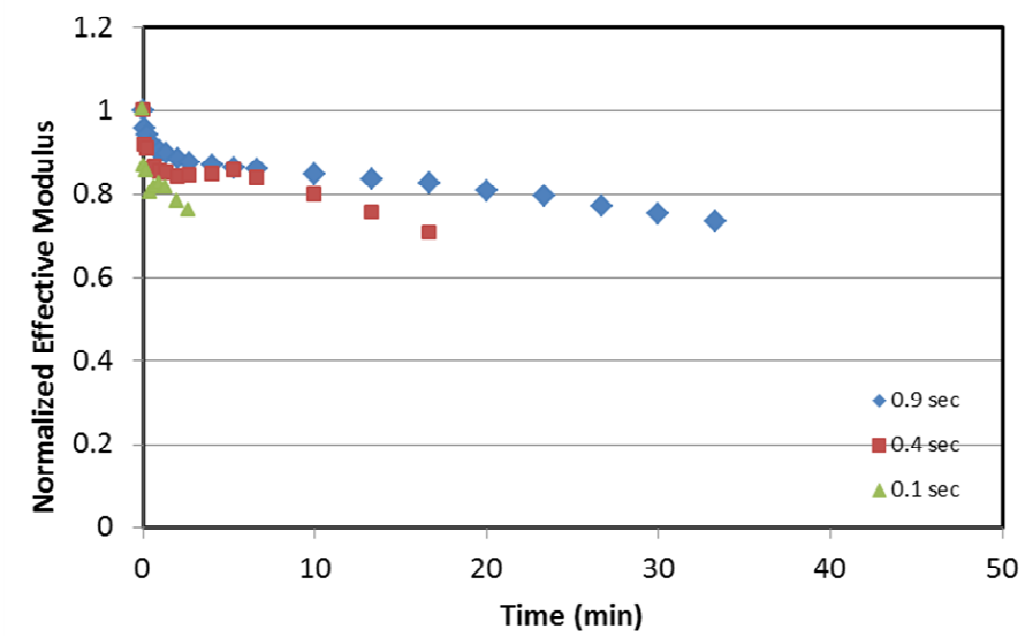

Figure 4-20. Effect of rest period with 35% loading of P_{fail} (DUS20)

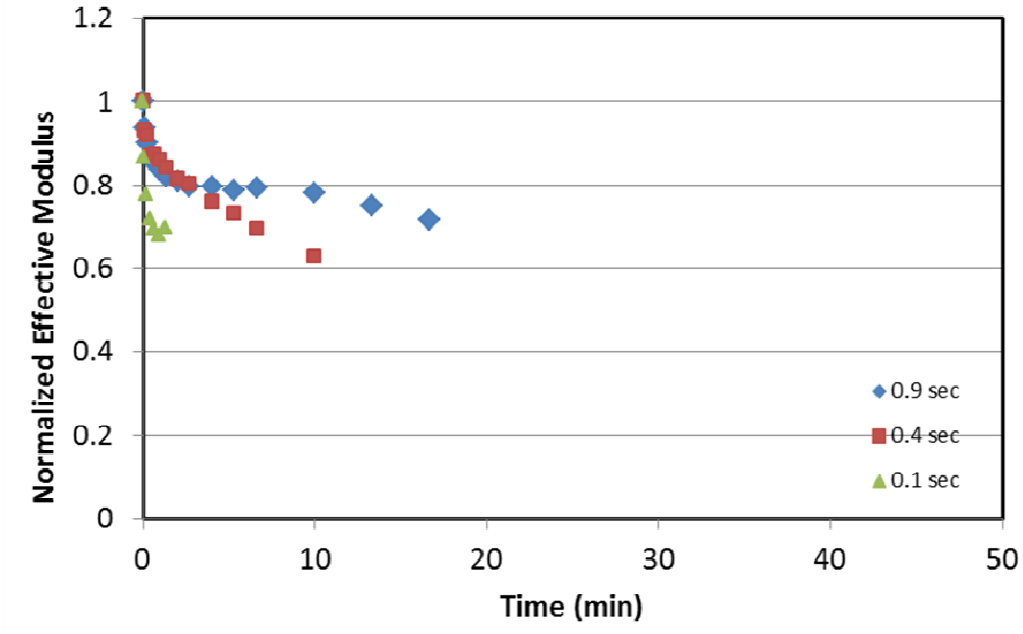

Figure 4-21. Effect of rest period with 40% loading of P_{fail} (DUS20)

In contrast, as can be seen in Figures 4-14 and 4-17, the use of lower load levels and/or longer rest periods could potentially yield relatively long test times, which is undesired. That is, in using longer rest periods, it may take longer to induce proper amounts of damage in the asphalt mixture. Figure 4-14 shows that the 0.9-second rest period yielded similar reduction in effective modulus for loading levels of 25% and 30% of the load at failure, P_{fail}. This appears to be evidence that during longer rest periods, healing is occurring and is having a dominant effect on response.

Based on the results of the six mixtures tested, it was concluded that a 0.4-second rest period is appropriate during the damage phase for all asphalt mixtures. With the 0.4-second rest period, delayed elasticity is not a problem and testing times are not terribly long. At the time, load levels of 25%, 30%, and 45% of P_{fail} were thought to be appropriate for the ductile, medium, and brittle groups, respectively. Upon further examination though, it was discovered that there appeared to be a linear relationship between modified brittleness index and load level for the six mixtures tested, as shown in Figure 4-22. Using this relationship, additional damage tests were performed on various mixtures (those other than the six previously tested). However, it was found that the relationship did not always hold. For instance, load levels given by the relationship sometimes resulted in fracture of the asphalt concrete specimen. Other times, load levels given by the relationship did not induce enough microdamage. As a result, the relationship was used only as a general guide in selecting appropriate loading levels. Depending of the mixture at hand, load levels may have had to be adjusted up or down. Eventually, this technique was done for all 24 mixtures (see Figure 4-13). Once this was accomplished for all mixtures, it was discovered that the relationship between modified brittleness index and load level was in fact logarithmic, not linear as previously thought. The new relationship is shown in Figure 4-23

for the dense-graded mixture and Figure 4-24 for the open-graded mixture. For all mixtures tested, this relationship holds. Load levels given by the relationship do not necessarily result in the same damage rate for all mixtures, but sufficient damage is induced, that being, 10% - 25% reduction in resilient modulus.

It should be noted that mixtures with high brittleness index are much more sensitive to changes in load than those with low modified brittleness index. For instance, it is very likely that a mixture with $I_{MB} = 0.5$ could be tested at 40% of P_{fail} and not result in failure. The only difference would be a greater reduction in modulus. However, if a mixture with $I_{MB} = 4.5$ were tested at 45% of P_{fail}, it is very likely that it would fail. Recall, once a micro-crack becomes a macro-crack, it is no longer healable. As a result, to ensure sufficient reduction in resilient modulus, it is recommended that mixtures with high I_{MB} values be tested at 40% of P_{fail} or below and mixtures with low I_{MB} values be tested at 20% of P_{fail} or above. If a specific reduction in resilient modulus is desired, load levels should be adjusted as necessary.

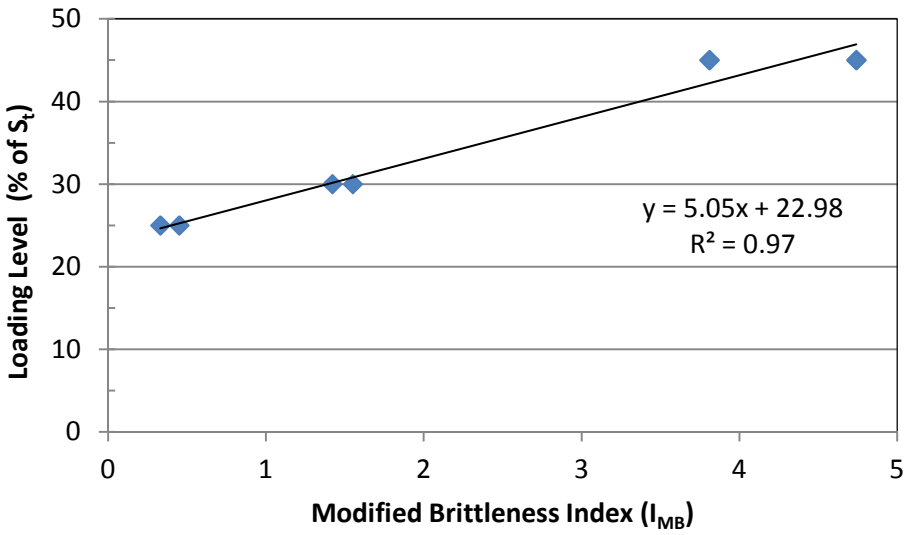

Figure 4-22. Original modified brittleness index vs. loading level relationship

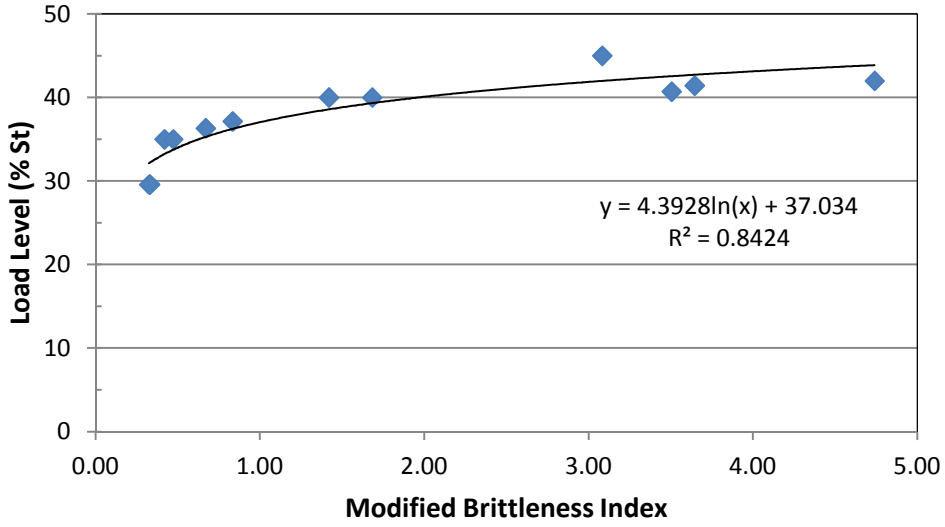

Figure 4-23. Final modified brittleness index vs. loading level (dense-graded)

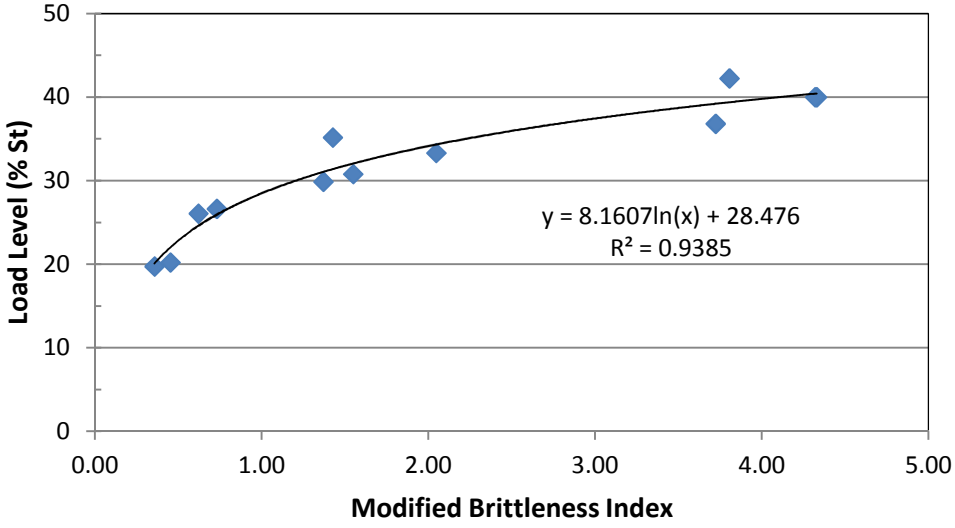

Figure 4-24. Final modified brittleness index vs. loading level (open-graded)

4.6 Data Acquisition

To adequately observe changes in effective modulus, it is imperative that data is acquired at a sufficient rate. When running the standard Superpave resilient modulus test, data is acquired at a rate of 500 points per cycle. This is based on a load cycle duration of 1.0 second (0.1-second load period, 0.9-second rest period). For the developed healing test, a 0.1-second load period and a 0.4-second rest period, for a total load cycle duration of 0.5 second, was found to be an appropriate loading procedure. Since this reduced the load cycle duration from 1.0 second to 0.5 second, data is acquired at a rate of 1000 points per second or 500 points per cycle.

Data acquisition occurs for both the damage phase and healing phase, separately. During the damage phase, repeated loading is continuous, but it is unnecessary to record every load cycle. So, data is recorded for six consecutive loading cycles at the times specified in Table 4-3. During the healing phase, load is only applied at discrete times as a means of obtaining effective modulus. Thus, data is only acquired and recorded at these times which are shown in Table 4-4. To deemphasize the minimal healing effect at longer healing times, data is acquired at times such that they are more or less equally spaced apart on natural log scale.

Table 4-3. Data acquisition times for damage phase

Acquisition	1	2	3	4	5	6	7	8	9	10
Time(sec)	0.67	6.67	13.3	26.67	40	60	80	120	160	240
Acquisition	11	12	13	14	15	16	17	18	19	
Time(sec)	320	400	600	800	1000	1200	1400	1600	1800	

Table 4-4. Data acquisition times for healing phase

Acquisition	1	2	3	4	5	6	7	8
Time(sec)	10	30	60	120	300	600	1200	1800

4.7 Healing Test

The developed healing test consists of two phases: a damage phase and a healing phase. For purposes of practicality, each phase was limited to 30 min, but there are no restrictions on testing time as long as enough time has been given to induce proper damage during the damage phase and recover the damage during the healing phase. During the damage phase, loading is continuous while during the healing phase, load is applied only at specified times to obtain resilient modulus measurements. The overall healing test is illustrated in Figure 4-25.

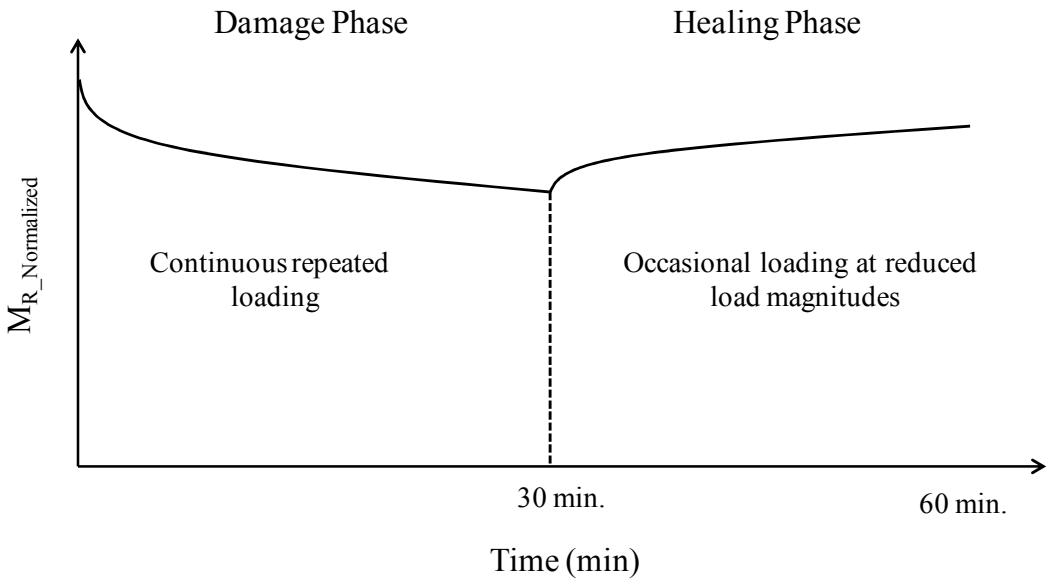

Figure 4-25. Healing test

Goals of the damage phase are summarized below:

- Want sufficient damage to evaluate healing effect
- Want to be in the linear damage range (i.e., no induced macrodamage)
- Want little or no healing during rest periods
- Want little delayed elasticity
- Want the shortest testing time possible

Goals of the healing phase are summarized below:

- Want little or no damage during healing phase
    - Decrease load level by 5%
    - Apply load only to obtain MR
- Want the shortest testing time possible

Testing protocol along with data analysis and interpretation methods are covered in subsequent chapters.

CHAPTER 5
TESTING PROTOCOL AND DATA INTERPRETATION

5.1 Overview

Healing test (including damage phase and healing phase) protocol is covered in this chapter. This protocol mainly includes testing procedure and data acquisition and interpretation. Standard Superpave IDT will be used in this research. The apparatus needed and specimen preparation procedures used by Roque et al. (1997b) are employed here.

Standard Superpave IDT tests (resilient modulus, creep, and strength tests) will precede the healing tests on materials to be evaluated. They will provide essential properties, which will be used for the purpose of determining load magnitudes for damage and healing phases.

5.2 Testing Procedure

The testing procedures are summarized in the following steps:

- Superpave IDT specimens were prepared following procedures in Roque et al. (1997b).
- Brass gauge points (5/16-inch diameter by 1/8-inch thick) were affixed with epoxy to each specimen face. Specimens were stored in a cabinet at a constant relative humidity of 50 percent for 3 days prior to testing to ensure uniform moisture conditions. Specimens were cooled at the test temperature for at least 3 hours before the test. Four extensometers, two on each face of the specimen, were mounted at a distance of 1.5 inch.

- The test specimen was placed into the Superpave IDT loading frame. A seating load of 10 pounds was applied to the test specimen to ensure proper contact between the specimen and loading heads.
- The specimen was then loaded by applying a repeated haversine load with 0.1-second loading and 0.4-second rest period for 30 min to induce damage to the specimen. The load was determined from the loading level versus modified brittleness index relationship as presented in Chapter 4. Test data were recorded by the computer software (data acquisition program) 19 times as shown in Table 4-3. Data was acquired at a rate of 1000 points per second for 6 loading cycles.
- The specimen was then unloaded and the healing phase began. Repeated haversine load with 0.1-second loading and 0.4-second rest period were applied onto the specimen for 6 cycles to obtain resilient modulus recovery data. The loading level was reduced by 5% to minimize potential for damage to be induced during the healing phase. Data was recorded at a rate of 1000 points per second 8 times during the 30-min healing phase with intervals shown in Table 4-4.

5.3 Damage Phase Data Interpretation

Resilient modulus is a convenient way to indicate damage and its recovery since repeated haversine load is used through the healing test. Resilient modulus is calculated by using total recoverable deformation (See Figure 5-1), which includes both the instantaneous recoverable and the time-dependent recoverable deformation during the unloading and rest period portion of each loading cycle. It should be pointed out that Poisson's ratio from the standard Superpave IDT resilient modulus test is used instead of the Poisson's ratio measured during the damage and

healing phases. The Poisson's ratio measured throughout the healing test is not reliable because damage is introduced to the specimen.

Typical horizontal strain gauge deformation versus time is presented in Figure 5-1. Once total recoverable deformation is determined, resilient modulus is calculated at 19 times throughout the damage phase (Roque et al. 1997b). Typical resilient modulus during damage phase is shown in Figure 5-2. Results were normalized with the resilient modulus at the beginning of damage phase.

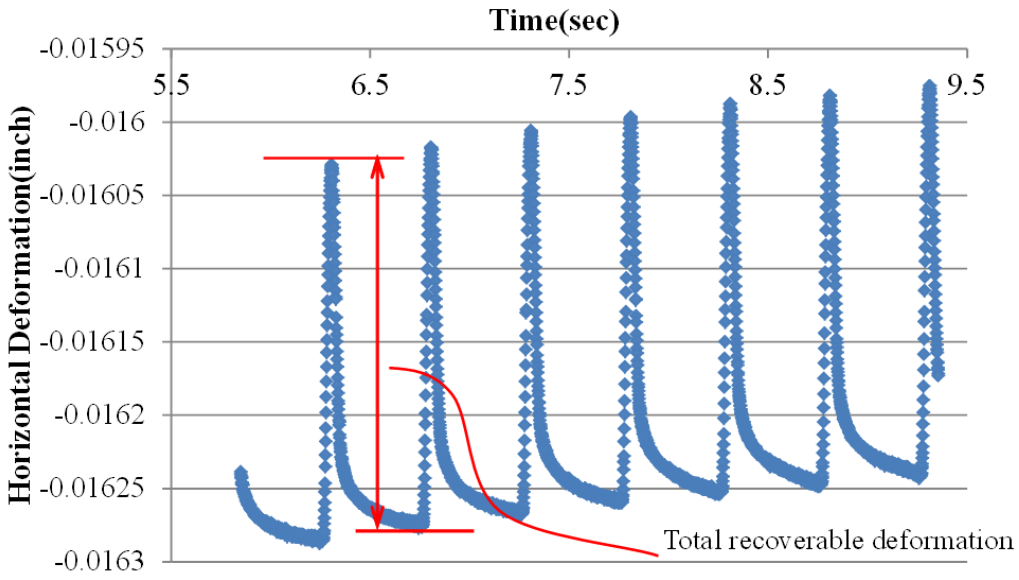

Figure 5-1. Horizontal strain gauge deformation

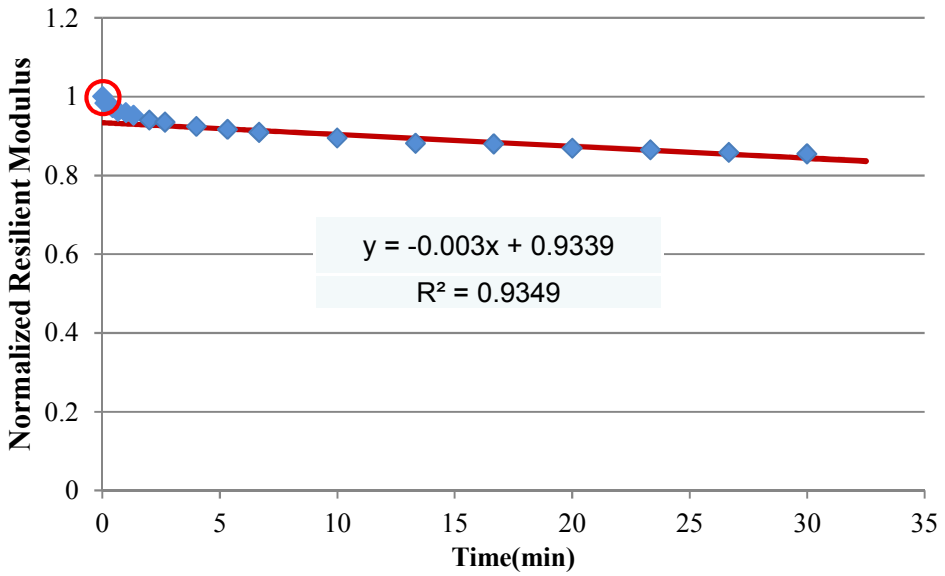

Figure 5-2. Typical normalized resilient modulus vs. time during damage phase

As reported by Grant (2001), mixtures typically stabilized (exhibit linear modulus reduction) after about 2 min of loading. Thus, linear regression analysis was performed on data obtained from 2 min to 30 min. Damage rate is defined as the slope of the regression curve as defined in Figure 5-2. Resilient modulus throughout the damage phase was normalized to the initial resilient modulus. Initial resilient modulus is the value at the very beginning of the test, as shown circled in Figure 5-2. The nonlinear resilient modulus reduction is primarily caused by local elevation of temperature in the specimen and reversal of steric hardening. Since evaluation and quantification of mixture healing is the goal of this project and the damage phase only serves as a tool to introduce damage to the specimen, damage evaluation and quantification will not be covered in this analysis. Damage phase testing results are presented in Appendix D.

5.4 Healing Phase Data Interpretation

For the healing phase, resilient modulus was also normalized to initial resilient modulus. Healing phase testing results are presented in Appendix D. The power model function used in the Superpave IDT creep curve fitting process was selected to describe the healing phase. This power model function is presented in equation 5-1. Typical healing phase data and curve fitting are presented in Figure 5-3. Power model parameters for all 24 mixture combinations as defined in Chapter 4 are presented in Table 5-1.

$$MR(t)=MR_0+MR_1t^m, \quad (5\text{-}1)$$

where,
MR(t)=Normalized resilient modulus at time, t, in healing phase
MR_0= Power model parameter, selected to be the normalized resilient modulus at t=0 in healing phase
MR_1 and m=Power model parameters

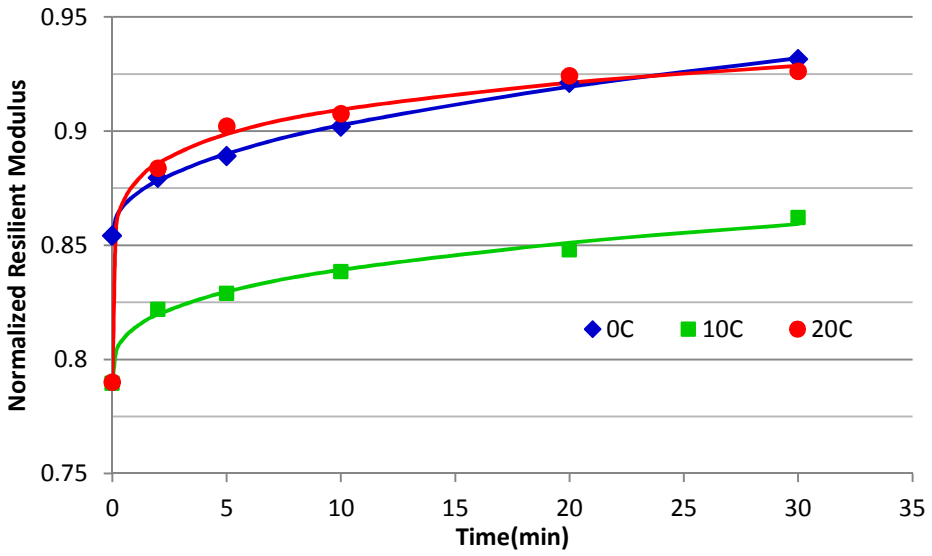

Figure 5-3. Typical normalized resilient modulus vs. time during healing phase

Table 5-1. Power model parameters

Mixture	m	MR_0	MR_1	Mixture	m	MR_0	MR_1
DUS00	0.4211	0.8541	0.0185	OMS00	0.4326	0.8539	0.0144
DUS10	0.2897	0.7895	0.0256	OMS10	0.2641	0.7525	0.0349
DUS20	0.1380	0.7901	0.0956	OMS20	0.1138	0.7189	0.0757
DUL00	0.5367	0.7855	0.0099	OML00	0.4000	0.8386	0.0165
DUL10	0.4410	0.7867	0.0195	OML10	0.2610	0.7560	0.0272
DUL20	0.2860	0.7333	0.0312	OML20	0.0945	0.6875	0.0615
DMS00	0.4122	0.8619	0.0204	ORS00	0.2643	0.8659	0.0283
DMS10	0.2226	0.7012	0.0331	ORS10	0.2161	0.7788	0.0314
DMS20	0.0733	0.8124	0.0202	ORS20	0.0945	0.7229	0.1003
DML00	0.3972	0.7651	0.0204	ORL00	0.2710	0.7953	0.0239
DML10	0.3283	0.6968	0.0267	ORL10	0.2392	0.7518	0.0390
DML20	0.2928	0.7150	0.0226	ORL20	0.0587	0.6716	0.0803

The slope of the healing phase curve (See Figure 5-3) at time t can be obtained through the derivative of the power model function with respect to time as shown in equation 5-2. It was observed that as the resilient modulus of the mixture was being recovered, the slope of the healing phase curve was decreasing. Therefore, it is reasonable to hypothesize that the slope of the healing phase curve will decrease to zero when the mixture is fully healed. In other words, the healing phase curve will become flat when the mixture is fully healed. It was also observed that the healing phase enters steady-state after around 10 minutes as compared with the rapid change in first 10 minutes. The slopes of the healing phase curve at times 10, 20 and 30 minutes were used to predict the normalized undamaged resilient modulus as presented in Figure 5-4.

$$\frac{dMR(t)}{dt} = MR_1 \cdot m \cdot t^{(m-1)} \tag{5-2}$$

where,
MR_1 and m=Power model parameters as defined in equation 5-1

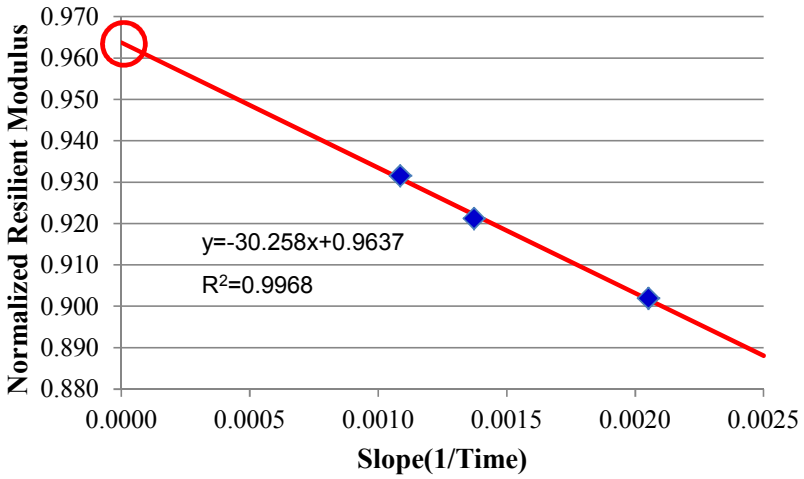

Figure 5-4. Typical normalized resilient modulus vs. slope of healing phase curve

Normalized undamaged resilient modulus can be predicted as the value circled in Figure 5-4. This normalized undamaged resilient modulus value was determined for all 24 mixture combinations and presented in Table 5-2. After the normalized undamaged resilient modulus is determined, the percentage of healing with time can then be calculated using equation 5-3. The percentage of healing can be considered a measurement of how close a particular mixture is to being fully healed. Finally, healing rate is taken as the plot of percentage of healing versus time.

Table 5-2. Undamaged normalized resilient modulus

Mixture	Undamaged MR	Mixture	Undamaged MR	Mixture	Undamaged MR	Mixture	Undamaged MR
DUS00	0.9637	DMS00	0.9662	OMS00	0.9403	ORS00	0.9515
DUS10	0.8770	DMS10	0.7882	OMS10	0.8609	ORS10	0.8561
DUS20	0.9399	DMS20	0.8725	OMS20	0.8261	ORS20	0.8662
DUL00	0.8869	DML00	0.8762	OML00	0.9292	ORL00	0.8746
DUL10	0.8917	DML10	0.7983	OML10	0.8386	ORL10	0.8555
DUL20	0.8326	DML20	0.7912	OML20	0.7705	ORL20	0.7662

$$Percentage\ of\ Healing = \frac{MR(t) - MR_0}{MR_{undamaged} - MR_0} \times 100\% \quad (5\text{-}3)$$

where,

MR(t) = Normalized resilient modulus at time, t, in healing phase

MR_0 = Normalized resilient modulus at time=0 in healing phase

$MR_{undamaged}$ = Undamaged normalized resilient modulus as defined in Figure 5-4

Percentage of healing data for all 24 mixture combinations tested are presented in Appendix E. As can be seen in Appendix E, the healing rate (defined as the slope of percentage of healing versus time curve) is time dependent. The healing rate decreases as healing phase time increases. Since healing rate is time dependent, no single healing rate can be obtained for each mixture as a measurement of how fast a mixture heals. A logarithmic function with single parameter 'a' was used to fit the percentage of healing versus time curve to represent mixture healing potential. Typical percentage of healing versus time data with the logarithmic function is presented in Figure 5-5. The healing rate parameter 'a' is defined as the coefficent of logarithm function as shown in Figure 5-5. Healing rate parameters for all 24 mixture combinations are presented in Table 5-3, and Figure 5-6 and 5-7 for dense-graded and open-graded mixture, respectively. The data presented in Table 5-3, Figure 5-6 and 5-7 indicated that mixture at higher temperature had higher healing potential than that at lower temperature. Likewise, short-term aged mixture had a higher healing potential than long-term aged mixture. For dense-graded mixture, binder modified mixture had higher healing potential than unmodified mixture. In addition, these results were in good agreement with expected trends.

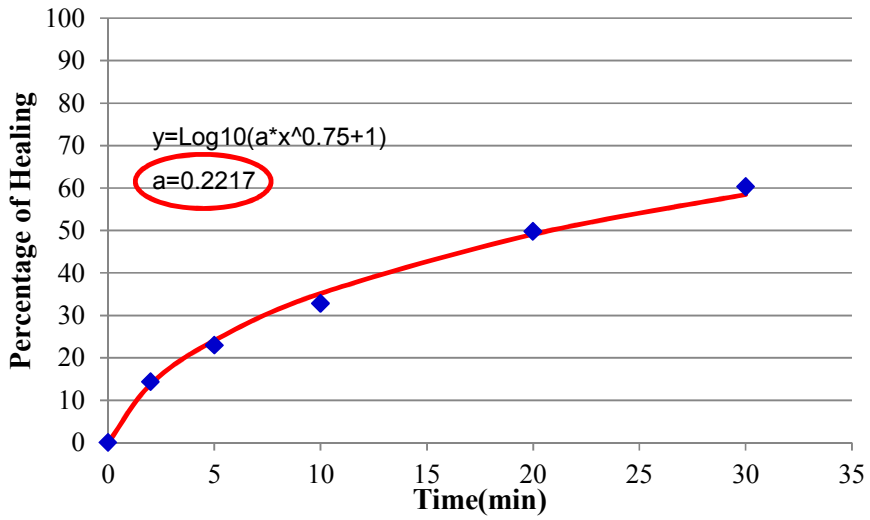

Figure 5-5. Typical percentage healing and fit curve vs. time

Table 5-3. Healing rate parameter, a

Mixture	a	Mixture	a	Mixture	a	Mixture	a
DUS00	0.3255	DMS00	0.4070	OMS00	0.3373	ORS00	0.5267
DUS10	0.4725	DMS10	0.5715	OMS10	0.5008	ORS10	0.6283
DUS20	0.8989	DMS20	1.1658	OMS20	1.2704	ORS20	1.1007
DUL00	0.2217	DML00	0.3391	OML00	0.3370	ORL00	0.4565
DUL10	0.4238	DML10	0.4663	OML10	0.5157	ORL10	0.6029
DUL20	0.5314	DML20	0.4930	OML20	0.6571	ORL20	1.4565

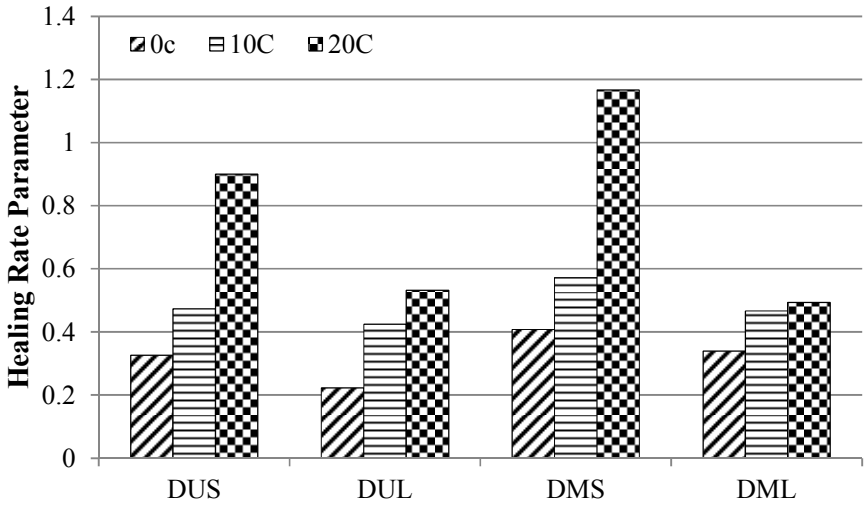

Figure 5-6. Healing rate parameter for dense-graded mixture

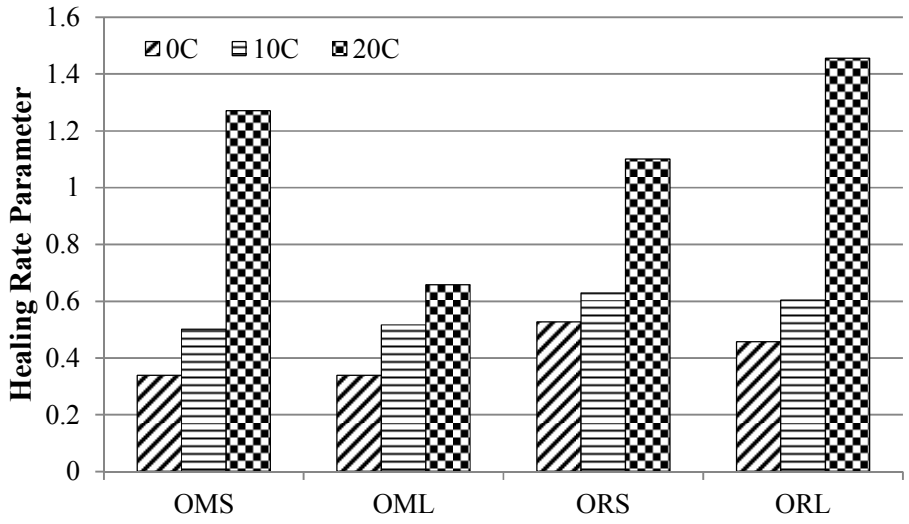

Figure 5-7. Healing rate parameter for open-graded mixture

It should be noted that specimens were damaged, but not brought to failure during the damage phase. In other words, DCSE and/or FE limit was not exceeded throughout the damage phase. This requirement was maintained for all mixtures tested by keeping the damage phase in linear range after initial quick resilient modulus reduction (See Figure 5-2). On the other hand, once damage phase passes beyond this linear range, little or no damage can be recovered since failure is introduced (See Figure 5-8).

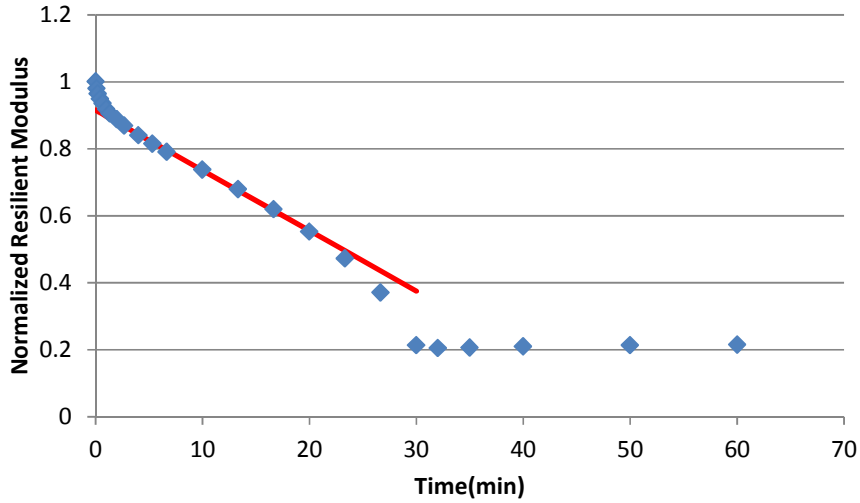

Figure 5-8. Typical damage and healing phase with failure limit exceeded

CHAPTER 6
CLOSURE

6.1 Summary and Findings

This study was conducted to develop a test method that will allow evaluation and quantification of the effects of healing on asphalt mixture. A new healing test, including both a damage phase and a healing phase was conceived, developed and validated for asphalt mixtures. Resilient modulus testing data were acquired throughout the duration of the healing test (damage and healing phase) to monitor damage accumulation and recovery on asphalt mixtures.

Appropriate loading was necessary for the damage phase of the healing test to obtain sufficient damage in the specimen without failing it in a reasonable amount of time (30 min in this study). A number of variables were evaluated: loading mode, including monotonic and repeated loading; rest period for repeated loading, including 0.1 sec, 0.4 sec and 0.9 sec; and loading magnitudes for repeated loading. Loading magnitudes were determined using modified brittleness index based on brittleness of the asphalt mixture. Healing tests were performed on 4 types of asphalt mixtures at two oxidation aging conditions (short-term and long-term aging) under three temperatures (0°C, 10°C and 20°C). Findings associated with this study are summarized as follows:

- Delayed elasticity associated with monotonic loading may cause error during healing phase since it is almost impossible to differentiate delayed elasticity from damage recovery. On the other hand, rest periods between repeated loading applications allow most delayed elasticity to be recovered.

- Short rest periods (0.1 and 0.2-second) resulted in excessively rapid damage development whereas long rest period (0.9-second) resulted in almost complete healing for typical STOA dense-graded mixture regardless of load level used.
- Intermediate rest period (0.4-second) resulted in a balance between delayed elasticity recovery and damage recovery, a controllable damage development, and a longer steady-state damage range.
- Loading level (as percent of strength) in the linear range of applied force versus horizontal deformation curve reduced the error of resultant resilient modulus calculated through stress-strain relationship. High loading magnitudes led not only to nonlinear response but also to excessive concentration at the loading strip on IDT specimens. On the other hand, low loading magnitude results in excessively long testing time to damage asphalt mixtures.
- Modified brittleness index defined as strength divided by failure strain (from Superpave IDT strength test) successfully separated asphalt mixtures based on brittleness at different temperatures.
- For the damage phase, higher loading magnitude and / or shorter rest period resulted in higher reduction in resilient modulus. Additionally, higher loading magnitude and / or shorter rest period caused more heating and reversal of steric hardening effects as long as DCSE and FE limits are were exceeded.
- Through trial and error, a natural logarithmic relationship between loading level and modified brittleness index was established for both dense-graded and open-graded mixture.

- During the damage phase, asphalt mixtures exhibited linear reduction in resilient modulus after about 2 min of loading. The initial nonlinear reduction in resilient modulus (first 2 min) was caused by local elevation of temperature in the specimen and reversal of steric hardening.
- In steady-state of healing phase (from 10 to 30 min), normalized resilient modulus has a linear relationship with the slope of normalized resilient modulus versus time curve. Normalized undamaged resilient modulus determined from this linear relationship is a good predictor of the normalized resilient modulus at the value at which the mixture has fully healed.
- Healing rate is time dependent throughout the healing phase. Healing rate parameter 'a' determined from fitting of the percentage of healing versus time curve is a good indicator of mixture healing potential.
- Mixture at higher temperature has greater healing potential than mixture at lower temperature; long-term aged mixture has less healing potential than short-term aged mixture; for dense-graded mixture, binder modified mixture has greater healing potential than unmodified mixture.
- Once the linear damage range is exceeded, little or no damage recovery will occur since the mixture failure limit has been exceeded.

6.2 Conclusions

After comprehensive evaluation of results from the healing test performed on all asphalt mixtures tested in this study, the following conclusions can be drawn:

- The developed healing test can successfully evaluate healing characteristics of asphalt mixture as well as quantify healing rates of asphalt mixture.
- Healing rate parameter, a, can be used to evaluate asphalt mixture healing potential.
- Modified brittleness index (strength divided by failure strain from Superpave IDT test) introduced in this study can be used to determine appropriate load levels for use in the damage phase of testing.
- Low temperature and aging reduce mixture healing potential; for dense-graded mixture, binder modification enchances asphalt mixture healing potential.
- Once fracture / failure are induced in asphalt mixtures, little or no damage can be recovered.

6.3 Recommendations

Based on the studies completed, the following items are recommended for further research:

- Results are presented in terms of resilient modulus. However, further attention should be given to transforming the results to dissipated creep strain energy (DCSE), such that healing rates can be incorporated in the HMA Fracture Mechanics model and prediction of pavement cracking performance.
- Perform damage phase test immediately after a full healing test (damage and healing phase) to determine whether the initial nonlinear quick drop of resilient modulus at the beginning of damage phase is a one-time phenomenon or not. This can help to evaluate whether rapid drop in resilient modulus is caused by local elevation of temperature in the specimen and reversal of steric hardening.

- A broader range of factors/mixture parameters should be evaluated using the developed healing test (e.g., binder types, dominant aggregate size range porosity, disruption factor, effective film thickness, ratio between coarse portion of fine aggregate and fine portion of fine aggregate, etc.).
- The healing test in this study was performed on laboratory produced specimens. To acquire more insight into healing behavior of asphalt mixture, field cores should be used as well.
- Results indicate that all load-induced damage may be fully healable. Thermal contraction (freeze-thaw without the presence of water) may be a source of non-healable damage and should be studied.
- Healing potential of plant mix, as opposed to laboratory generated mix, should be evaluated as well.

LIST OF REFERENCES

AASHTO (2001a). Standard Practice for Mixture Conditioning of Hot Mix Asphalt, AASHTO PP2, Washington, D.C.

AASHTO (2001b). Standard Method of Test for Bulk Specific Gravity of Compacted Bituminous Mixtures Using Saturated Surface-Dry Specimens, AASHTO T 166, Washington, D.C.

Asphalt Institute. (2001). Superpave Mix Design. Superpave Series No.2 (SP-2). Asphalt Institute. Lexington, KY.

ASTM (2002a). Standard Test Method for Bulk Specific Gravity and Density of non-absorptive Compacted Bituminous Mixtures, ASTM D 2726, West Conshohocken, PA.

ASTM (2002b). Standard Test Method for Bulk Specific Gravity and Density of Compacted Bituminous Mixtures Using Automatic Vacuum Sealing Method, ASTM D 6752, West Conshohocken, PA.

Bhasin, A., Palvadi, S., and Little, D.N. (2011). "Influence of Aging and Temperature on Intrinsic Healing of Asphalt Binders," Transportation Research Record 2207, Transportation Research Board, Washington, D.C., pp. 70-78.

Buchanan, M.S., and White, T.D. (2005). "Hot Mix Asphalt Mix Design Evaluation Using the Corelok Vacuum-Sealing Device," Journal of Materials in Civil Engineering, Vol. 17(2), pp. 137-142.

Buttlar, W. G. and Roque, R. (1994). "Development and Evaluation of the Strategic Highway Research Program Measurement and Analysis System for Indirect Tensile Testing at Low Temperatures," In Transportation Research Record: Journal of the Transportation Research Board, No. 1454, National Research Council, National Academy Press, Washington, D. C., pp. 163-171.

Carpenter, S. H., and Shen, S. (2006). "A Dissipated Energy Approach to Study HMA Healing in Fatigue," Transportation Research Record 1970, Transportation Research Board, Washington, D.C., pp. 178–185.

Cooley, L. A., Prowell, B. D., Hainin, M. R., Buchanan, M. S., and Harrington, J. (2002). "Bulk Specific Gravity Round Robin Using the Corelok Vacuum Sealing Device," NCAT Report 02-11, National Center for Asphalt Technology, Auburn, AL.

Daniel, J.S., and Kim, Y.R. (2001). "Laboratory Evaluation of Fatigue Damage and Healing of Asphalt Mixtures," Journal of Materials in Civil Engineering, Vol. 13(6), pp. 434-440.

FDOT (2007). Standard Specifications for Road and Bridge Construction, Florida Department of Transportation, Tallahassee, FL.

Francken, L. (1979). “Fatigue Performance of a Bituminous Road Mix under Realistic Test Conditions,” Transportation Research Record 712, Transportation Research Board, Washington, D. C., pp. 30-36.

Ghuzlan, K.A., and Carpenter, S.H. (2000). “Energy-Derived, Damage-Based Failure Criterion for Fatigue Testing,” Transportation Research Record 1723, Transportation Research Board, Washington, D.C., pp. 141–149.

Grant, T.P (2001). “Determination of Asphalt Mixture Healing Rate Using the Superpave Indirect Tensile Test”, Thesis (M.E.), University of Florida, Gainesville, FL.

Kim, B., and Roque, R. (2006). “Evaluation of Healing Property of Asphalt Mixture,” Transportation Research Record 1970, Transportation Research Board, Washington, D.C., pp. 84-91.

Kim, Y. S. (1988). ‘‘Evaluation of Healing and Constitutive Modeling of Asphalt Concrete by Means of the Theory of Nonlinear Viscoelasticity and Damage Mechanics,’’ PhD Dissertation, Texas A&M University, College Station, TX.

Kim, Y., and Kim, Y.R. (1997). “In Situ Evaluation of Fatigue Damage Growth and Healing of Asphalt Concrete Pavements Using Stress Wave Method,” Transportation Research Record 1568, Transportation Research Board, Washington, D.C., pp. 106-113.

Koh, C. and Roque, R. (2010a). “Characterization of the Tensile Properties of Open Graded Friction Course Mixtures Based on Direct and Indirect Tension Tests,” Journal of Testing and Evaluation, Vol. 38(4), pp. 1-12.

Koh, C. and Roque, R. (2010b). “Use of Nonuniform Stress-State Tests to Determine Fracture Energy of Asphalt Mixtures Accurately,” Transportation Research Record 2181, Transportation Research Board, Washington, D.C., pp. 55-66.

Li, W. (2009). ‘‘Evaluation of Hybrid Binder for Dense and Open-Graded Asphalt Mixtures,’’ PhD Dissertation, University of Florida, Gainesville, FL.

Little, D.N. and Bhasin, A. (2007). “Exploring Mechanism of Healing in Asphalt Mixtures and Quantifying its Impact,” Springer Series in Material Science, Vol. 100, pp. 205-218.

Lytton, R. L. (2000). ‘‘Characterizing Asphalt Pavement for Performance,’’ Transportation Research Record 1723, Transportation Research Board, Washington, D.C., pp. 5-16.

Mallick, R., Kandhal, P., Cooley, A., and Watson, D. (2000). “Design, Construction and Performance of New Generation Open-Graded Friction Courses,” National Center for Asphalt Technology Report 00-01, NCAT, Auburn, AL.

Monismith, C.L., Epps, J.A. and Finn, F.N. (1985). “Improved Asphalt Mix Design,” Journal of the Association of Asphalt Paving Technologists, Vol. 55, pp. 347-406.

Monismith, C.L. and Finn, N. (1977). "Flexible Pavement Design: State of the Art – 1975," Transportation Engineering Journal, Vol. 103(1), pp. 1-53.

Oliensis, G.L. (1964). "Behavior of Asphalts during Prolonged Weathering as Influenced by Relative Homogeneity of Their Internal Structures," American Society for Testing and Materials -- Special Technical Publications, Pub. 347, pp. 58-69.

Roque, R. and Buttlar, W. G. (1992). "The Development of a Measurement and Analysis System to Accurately Determine Asphalt Concrete Properties Using the Indirect Tensile Mode," Journal of the Association of Asphalt Paving Technologists, Vol.61, pp. 304-332.

Roque, R., Buttlar, W. G., Ruth, B. E., and Dickson, S. W., (1997a). "Short-Loading-Time Stiffness from Creep, Resilient Modulus, and Strength Tests Using Superpave Indirect Tension Test," Transportation Research Record 1630, Transportation Research Board, Washington, D.C., pp. 10-20.

Roque, R., Buttlar, W. G., Ruth, B. E., Tia, M., Dickson, S. W., and Reid, B. (1997b). "Evaluation of SHRP Indirect Tension Tester to Mitigate Cracking in Asphalt Pavements and Overlays," Final Report of Florida Department of Transportation, University of Florida, Gainesville, FL.

Schapery, R. A. (1984). ''Correspondence Principles and a Generalized J Integral for Large Deformation and Fracture Analysis of Viscoelastic Media.'' International Journal of Fracture, Vol. 25, pp. 195–223.

Shen, S. and Carpenter, S.H. (2005). ''Application of the Dissipated Energy Concept in Fatigue Endurance Limit Testing,'' Transportation Research Record 1929, Transportation Research Board, Washington, D.C., pp. 165-173.

Shen, S., Chiu, H., and Huang, H. (2010). "Characterization of Fatigue and Healing in Asphalt Binders," Journal of Materials in Civil Engineering, Vol. 22(9), pp. 846-852.

Si, Z., Little, D.N., and Lytton, R.L. (2002a). "Characterization of Microdamage and Healing of Asphalt Concrete Mixtures," Journal of Materials in Civil Engineering, Vol. 14(6), pp. 461-470.

Si, Z., Little, D.N., and Lytton, R.L. (2002b). "Evaluation of Fatigue Healing Effect of Asphalt Concrete by Pseudo Stiffness," Transportation Research Record 1789, Transportation Research Board, Washington, D.C., pp. 73-79.

Soltani, A. and Anderson, D.A. (2005). "New Test Protocol to Measure Fatigue Damage in Asphalt Mixtures," Road Materials and Pavement Design, Vol. 6, pp. 485-514.

Song, I., Little, D., Masad, E., and Lytton,R. (2005). "Comprehensive Evaluation of Damage in Asphalt Mastics Using X-ray CT, Continuum Mechanics, and Micromechanics," Journal of the Association of Asphalt Paving Technologists, Vol. 74, pp. 885-920.

Tashman, L., Masad, E., Little, D., and Lytton, R. (2004). "Damage Evolution in Triaxial Compression Tests of HMA at High Temperatures," Journal of the Association of Asphalt Paving Technologists, Vol. 73, pp. 53-87.

Varadhan, A. (2004). "Evaluation of Open Graded and Bonded Friction Course for Florida," Master's Thesis, University of Florida, Gainesville, FL.

Wool, R. P. and O'Connor, K.M. (1981). "A Theory of Crack Healing in Polymers," Journal of Applied Physics, Vol. 52(10), pp. 5953–5963.

APPENDIX A
ASPHALT MIXTURE INFORMATION

Table A-1. Dense gradation Job Mix Formula (JMF)

Sieve Size	Percent Passing				
	33%	7%	50%	10%	100%
	# 78 Stone	# 89 Stone	W-10 Screenings	Local Sand	JMF
3/4"	100.0	100.0	100.0	100.0	100.0
1/2"	97.0	100.0	100.0	100.0	99.0
3/8"	59.0	99.7	100.0	100.0	86.5
# 4	9.0	30.0	100.0	100.0	65.1
# 8	4.0	4.0	70.0	100.0	46.6
# 16	2.0	2.0	42.0	100.0	31.8
# 30	2.0	1.0	25.0	94.0	22.6
# 50	1.0	1.0	16.0	53.0	13.7
# 100	1.0	1.0	10.0	11.0	6.5
# 200	1.0	1.0	7.0	3.0	4.2
G_{sb}	2.809	2.799	2.770	2.626	2.770

Table A-2. Dense gradation batch weights (cumulative)

Sieve Size	Retained Weight, g			
	# 78 Stone	# 89 Stone	W-10 Screenings	Local Sand
3/4"	0.0	1485.0	1800.0	4050.0
1/2"	44.6	1485.0	1800.0	4050.0
3/8"	608.9	1485.9	1800.0	4050.0
# 4	1351.4	1705.5	1800.0	4050.0
# 8	1425.6	1787.4	2475.0	4050.0
# 16	1455.3	1793.7	3105.0	4050.0
# 30	1455.3	1796.9	3487.5	4077.0
# 50	1470.2	1796.9	3690.0	4261.5
# 100	1470.2	1796.9	3825.0	4450.5
# 200	1470.2	1796.9	3892.5	4486.5
Pan	1485.0	1800.0	4050.0	4500.0
Sum	1485.0	315.0	2250.0	450.0

Table A-3. Open gradation Job Mix Formula (JMF)

Sieve Size	Percent Passing				
	44.7%	49.4%	3.2%	2.7%	100%
	S1A Stone	S1B Stone	Screenings	Filler	JMF
3/4"	100.0	100.0	100.0	100.0	100.0
1/2"	79.0	100.0	100.0	100.0	90.6
3/8"	36.0	92.0	100.0	100.0	67.4
# 4	7.0	26.0	100.0	100.0	21.9
# 8	3.0	7.0	68.0	100.0	9.7
# 16	3.0	3.0	67.0	100.0	7.7
# 30	3.0	3.0	55.0	100.0	7.3
# 50	3.0	2.0	35.0	100.0	6.1
# 100	2.0	2.0	14.0	100.0	5.0
# 200	1.0	1.0	3.0	100.0	3.7
G_{sb}	2.425	2.451	2.527	2.600	2.445

Table A-4. Open gradation batch weights (cumulative)

Sieve Size	Retained Weight, g			
	S1A Stone	S1B Stone	Screenings	Filler
3/4"	0.0	2011.5	4234.5	4378.5
1/2"	422.4	2011.5	4234.5	4378.5
3/8"	1287.4	2189.3	4234.5	4378.5
# 4	1870.7	3656.5	4234.5	4378.5
# 8	1951.2	4078.9	4280.6	4378.5
# 16	1951.2	4167.8	4282.0	4378.5
# 30	1951.2	4167.8	4299.3	4378.5
# 50	1951.2	4190.0	4328.1	4378.5
# 100	1971.3	4190.0	4358.3	4378.5
# 200	1991.4	4212.3	4374.2	4378.5
Pan	2011.5	4234.5	4378.5	4500.0
Sum	2011.5	2223.0	144.0	121.5

APPENDIX B
BULK SPECIFIC GRAVITY RESULTS

Table B-1. Bulk specific gravity test results for open-graded mixture with modified binder

Sample ID		A	B	C	D	E	F	G	H	I	J	K	L	M
		Bag Weight (g)	Weight before Sealing (g)	Sealed Sample Weight in Water (g)	Weight after Water Submersion (g)	Ratio B/A	Bag Volume Correction from Table	Total Volume (A+D)-C	Volume of Bag A/F	Volume of Sample G-H	G_{mb} (g/cm^3)	Maximum Specific Gravity	% Air Voids	Average G_{mb}
STOA	OMS_A	46.3	4752.9	2360.0	4752.9	102.654	0.689	2439.2	67.18	2372.02	2.004	2.309	13.22	1.98
	OMS_B	46.3	4752.9	2345.0	4752.9	102.654	0.689	2454.2	67.18	2387.02	1.991	2.309	13.77	
	OMS_C	46.3	4765.3	2347.0	4765.3	102.922	0.689	2464.6	67.22	2397.38	1.988	2.309	13.91	
	OMS_D	47.3	4772.7	2350.1	4772.7	100.903	0.692	2469.9	68.34	2401.56	1.987	2.309	13.93	
	OMS_E	47.2	4789.9	2341.3	4789.9	101.481	0.691	2495.8	68.29	2427.51	1.973	2.309	14.54	
	OMS_F	46.3	4769.5	2345.2	4769.5	103.013	0.689	2470.6	67.24	2403.36	1.985	2.309	14.05	
	OMS_G	46.3	4766.9	2309.0	4766.9	102.957	0.689	2504.2	67.23	2436.97	1.956	2.309	15.28	
LTOA	OML_A	46.3	4770.7	2319.2	4770.7	103.039	0.689	2497.8	67.24	2430.56	1.963	2.309	14.99	1.95
	OML_B	46.3	4757.4	2281.0	4757.4	102.752	0.689	2522.7	67.20	2455.50	1.937	2.309	16.09	
	OML_C	46.3	4757.4	2251.6	4757.4	102.752	0.689	2552.1	67.20	2484.90	1.915	2.309	17.08	
	OML_D	47	4770.0	2323.1	4770.0	101.489	0.691	2493.9	68.00	2425.90	1.966	2.309	14.84	
	OML_E	47.2	4782.3	2324.3	4782.3	101.320	0.691	2505.2	68.27	2436.93	1.962	2.309	15.01	
	OML_F	46.3	4764.7	2306.8	4764.7	102.909	0.689	2504.2	67.22	2436.98	1.955	2.309	15.32	
	OML_G	46.3	4771.8	2326.5	4771.8	103.063	0.689	2491.6	67.25	2424.35	1.968	2.309	14.76	

Table B-2. Bulk specific gravity test results for open-graded mixture with asphalt rubber binder

Sample ID		A	B	C	D	E	F	G	H	I	J	K	L	M
		Bag Weight (g)	Weight before Sealing (g)	Sealed Sample Weight in Water (g)	Weight after Water Submersion (g)	Ratio B/A	Bag Volume Correction from Table	Total Volume (A+D)-C	Volume of Bag A/F	Volume of Sample G-H	G_{mb} (g/cm^3)	Maximum Specific Gravity	% Air Voids	Average G_{mb}
STOA	ORS_A	49.85	4770.9	2320.0	4770.9	95.705	0.701	2500.75	71.14	2429.61	1.964	2.309	14.96	1.97
	ORS_B	49.85	4770.9	2324.7	4770.9	95.705	0.701	2496.05	71.14	2424.91	1.967	2.309	14.79	
	ORS_C	49.85	4804.8	2335.9	4804.8	96.385	0.700	2518.75	71.25	2447.50	1.963	2.309	14.98	
	ORS_D	49.85	4804.8	2320.3	4804.8	96.385	0.700	2534.35	71.25	2463.10	1.951	2.309	15.52	
	ORS_E	49.85	4794.9	2337.0	4794.9	96.187	0.700	2507.75	71.22	2436.53	1.968	2.309	14.77	
	ORS_F	49.85	4794.9	2337.7	4794.9	96.187	0.700	2507.05	71.22	2435.83	1.968	2.309	14.75	
	ORS_G	47.5	4790.4	2390.0	4790.4	100.851	0.692	2447.9	68.62	2379.28	2.013	2.309	12.80	
	ORS_H	47.5	4790.4	2390.0	4790.4	100.851	0.692	2447.9	68.62	2379.28	2.013	2.309	12.80	
	ORS_I	46.3	4785.5	2299.5	4785.5	103.359	0.688	2532.3	67.29	2465.01	1.941	2.309	15.92	
	ORS_J	46.3	4782.9	2321.0	4782.9	103.302	0.688	2508.2	67.28	2440.92	1.959	2.309	15.14	
LTOA	ORL_A	49.85	4791.3	2305.8	4791.3	96.114	0.700	2535.35	71.21	2464.14	1.944	2.309	15.79	1.96
	ORL_B	49.85	4791.3	2312.7	4791.3	96.114	0.700	2528.45	71.21	2457.24	1.950	2.309	15.55	
	ORL_C	49.85	4784.0	2323.6	4784.0	95.968	0.700	2510.25	71.18	2439.07	1.961	2.309	15.05	
	ORL_D	49.85	4784.0	2323.6	4784.0	95.968	0.700	2510.25	71.18	2439.07	1.961	2.309	15.05	
	ORL_E	49.85	4756.6	2311.7	4756.6	95.418	0.701	2494.75	71.09	2423.66	1.963	2.309	15.00	
	ORL_F	49.85	4756.6	2318.0	4756.6	95.418	0.701	2488.45	71.09	2417.36	1.968	2.309	14.78	
	ORL_G	49.85	4810.9	2353.4	4810.9	96.508	0.699	2507.35	71.28	2436.07	1.975	2.309	14.47	
	ORL_H	49.85	4810.9	2358.0	4810.9	96.508	0.699	2502.75	71.28	2431.47	1.979	2.309	14.31	
	ORL_I	46.3	4780.7	2319.5	4780.7	103.255	0.688	2507.5	67.28	2440.22	1.959	2.309	15.15	
	ORL_J	46.3	4785.2	2298.0	4785.2	103.352	0.688	2533.5	67.29	2466.21	1.940	2.309	15.97	

APPENDIX C
SUPERPAVE TEST RESULTS

Table C-1. Superpave IDT test results

	Aging	Temp.	m-value	D_1 (1/psi)	St (MPa)	MR (GPa)	FE (kJ/m3)	$DCSE_f$(kJ/m3)	Creep Rate (1/psi-sec)	D(t) (1/GPa)	Failure Strain (με)
Dense (PG 67-22)	STOA	0°C	0.529	2.25E-07	3.05	15.28	1.80	1.50	4.59E-09	1.330	870.23
		10°C	0.668	4.77E-07	2.14	10.85	4.20	3.99	3.20E-08	7.055	2566.05
		20°C	0.740	2.00E-06	1.16	6.34	2.90	2.79	2.46E-07	47.994	3556.95
	LTOA	0°C	0.479	1.66E-07	3.56	18.43	1.70	1.36	2.18E-09	0.735	751.07
		10°C	0.532	4.48E-07	2.25	11.99	2.20	1.99	9.43E-09	2.619	1336.78
		20°C	0.680	1.07E-06	1.19	6.37	2.50	2.39	7.99E-08	17.081	2838.78
Dense (PG 76-22)	STOA	0°C	0.423	3.57E-07	3.20	17.40	2.30	2.01	2.81E-09	1.013	1038.17
		10°C	0.534	7.54E-07	2.23	10.55	5.50	5.26	1.61E-08	4.414	3326.20
		20°C	0.623	1.70E-06	1.32	5.72	3.90	3.75	7.81E-08	18.189	3988.09
	LTOA	0°C	0.360	2.27E-07	3.55	17.40	2.40	2.04	9.79E-10	0.443	974.00
		10°C	0.413	5.43E-07	2.59	11.37	3.50	3.21	3.88E-09	1.414	1824.64
		20°C	0.551	1.08E-06	1.38	6.21	2.90	2.75	2.68E-08	7.114	2919.52
Open (PG 76-22)	STOA	0°C	0.393	2.98E-07	1.87	10.48	0.60	0.43	1.76E-09	0.708	491.42
		10°C	0.434	8.83E-07	1.58	7.83	1.20	1.00	7.65E-09	2.657	1107.59
		20°C	0.646	1.51E-06	1.09	4.29	2.50	2.36	8.49E-08	19.049	3050.47
	LTOA	0°C	0.291	3.02E-07	1.98	10.18	0.50	0.31	6.57E-10	0.386	457.41
		10°C	0.365	9.02E-07	1.50	8.53	0.70	0.60	4.11E-09	1.741	732.86
		20°C	0.520	1.31E-06	1.03	5.15	1.10	1.00	2.47E-08	7.011	1409.67
Open (ARB-12)	STOA	0°C	0.400	4.80E-07	1.67	9.84	0.50	0.36	3.06E-09	1.185	448.59
		10°C	0.533	5.87E-07	1.45	9.10	1.20	1.08	1.25E-08	3.500	1058.80
		20°C	0.717	1.24E-06	1.07	4.52	2.00	1.87	1.25E-07	25.304	2364.51
	LTOA	0°C	0.324	4.46E-07	1.93	11.35	0.50	0.34	1.35E-09	0.670	446.92
		10°C	0.427	6.26E-07	1.57	10.16	1.10	0.98	5.13E-09	1.824	1013.60
		20°C	0.585	9.62E-07	1.10	4.92	1.50	1.38	3.19E-08	7.988	1772.16

APPENDIX D
DAMAGE PHASE AND HEALING PHASE RESULTS

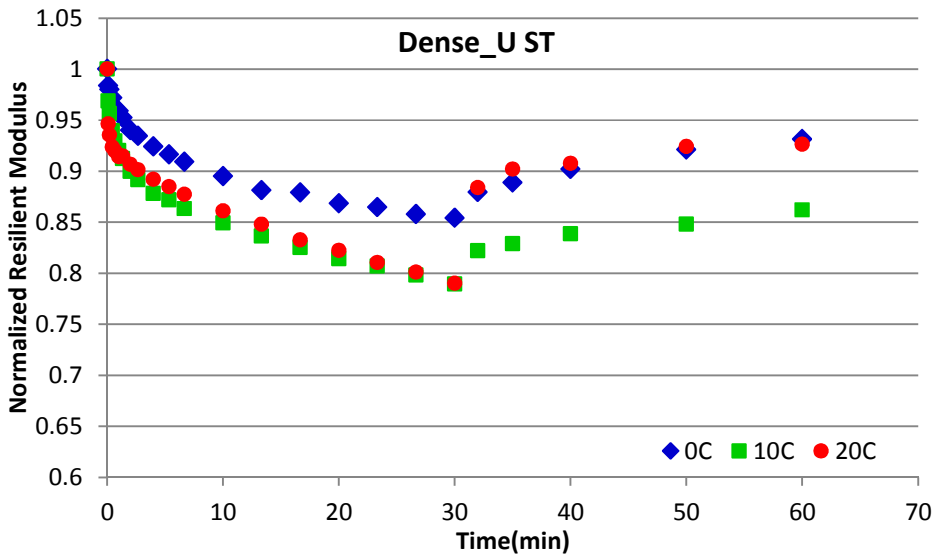

Figure D-1. Damage and healing phase for dense-graded unmodified short-term aged mixtures

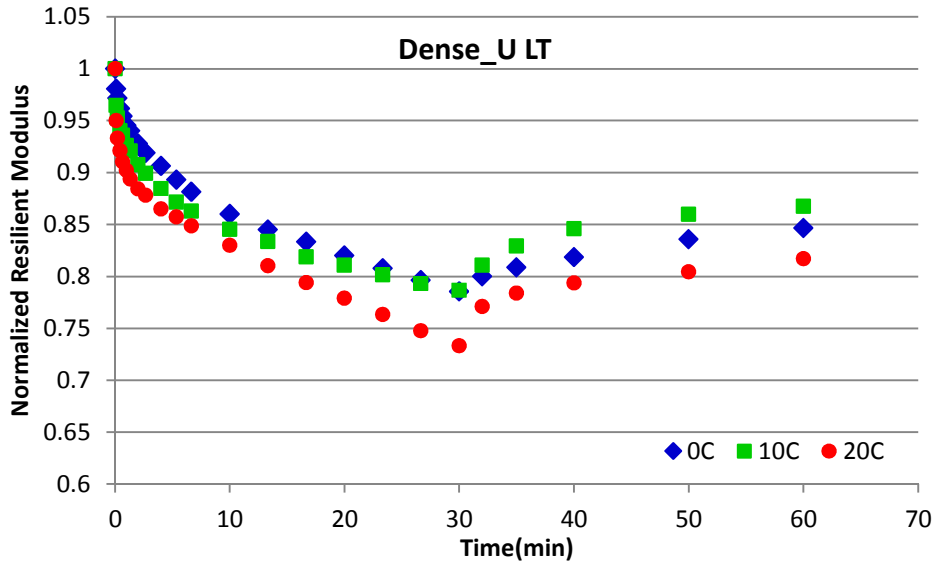

Figure D-2. Damage and healing phase for dense-graded unmodified long-term aged mixtures

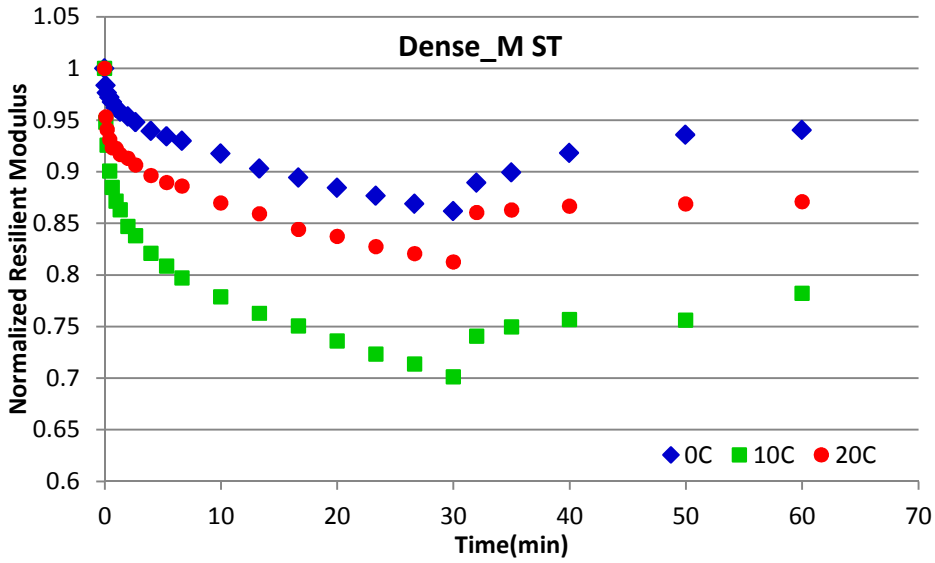

Figure D-3. Damage and healing phase for dense-graded modified short-term aged mixtures

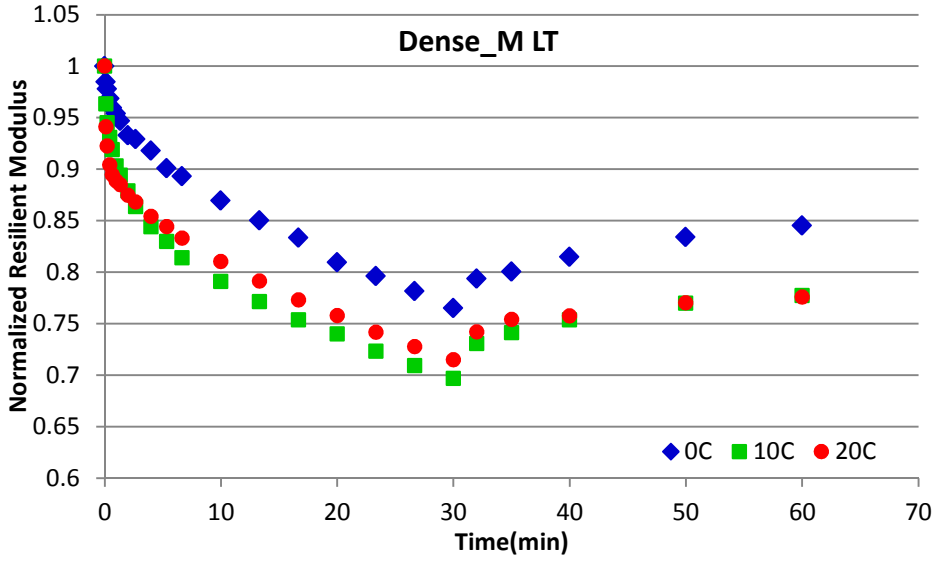

Figure D-4. Damage and healing phase for dense-graded modified long-term aged mixtures

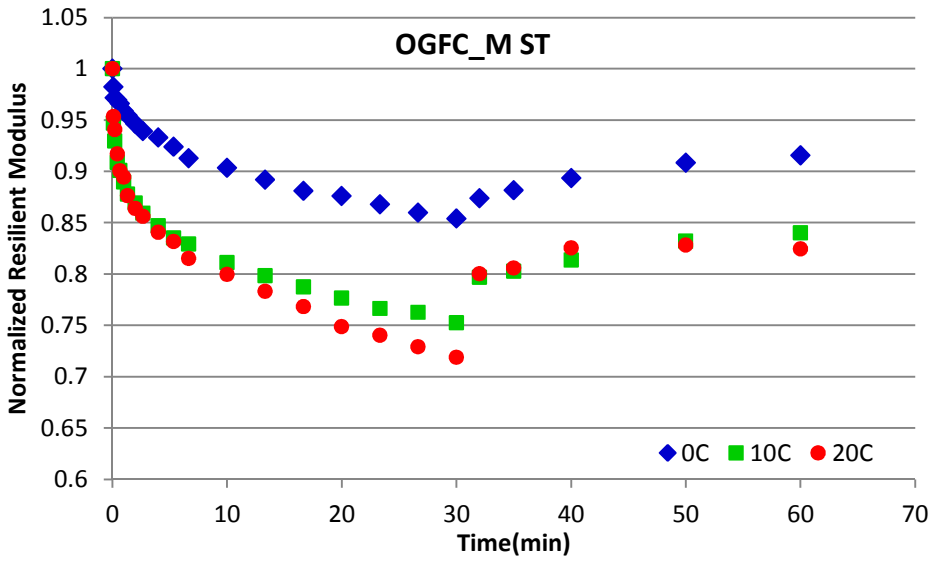

Figure D-5. Damage and healing phase for open-graded modified short-term aged mixtures

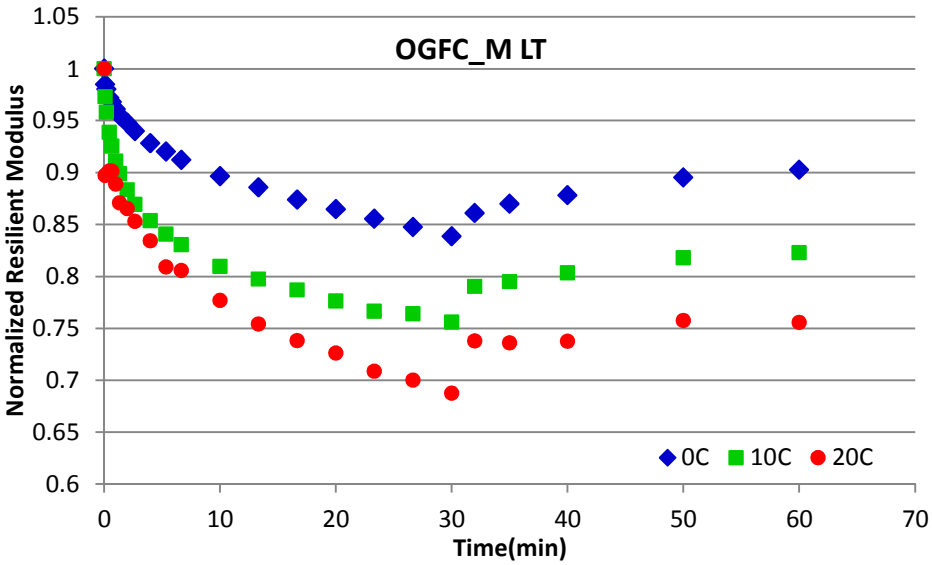

Figure D-6. Damage and healing phase for open-graded modified long-term aged mixtures

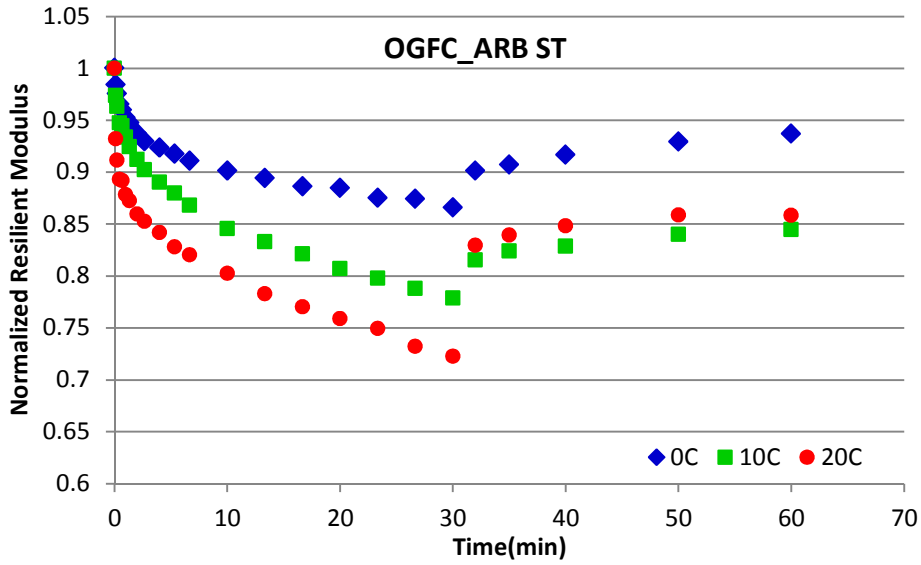

Figure D-7. Damage and healing phase for open-graded asphalt rubber short-term aged mixtures

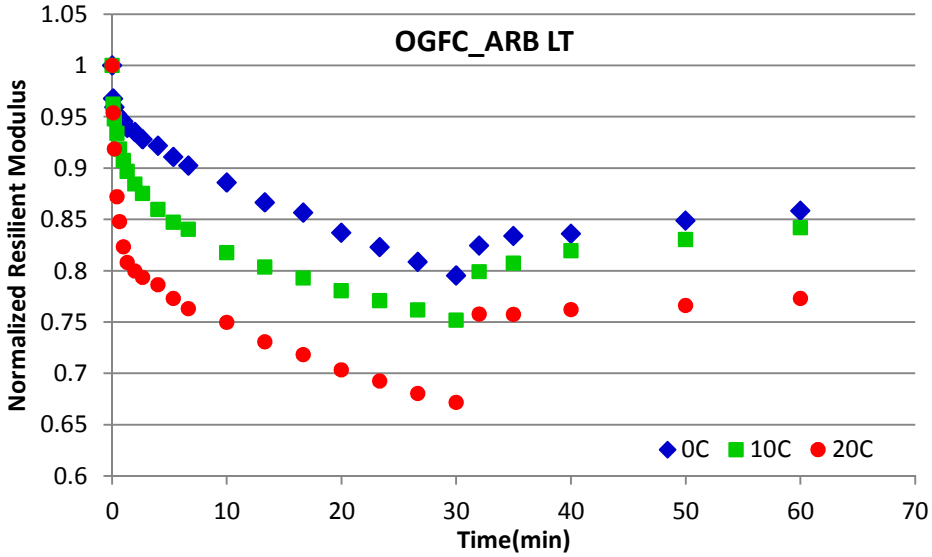

Figure D-8. Damage and healing phase for open-graded asphalt rubber long-term aged mixtures

APPENDIX E
PERCENTAGE OF HEALING RESULTS

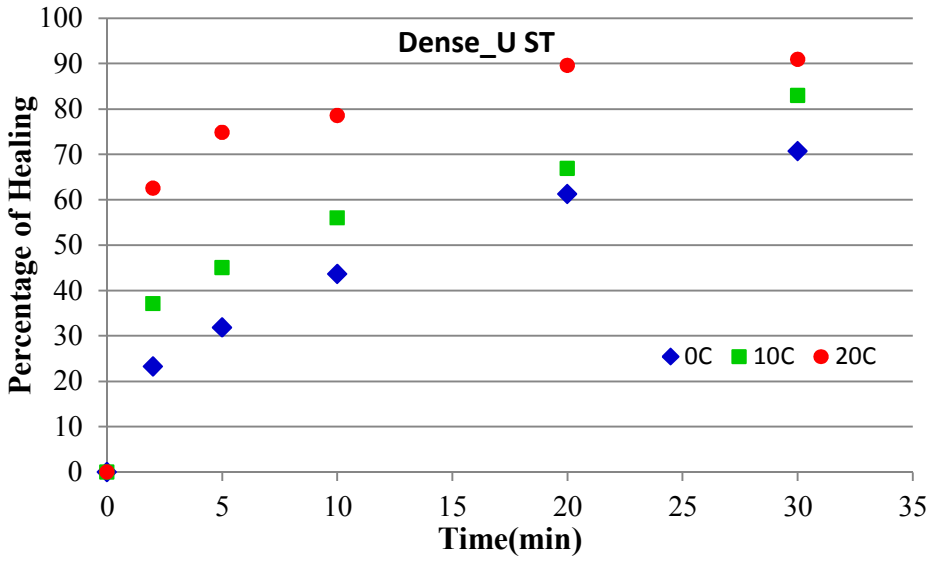

Figure E-1. Percentage of healing for dense-graded unmodified short-term aged mixtures

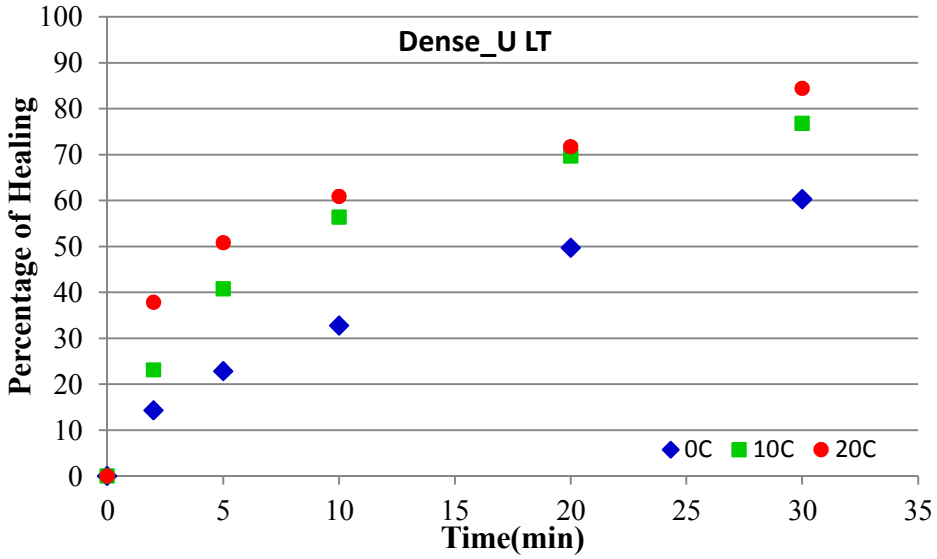

Figure E-2. Percentage of healing for dense-graded unmodified long-term aged mixtures

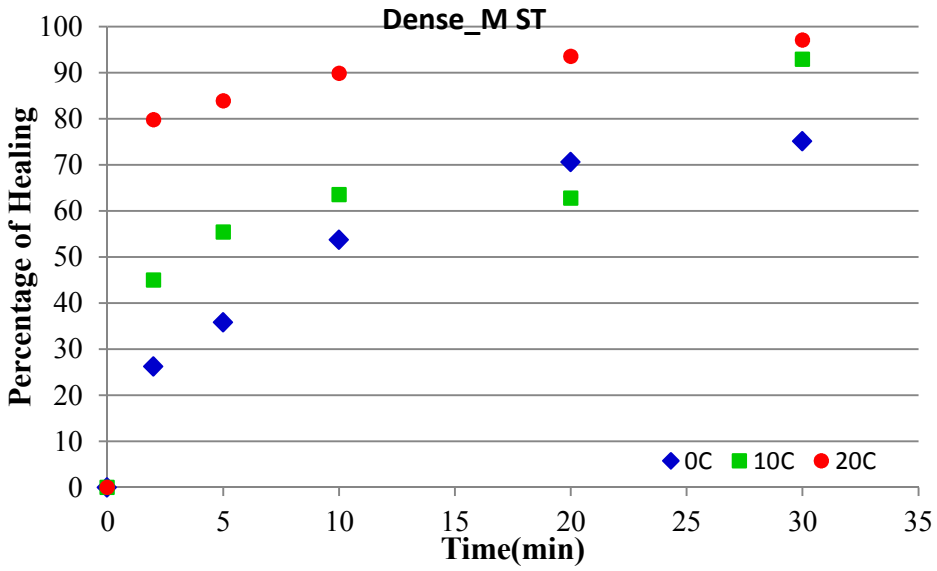

Figure E-3. Percentage of healing for dense-graded modified short-term aged mixtures

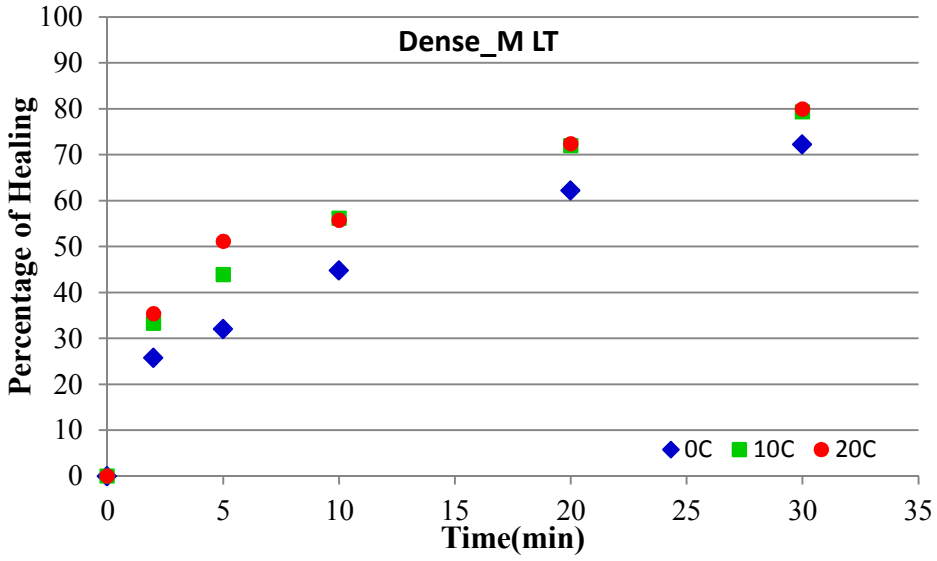

Figure E-4. Percentage of healing for dense-graded modified long-term aged mixtures

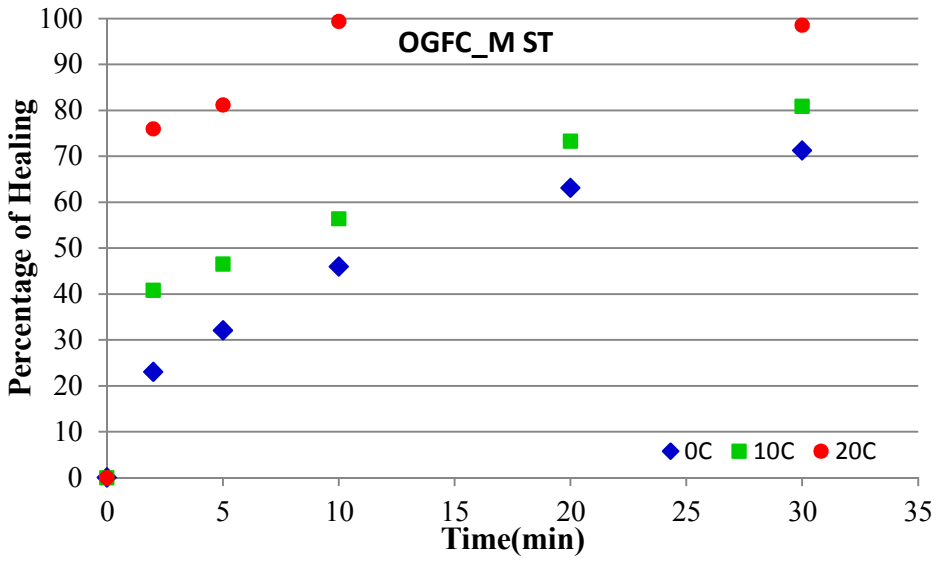

Figure E-5. Percentage of healing for open-graded modified short-term aged mixtures

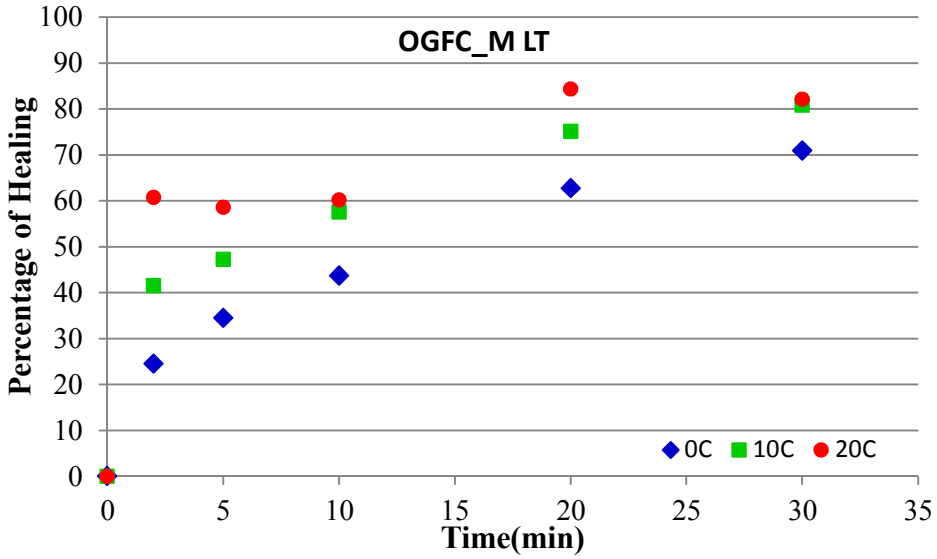

Figure E-6. Percentage of healing for open-graded modified long-term aged mixtures

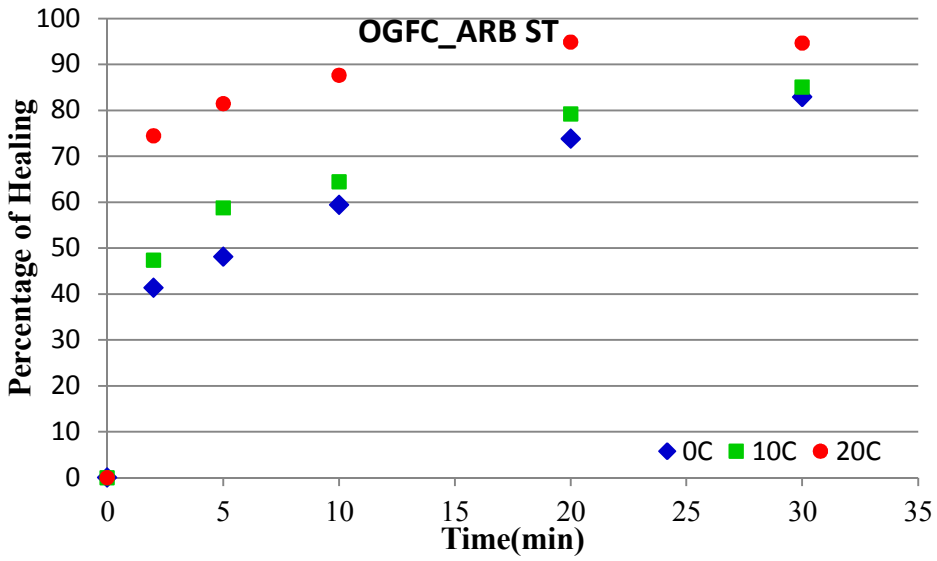

Figure E-7. Percentage of healing for open-graded asphalt rubber short-term aged mixtures

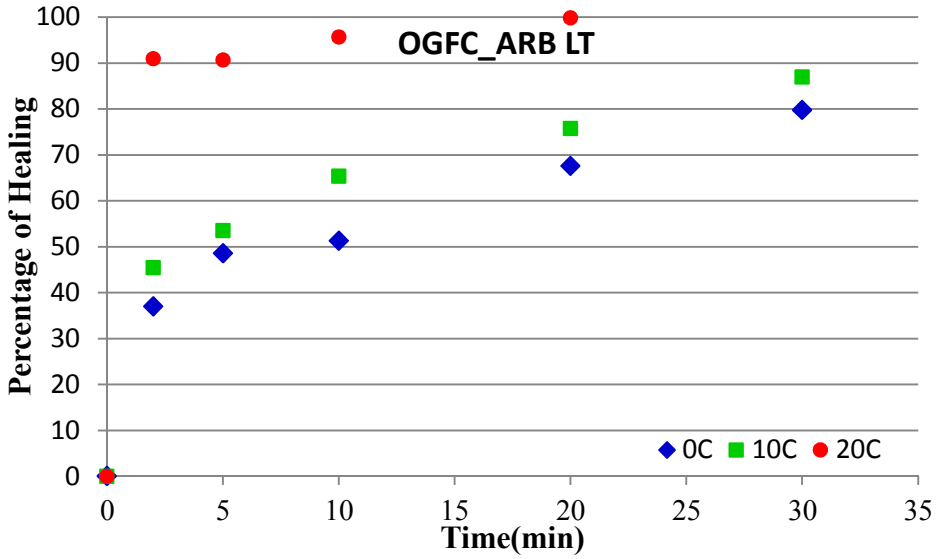

Figure E-8. Percentage of healing for open-graded asphalt rubber long-term aged mixtures